DEFENSE TECHNICAL INFORMATION CENTER

Information for the Defense Community

DTIC® has determined on 04 / 08 / 2016 that this Technical Document has the Distribution Statement checked below. The current distribution for this document can be found in the DTIC® Technical Report Database.

☑ **DISTRIBUTION STATEMENT A.** Approved for public release; distribution is unlimited.

☐ **© COPYRIGHTED.** U.S. Government or Federal Rights License. All other rights and uses except those permitted by copyright law are reserved by the copyright owner.

☐ **DISTRIBUTION STATEMENT B.** Distribution authorized to U.S. Government agencies only (fill in reason) (date of determination). Other requests for this document shall be referred to (insert controlling DoD office).

☐ **DISTRIBUTION STATEMENT C.** Distribution authorized to U.S. Government Agencies and their contractors (fill in reason) (date determination). Other requests for this document shall be referred to (insert controlling DoD office).

☐ **DISTRIBUTION STATEMENT D.** Distribution authorized to the Department of Defense and U.S. DoD contractors only (fill in reason) (date of determination). Other requests shall be referred to (insert controlling DoD office).

☐ **DISTRIBUTION STATEMENT E.** Distribution authorized to DoD Components only (fill in reason) (date of determination). Other requests shall be referred to (insert controlling DoD office).

☐ **DISTRIBUTION STATEMENT F.** Further dissemination only as directed by (insert controlling DoD office) (date of determination) or higher DoD authority.

Distribution Statement F is also used when a document does not contain a distribution statement and no distribution statement can be determined.

☐ **DISTRIBUTION STATEMENT X.** Distribution authorized to U.S. Government Agencies and private individuals or enterprises eligible to obtain export-controlled technical data in accordance with DoDD 5230.25; (date of determination). DoD Controlling Office is (insert controlling DoD office).

SIU School of Medicine

December 22, 2015

Defense Technical Information Center
8725 John J Kingman Rd., Ste 0944
Fort Belvoir, VA 22060-6218

As required, enclosed is the final technical report for Award N00014-13-1-0569, "Cell source and mechanism of hair cell regeneration in the neonatal mouse cochlea", PI, Cox. As required, this report has also been sent to the technical representative and the Chicago administrative office. If you have any questions concerning the report, please contact me.

Sincerely,

Pamela Burk

Pamela Burk
Grants and Contracts Administrator
217-545-8174
pburk@siumed.edu

I. **Heading: Final Report Period April 1, 2013 – September 30, 2015**

A. PI: Brandon C. Cox bcox@siumed.edu
B. Southern Illinois University, School of Medicine, Springfield IL 62702
C. Award# N00014-13-1-0569
D. *Cell source and mechanism of hair cell regeneration in the neonatal mouse cochlea*

II. Scientific and Technical Objectives

Specific Aims:
Aim 1: To determine the cell source of regenerated hair cells in the neonatal mouse cochlea.
Aim 2: To determine the mechanism of hair cell regeneration in the neonatal mouse cochlea.

Non-mammalian vertebrates such as birds, fish, and amphibians can regenerate hair cells (HCs) after damage. This occurs when neighboring supporting cells (SCs) produce new HCs by either a change in cell fate (termed direct transdifferentiation) or by cell division (termed mitotic regeneration). In contrast, damage to auditory HCs, caused by noise exposure or other factors, is permanent in humans and other mature mammals. However, we have recently developed a novel method to damage HCs in the neonatal mouse cochlea *in vivo* and observed spontaneous HC regeneration. Regenerated HCs are similar to endogenous HCs expressing espin+ stereocilia and several HC markers, including prestin, a protein specific to outer HCs that is necessary for the amplification of sound. Our findings demonstrate that, in contrast to common belief, the neonatal mouse cochlea does have the capacity to regenerate HCs after damage and is one step closer to regenerating HCs in humans. This award was focused on further investigation of the cell source, mechanism, and genes involved in the HC regeneration process that occurs in the neonatal mouse cochlea. During the funding period, we completed the original Aim 1 using fate-mapping to demonstrate that SCs act as the cell source of regenerated HCs in the neonatal mouse cochlea. However there are seven SC subtypes in the cochlea and little is known about the capacity of individual subtypes to convert into HCs. We thus expanded Aim 1 to investigate which SC subtypes have the ability to act the cell source of regenerated HCs. Aim 2's focus has not changed from the original proposal and is focused on the molecular mechanism which underlies the HC regeneration process in the neonatal mouse cochlea.

III. Approach

The proposed approach for Aim 1 used mouse genetics to fate-map SCs during the HC regeneration process. We have continued to use mouse genetics for this approach but the specific genetic strategy was changed from the original design. To fate-map SCs as a group we used Hes5-nlsLacZ knock-in mice (Imayoshi et al., 2010) since LacZ is strongly expressed in the majority of SCs within the cochlea. The Hes5-nlsLacZ mouse was bred with Atoh1-CreER::Rosa26-loxP-stop-loxP-DTA mice to trace LacZ+ SCs after HCs were killed by expression of the toxin, DTA. We also collaborated with Dr. Alan Cheng at Stanford University to perform similar fate-mapping experiments in his model of neonatal HC damage (see section V). As mentioned in section II we expanded Aim 1 to fate-map individual SC subtypes. To achieve this we created an Atoh1-rtTA mouse line so that the tetracycline inducible system could be used to kill HCs (by combining Atoh1-rtTA with TetO-DTA mice which will express DTA in HCs and cause cell death). This allows the use of the Cre/loxP system to fate-map individual SC subtypes. Unfortunately this strategy was problematic (explained in section V) and we changed our strategy to use the recently developed Pou4f3^{DTR} mouse line to kill HCs. Pou4f3^{DTR} mice express the human diphtheria toxin receptor (DTR) in HCs. Selective HC death is induced by injection of diphtheria toxin. We combined Pou4f3^{DTR} mice with three different CreER mouse lines to target different SC subtypes for fate-mapping during the HC regeneration process. The proposed approach for Aim 2 did not changed. We used gene expression arrays during the HC regeneration process and validated these changes using immunostaining and qPCR.

IV. Concise Accomplishments

The study demonstrating that the neonatal mouse cochlea can spontaneously regenerate HCs after damage and that SCs are the cell source of regenerated HCs based on fate-mapping studies was published (Cox et al., 2014 *Development*). This publication was the first to demonstrate that HC regeneration can occur in mammals. To expand the fate-mapping studies in Aim 1 to individual SCs subtypes, we generated the needed tetracycline inducible mouse model (Atoh1-rtTA). Characterization of Atoh1-rtTA mice showed it to be HC-specific using two different TetO-reporter lines (published in Cox et al., 2014 *Sci Reports*). The Atoh1-rtTA mouse line is the first to specifically target HCs using the tetracycline inducible system and provides a powerful tool for the field. We then bred Atoh1-rtTA mice with TetO-DTA mice and gave doxycycline to induce expression of DTA and to cause HC death. Unfortunately, no HC death was observed in Atoh1-rtTA::TetO-DTA mice. We therefore imported the Pou4f3^{DTR} mouse line from the University of Washington to induce HC death by injection of diphtheria toxin. To determine which CreER lines would be the most useful to fate-map SCs subtypes, we modified the reporter line and tamoxifen induction paradigm for four CreER lines (Plp-CreER, Prox1-CreER, FGFR3-iCreER, and Sox2-CreER). Publication of this work is planned for submission to the *Journal of the Association for Research in Otolaryngology* before the end of 2015. Two of these lines (Plp-CreER and Prox1-CreER) have proven to be useful in targeting two sets of SC subtypes and a new Cre line (GLAST-CreER) was recently demonstrated to target a third subset of SC subtypes (Mellado Lagarde et al., 2014). The actual fate-mapping of SC subtypes using Pou4f3^{DTR} mice (to kill HCs) bred with these Cre/loxP mouse lines (to fate-map three different SC subtypes during the HC regeneration process) are still in progress. For Aim 2, analysis of the gene expression arrays suggested that the Notch pathway is involved. We validated these results using real-time qPCR and immunostaining. Specifically we observed decreased expression of the Notch ligands Delta1, Jagged1 and Jagged2, as well as the Notch target genes, Hey1, HeyL, and Hes5. This data was used to apply for, and successfully obtain, a 3 year grant from the Department of Defense's Congressionally Directed Medical Research Program (CDMRP) under the Neurosensory and Rehabilitation Research Award (award #W81XWH-15-1-0475).

V. Expanded Accomplishments:

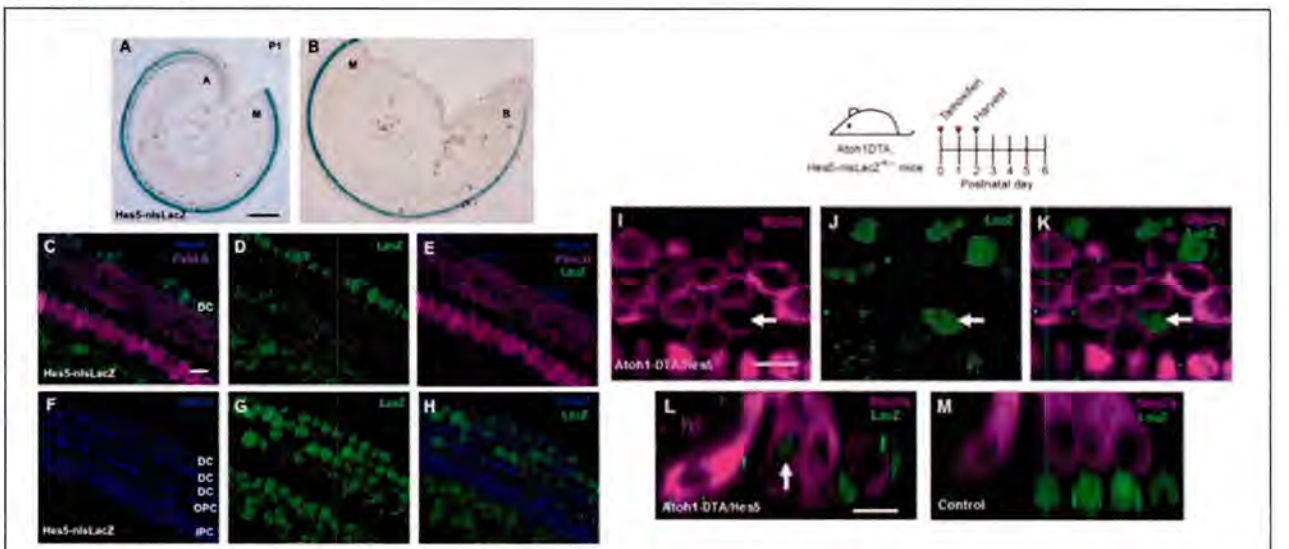

Figure 1. Fate mapping of SCs in the Atoh1DTA model. (**A,B**) X-Gal staining (blue) in Hes5-nlsLacZ cochlea at P1. Cochlear turns are labeled as apical (A), middle (M) and basal (B). (**C-H**) Confocal images of the apical turn of Hes5-nlsLacZ mice at P1. LacZ expression is detected with anti-β-gal antibody (green) and is specific to SCs. HCs are labeled by parvalbumin (PVALB; magenta). Deiter's cells (DC), outer pillar cells (OPC) and inner pillar cells (IPC) are labeled by Prox1 (blue). (**I-K**) Confocal images of LacZ+ (green) HCs (Myo7a, magenta) in the apical turn of Atoh1DTA::Hes5-nlsLacZ$^{+/-}$ mice at P2. (**L**) Cross-section focused on the LacZ+ HC labeled by the arrow in I-K. (**M**) Cross-section of a littermate control at P2, in which all LacZ+ cells are in the SC nuclear layer. Scale bars: 200 μm in A,B; 10 μm in C-M.

Aim 1: To kill HCs in the neonatal mouse cochlea *in vivo*, we used a HC-specific inducible Cre line, Atoh1-CreER, to drive expression of diphtheria toxin fragment A (DTA). When tamoxifen was administrated at postnatal day (P) 0 and P1, CreER was activated in ~80-90% of HCs (Chow et al., 2006; Weber et al., 2008). Beginning 2 days after tamoxifen administration, Atoh1-CreER::ROSA26-loxP-stop-loxP-DTA (Atoh1DTA) mice show rapid and

reproducible loss of both inner and outer HCs. We then performed fate-mapping studies of SCs in the Atoh1DTA model. Although fate-mapping is primarily performed using the Cre/loxP system, we were already using this system to kill HCs and thus needed another mouse genetic tool to trace SCs. Since Hes5 is known to be expressed in SCs of the postnatal cochlea (Hartman et al., 2009; Lanford et al., 2000; Li et al., 2008; Zine et al., 2001), we characterized a recently generated Hes5-nlsLacZ knock-in allele (Imayoshi et al., 2010). LacZ was strongly expressed throughout the P1 cochlea (Figure 1A-B) and labeled many SC subtypes including the majority of Deiter's cells and outer pillar cells, with mosaic labeling of inner phalangeal cells (Figure 1C-H). LacZ expression was not detected in inner pillar cells or HCs. For fate-mapping, we generated Atoh1DTA::Hes5-nlsLacZ$^{+/-}$ mice. After tamoxifen injection at P0/P1, we first observed LacZ+ HCs at P2 (Figure 1I-L), whereas no LacZ+ HCs were found in control samples that were lacking either the Cre or DTA allele (Figure 1M) or at P1 in experimental or control cochleae (n=3). This finding indicates that after HC damage, SCs have changed cell fate and differentiated into HCs *in vivo* and are thus the cell source of regenerated HCs.

To confirm these findings we collaborated with Dr. Alan Cheng at Stanford University to perform similar fate-mapping experiments in his model of neonatal HC damage. Dr. Cheng's model is a knock-in mouse in which expression of the human diphtheria toxin receptor (DTR) is driven by the Pou4f3 promoter (Pou4f3$^{DTR/+}$) (Golub et al., 2012; Mahrt et al., 2013) and selective HC death is induced by injection of diphtheria toxin (DT), because Pou4f3 is exclusively expressed by HCs in the inner ear (Erkman et al., 1996; Xiang et al., 1998). Fate-mapping of SCs with the Pou4f3$^{DTR/+}$ model was performed using the Lgr5-EGFP-IRES-CreER allele (Lgr5-CreER) (Barker et al., 2007) bred with the ROSA26$^{CAG\text{-}tdTomato}$ reporter line (Madisen et al., 2010). In Pou4f3$^{DTR/+}$::Lgr5-CreER$^{+/-}$::ROSA26$^{CAG\text{-}tdTomato/+}$ mice, tamoxifen was given at P1 to label Lgr5+ SCs with tdTomato and DT was injected ~8 hours later to kill HCs. Similar to the fate-mapping in the Atoh1DTA model, a large number of tdTomato+ HCs were detected after HC damage which confirms that SCs are the cell source of regenerated HCs (for more details see Cox et al., 2014 *Development*).

Both methods of fate-mapping targeted broad populations of SCs, but different SC subtypes may vary in their capacity to serve as the source of regenerated HCs. Therefore we expanded the fate-mapping studies in Aim 1 to individual SC subtypes. To perform these experiments, we need to use the Cre/loxP system to fate-map SC subtypes and thus generated a new mouse line that uses the tetracycline inducible system to kill HCs. The tetracycline inducible system uses the rtTA protein that binds to the promoter and activates transcription of a second transgene which contains a tetracycline operator (TetO). The rtTA protein can only bind to TetO and activate transcription in the presence of doxycycline (a more potent analogue of tetracycline) (Gossen et al., 1995). We generated Atoh1-rtTA mice using the well characterized Atoh1 enhancer to drive expression of the reverse tetracycline transactivator (rtTA) protein in HCs. (Atoh1-rtTA was later combined with the commercially available TetO-DTA mouse line to kill HCs.) Atoh1-rtTA activity was measured using two tetracycline operator (TetO) reporter alleles. Each of the five Atoh1-rtTA founder lines was bred with a TetO-mCherry or a TetO-LacZ reporter mouse and double transgenic offspring (Atoh1-rtTA+::TetO-reporter+) given doxycycline in the food to the nursing mother from P0-P3 as well as an injection of doxycycline given to the pups at P1 were evaluated at P3 for rtTA activity. All founder lines showed robust reporter expression in the majority of cochlear HCs (Founder 7 is shown in Figure 2). This thorough characterization of five founder lines demonstrated that Atoh1-rtTA is specifically expressed in cochlear HCs and was recently published (Cox et al., 2014 *Sci Reports*). The Atoh1-rtTA mouse line provides a powerful tool for the field and can be used in combination with other existing Cre/loxP mouse lines to manipulate gene expression in two distinct cell types *in vivo*.

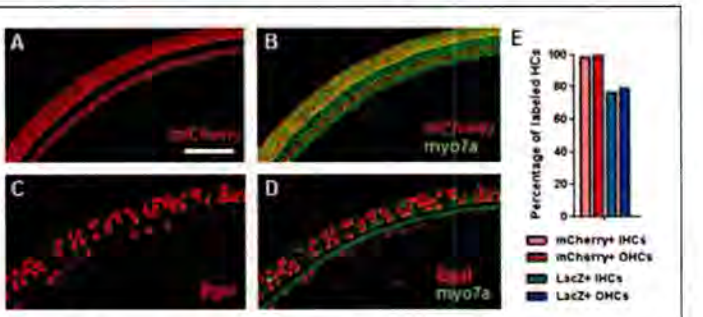

Figure 2. Characterization of the Atoh1-rtTA mouse line. Founder 7 Atoh1-rtTA mice bred with the TetO-mCherry reporter (**A-B**) or the TetO-LacZ reporter (**C-D**) were induced with doxycycline from P0-P3 and samples were analyzed at P3. mCherry and LacZ (detected with a βgal antibody) were expressed only in HCs (myo7a, green). **E,** Quantification of mCherry+ and LacZ+ HCs. IHCs: inner hair cells, OHCs: outer hair cells. Scale Bar: 50 μm

To induce HC death and stimulate the HC regeneration process with this model, Atoh1-rtTA mice were bred with the commercially available TetO-DTA mouse line and given doxycycline in the food to the nursing mother from P0 to P3, as well as an injection of doxycycline given to the pups at P1. Unfortunately, no HC death was observed in Atoh1-rtTA::TetO-DTA mice (Figure 3). This was unexpected since the TetO-DTA mouse line has been used successfully in other fields of research. However it is possible that a spontaneous mutation occurred in the TetO-DTA mouse line or there was downregulation of DTA. We have therefore imported the Pou4f3^{DTR} mouse line from the University of Washington to induce HC death. Pou4f3^{DTR} mice express the human diphtheria toxin receptor (DTR) in HCs and selective HC death is induced by injection of diphtheria toxin. Therefore the Cre/loxP system can still be used to fate-map SC subtypes. Previous studies have shown that HC regeneration occurs in the neonatal mouse cochlea of Pou4f3^{DTR} mice after injection of diphtheria toxin at P1 (Cox et al., 2014 *Development*).

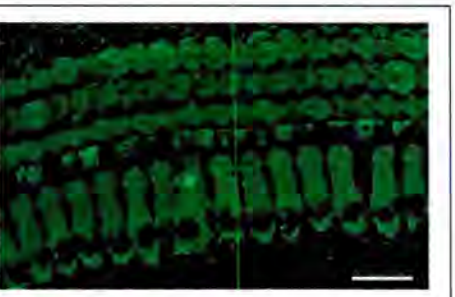

Figure 3. HCs remain intact after Dox induction in Atoh1-rtTA::TetO-DTA mice. Confocal image of HCs (myo7a, green) in Atoh1-rtTA::TetO-DTA mice that were given doxycycline in the food to the nursing mother from P0 to P3 as well as an injection of doxycycline at P1. No HC loss was detected at P9. Scale bar: 20 μm.

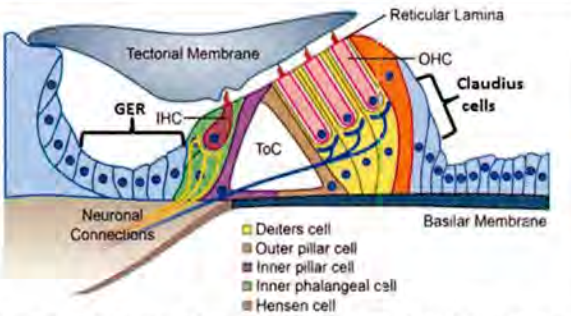

Figure 4. SC subtypes found within the cochlea. GER: greater epithelial ridge, IHC: inner HCs, OHC: outer HCs, ToC: tunnel of Corti. Image modified from (Image modifed from Mellado Lagarde et al., 2013).

The known SC subtypes in the mouse cochlea include Claudius cells, Hensen's cells, Deiter's cells, inner pillar cells, outer pillar cells, and inner phalangeal cells (Figure 4). There are also cells medial to inner phalangeal cells called the greater epithelial ridge (GER) which are known to possess plasticity. Previously published CreER lines that target SCs have Cre expression in multiple subtypes and some even show Cre expression in HCs (Cox et al., 2012). However, these findings are based on tamoxifen induction paradigms that are quite robust. Altering the tamoxifen concentration and number of injections can decrease the Cre expression pattern and increase cell-type specificity. There are also several reporter lines which have different expression patterns even when the same CreER line and tamoxifen induction paradigm are used. To determine which CreER lines would be the most useful to fate-map SCs subtypes, we modified the tamoxifen induction paradigm and used two different reporter lines (Rosa26$^{CAG\text{-}tdTomato}$ and CAG-eGFP) to increase the SC subtype specificity of the Cre expression pattern in four CreER lines (Plp-CreER, Prox1-CreER, FGFR3-iCreER, and Sox2-CreER).

Plp-CreER has previously been reported to label inner phalangeal cells, as well as some pillar and Deiter's cells and in the neonatal mouse cochlea (Gomez-Casati, 2010; Cox et al, 2012; et al, 2014; Mellado-Lagarde et al, 2014). Similar to the previous reports, tamoxifen injection (3mg/40g, IP) at P0/P1 in Plp-CreER$^{+/-}$::ROSA26$^{CAG\text{-}tdTomato+/loxP}$ mice labeled fewer inner phalangeal cells in the apical turn of the cochlea (46.4% ± 3.7%) compared to the middle turn (80.2% ± 2.1%; $p<0.05$), however there was no difference when either was compared to the basal turn (75.4% ± 19.4%) (Figures 5A & 6). This paradigm also showed SC labeling lateral to inner HCs in pillar and Deiter's cells. Specifically, 13.5% ± 4.6% of inner pillar cells were labeled throughout the organ of Corti, while there were 13.4% ± 2.2% tdTomato+ outer pillar cells in the apex and lower numbers of labeled outer pillar cells in the base (4.7% ± 1.5%, $p<0.05$) (Figures 5K-M & 6). There also appeared to be an opposite pattern for Deiter's cell labeling with fewer tdTomato+ Deiter's cells in the apex (6.0% ± 1.7%) and middle (9.5% ± 2.8%) than in the base (29.2% ± 4.8%; $p<0.001$) (Figures 5K-M & 6).

To achieve greater specificity to inner phalangeal cells, we reduced the tamoxifen injection paradigm to one injection at either P0 only or P1 only, while maintaining the same dose (3mg/40g). Expression of tdTomato in inner phalangeal cells of Plp-CreER$^{+/-}$::ROSA26$^{CAG\text{-}tdTomato+/loxP}$ mice that received tamoxifen at P0 only did not differ from tamoxifen injections at P1 only or at both P0/P1 (Figures 5A, E-M & 6). While there was also no difference in the number of tdTomato+ inner and outer pillar cells with a P0 only or P1 only injection compared to the P0/P1

injection, the P0 only injection labeled fewer Deiter's cells in the base of cochlea (11.1% ± 3.6% vs. 29.2% ± 4.8% with the P0/P1 injection) (Figures 5E-M & 6).

Because reduction in tamoxifen dose did not increase inner phalangeal cell specificity, we next generated Plp-CreER$^{+/-}$::CAG-eGFP$^{+/loxP}$ mice to determine if a less robust reporter would reduce off target labeling. When Cre recombination was induced with tamoxifen (3mg/40g, IP) at P0/P1, no difference was observed in inner phalangeal cell labeling between GFP and tdTomato samples in the apex or base, however in the middle turn there were fewer eGFP+ inner phalangeal cells (28.0% ± 3.3%) than tdTomato+ inner phalangeal cells (80.2% ± 2.2%; p>0.01) (Figures 5T-V & 6). Similarly, with the same tamoxifen induction paradigm, reduction in eGFP+ Deiter's cells was observed in the base of Plp-CreER$^{+/-}$::CAG-eGFP$^{+/loxP}$ mice (9.5% ± 9.5%) compared to the number of tdTomato+ Deiter's cells (29.2% ± 4.8%; p>0.05) (Figures 5T-V & 6). There was no difference in inner and outer pillar cell labeling between eGFP and tdTomato reporter lines with tamoxifen induction (3mg/40g, IP) at P0/P1 (Figures 5T-V & 6).

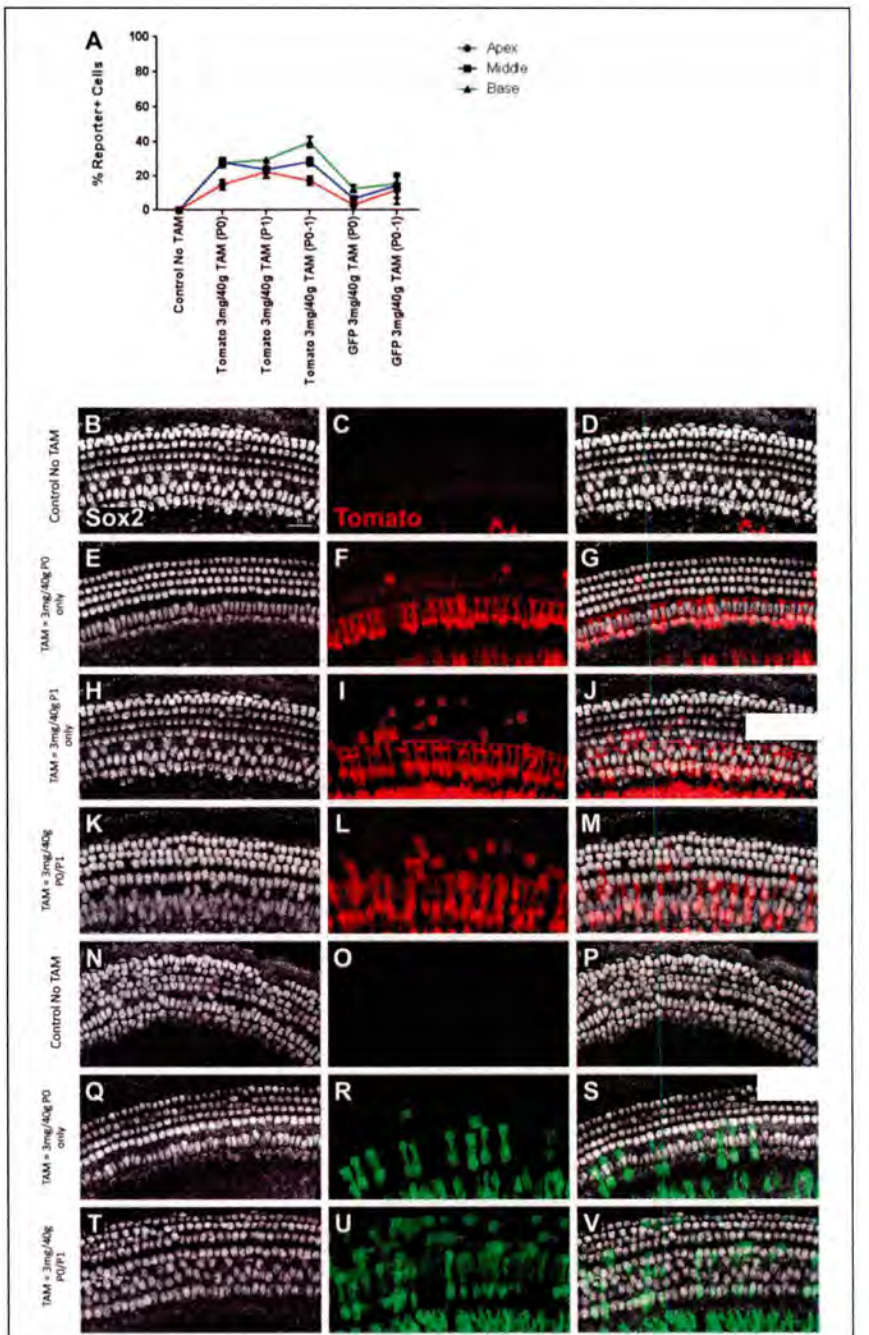

Figure 5. Plp-CreER targets inner phalangeal cells. A, Quantification of total reporter+ SCs after different doses of tamoxifen was given to either Plp-CreER::Rosa26$^{CAG\text{-}tdTomato}$ or Plp-CreER$^{+/-}$::CAG-eGFP$^{+/loxP}$ mice. **B-V,** Confocal images of Tomato (red) expression in Plp-CreER::Rosa26$^{CAG\text{-}tdTomato}$ mice or eGFP (green) expression in Plp-CreER$^{+/-}$::CAG-eGFP$^{+/loxP}$ mice given various doses of tamoxifen. Scale bar: 25 μm.

Since minimal changes in the Plp-CreER expression pattern occurred with the CAG-eGFP$^{+/loxP}$ reporter, we also investigated a lower dose of tamoxifen to achieve greater inner phalangeal cell-specificity. Reducing the amount of tamoxifen given to Plp-CreER$^{+/-}$::CAG-eGFP$^{+/loxP}$ mice to a single injection (3mg/40g, IP) at P0 only reduced the number of eGFP+ cells only in specific turns of the cochlea. The eGFP+ inner phalangeal cells in the middle turn were reduced (22.9% ± 4.7%) compared to Plp-CreER$^{+/-}$::ROSA26$^{CAG\text{-}tdTomato+/loxP}$ mice (80.2% ± 2.2%; p>0.01) (Figures 5E-G, Q-S & 6). Outer pillar cells were also reduced in the middle turn (0.6% ± 0.6% eGFP+ compared to 16.1% ± 3.2% tdTomato+; p>0.05) and Deiter's cells were reduced in the base (2.6% ± 1.5% eGFP+ compared to 29.2% ± 4.8% tdTomato+) (Figures 5E-G, Q-S & 6). Neither Plp-CreER$^{+/-}$::ROSA26$^{CAG\text{-}tdTomato+/loxP}$ nor Plp-CreER$^{+/-}$::CAG-eGFP$^{+/loxP}$ mice showed reporter expression in HCs throughout the cochlea. Finally, no tdTomato+ or eGFP+ cells were detected in Plp-CreER control mice which did not receive tamoxifen (Figures 5A-D, N-P & 6).

From this data we concluded that the best method to fate-map inner phalangeal cells is to use Plp-CreER::Rosa26$^{CAG\text{-}tdTomato}$ mice given tamoxifen (3mg/40g, IP) at P0 only. However fewer cells will be traced in the apical turn.

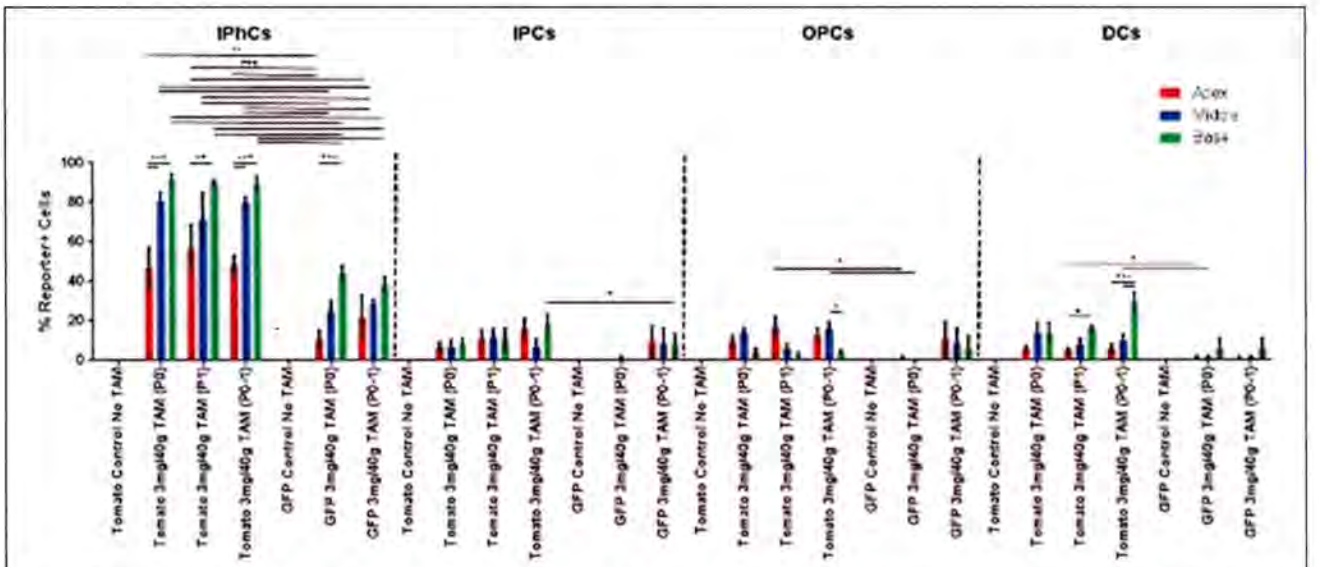

Figure 6. Quantification of Plp-CreER expression in different SC subtypes. SC subtypes that expressed either the tdTomato or eGFP reporter were quantified in two randomly chosen 200 µm regions per cochlear turn, averaged, and expressed as a percentage of labeled cells compared to total cells. IPhCs: inner phalangeal cells, IPCs: inner pillar cells, OPCs: outer pillar cells, DCs: Deiter's cells. (*p<0.05, **p <0.01, ***p<0.001 as determined by a two-way ANOVA with a Tukey'spost-hoc test) (N =3-4).

Prox1-CreER has previously been reported to label pillar and Deiter's cells and in the neonatal mouse cochlea (Yu et al., 2010; Mellado-Lagarde et al, 2013). Similar to the previous reports, tamoxifen injection (3mg/40g, IP) at P0/P1 in Prox1-CreER$^{+/-}$::ROSA26$^{CAG\text{-}tdTomato+/loxP}$ mice showed tdTomato expression specific to only pillar and Deiter's cells. The tdTomato labeling of pillar and Deiter's cells combined was higher in the apex (69.9% ± 1.2%) compared to middle (57.2% ± 1.5%; p<0.05) and basal turns (44.3% ± 3.3%; p<0.001) (Figure 7A, K-M & 8). Similar to the previous report, there was differential labeling among SC subtypes. Specifically, tdTomato was expressed in fewer inner pillar cells (25.2% ± 2.8%) compared to outer pillar cells (70.2% ± 2.6%; p<0.001) and Deiter's cells (77.3% ± 1.1%; p<0.001) (Figure 7K-M & 8). In addition, the number of tdTomato+ inner pillar cells showed a gradient across cochlear turns from apex (45.9% ± 1.6%) to middle (22.2% ± 6.5%; p<0.01) to base (7.4% ± 1.2%; p<0.001) (Figure 7K-M & 8). There was no difference in tdTomato+ outer pillar cells across turns. However, significantly fewer Deiter's cells expressed tdTomato in the base (61.7% ± 4.0%) compared to the apex (90.0% ± 3.0%; p<0.01) and middle (80.7% ± 0.6%; p<0.001) (Figure 7K-M & 8).

Because so few inner pillar cells were labeled with this induction paradigm, we attempted to increase the number of tdTomato+ inner pillar cells by inducing Cre-mediated recombination with a higher dose of tamoxifen. In Prox1-CreER$^{+/-}$::Rosa26$^{CAG\text{-}tdTomato+/loxP}$ mice injected (IP) with 5mg/40g tamoxifen at P0/P1, again we observed fewer tdTomato+ inner pillar cells, than outer pillar cells or Deiter's cells across the whole cochlea (Figure 7A, N-P & 8). We did not observe an increase in tdTomato labeling in inner pillar cells at this dose (24.5% ± 0.9%) compared to the 3mg/40g dose (25.2% ± 2.8%), nor did increasing the dose increase tdTomato expression in outer pillar cells or Deiter's cells (Figure 7K-P & 8). Interestingly, however, 17 outer HCs and 1 inner HC in the apical tip of one sample expressed tdTomato with the 5mg/40g dose (data not shown).

We next attempted to eliminate inner pillar cell labeling to make Prox1-CreER specific to just outer pillar cells and Deiter's cells using two different adjustments to the tamoxifen regimen. In Prox1-CreER$^{+/-}$::Rosa26$^{CAG\text{-}tdTomato+/loxP}$ mice injected with tamoxifen (3mg/40g, IP) at P0 only, there were no differences in the number of tdTomato+ inner pillar cells, outer pillar cells, or Deiter's cells compared to the P0/P1 injection with the same dose (Figure

7H-M & 8). Similarly, when the tamoxifen dose was reduced to 0.75mg/40g (IP) at P0 only, there was no significant difference in the number of tdTomato+ inner pillar cells (16.8% ± 4.0%) compared to the 3mg/40g dose given at either P0/P1 or P0 only (Figure 7E-M & 8). However tdTomato expression was reduced in outer pillar cells (36.1% ± 6.8%; p< 0.001) and Deiter's cells (35.7% ± 4.5%; p< 0.001) (Figure 7E-M & 8).

From this data we concluded that the best method to fate-map pillar and Deiter's cells is to use Prox1-CreER::Rosa26$^{CAG\text{-}tdTomato}$ mice given tamoxifen (3mg/40g, IP) at P0 only. However fewer inner pillar cells will be traced.

We performed similar studies with FGFR3-iCreER and Sox2-CreER mouse lines. However these Cre lines are known to be expressed in both SCs and HCs (Cox et al., 2012; Walters et al., 2015). Therefore the goal was to eliminate HC labeling. With the FGFR3-iCreER line, a 10-fold reduction in tamoxifen dose or changing to the CAG-eGFP reporter resulted in a large reduction of labeled HCs. However, a significant number

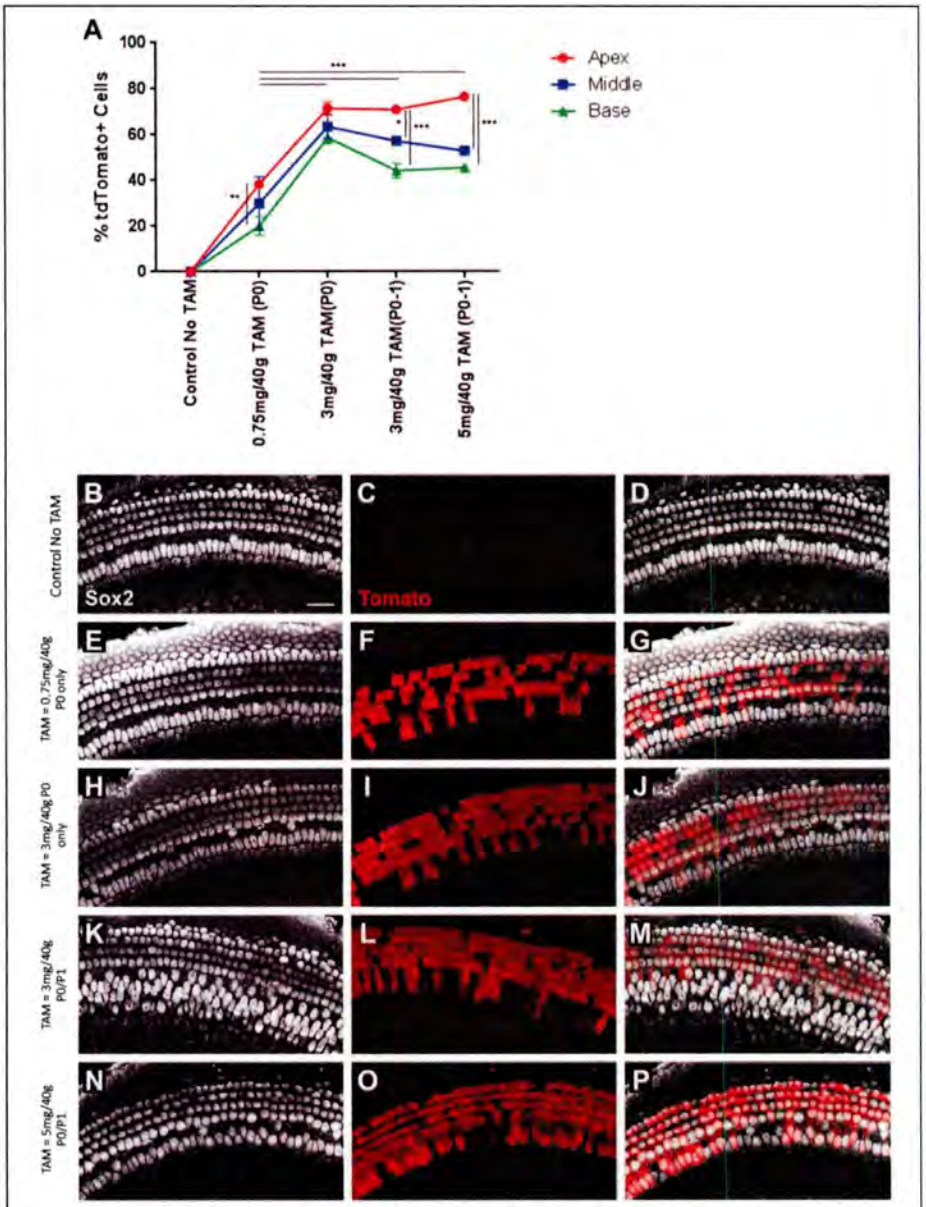

Figure 7. Prox1-CreER targets pillar and Deiter's cells. A, Quantification of total reporter+ SCs after different doses of tamoxifen was given to Prox1-CreER::Rosa26$^{CAG\text{-}tdTomato}$ mice. **B-P**, Confocal images of Tomato (red) expression in Prox1-CreER::Rosa26$^{CAG\text{-}tdTomato}$ mice given various doses of tamoxifen. Scale bar: 25 µm.

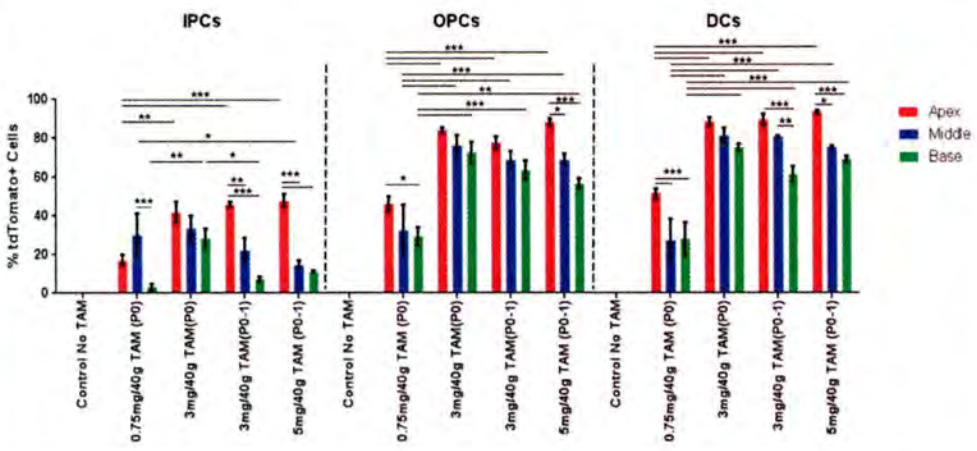

Figure 8. Quantification of Prox1-CreER expression in different SC subtypes. SC subtypes that expressed the tdTomato reporter were quantified in two randomly chosen 200 µm regions per cochlear turn, averaged, and expressed as a percentage of labeled cells compared to total cells. IPCs: inner pillar cells, OPCs: outer pillar cells, DCs: Deiter's cells. (*p<0.05, **p <0.01, ***p<0.001 as determined by a two-way ANOVA with a Tukey's post-hoc test) (N =3-4).

of reporter+ HCs remained in the apical turn (data not shown) and therefore we do not plan to use FGFR3-iCreER mice for our fate-mapping study.

Reducing the tamoxifen dose in Sox2-CreER$^{+/-}$::ROSA26$^{CAG\text{-}tdTomato+/loxP}$ mice produced a minimal effect on the number of labeled HCs or SCs. However, changing to the CAG-eGFP reporter resulted in a significant decrease in labeled HCs, but reporter+ SCs also decreased from ~100% to ~65% (data not shown). Therefore we also do not plan to use Sox2-CreER for our fate-mapping study.

Publication of this work is planned for submission to the *Journal of the Association for Research in Otolaryngology* before the end of 2015. The actual fate-mapping of SC subtypes using Pou4f3^{DTR} mice (to kill HCs) bred with Plp-CreER or Prox1-CreER (to fate-map different SC subtypes during the HC regeneration process) are still in progress. In addition, a new Cre line (GLAST-CreER) was recently demonstrated to target inner phalangeal cells and 75% of cells in the GER (Mellado Lagarde et al., 2014). We plan to also use GLAST-CreER in our fate-mapping studies so that GER cells can also be studied. We are still searching for other Cre lines to target Hensen cells, and Claudius cells.

Aim 2: To investigate the molecular mechanism(s) which underlies the HC regeneration process in the neonatal mouse cochlea, we performed gene expression arrays during the HC regeneration process in the Atoh1DTA model. Specifically, we isolated the apical turn of Atoh1DTA and control cochlea since the vast majority of HC regeneration occurs in this region. Samples were taken at P2, when the first evidence of new HCs was observed, for gene expression analysis. When directly comparing Atoh1DTA and control samples, there were only 24 gene that had a 1.5 fold change at a p value of <0.05 (Figure 9). Of these, three known HC genes were downregulated in Atoh1DTA samples which confirms that HC damage occurred. We next performed a more sophisticated analysis to see which genes correlated with changes in Otoferlin expression since Otoferlin is marker of mature inner HCs. In the Atoh1DTA model, mature inner HCs are killed, thus genes that correlate with or are opposite to Otoferlin expression may be related to the HC regeneration process. We found that several genes in the Notch and Wnt pathways were positively correlated with a decrease in Otoferlin (Figure 9). Since p<0.05 is consider weak for gene expression array analysis, we chose to further investigate the Notch pathway in our model instead of conducting additional gene arrays.

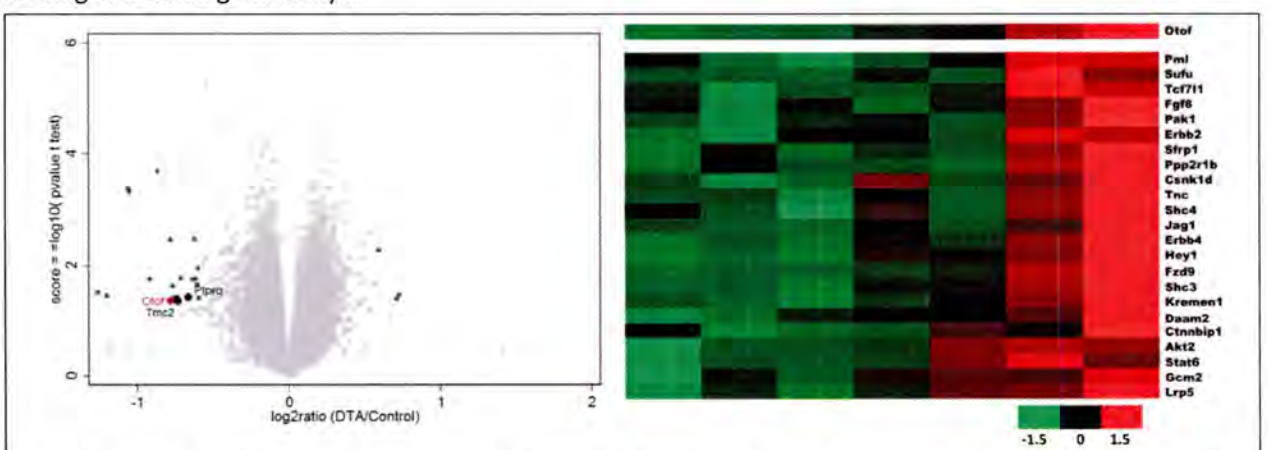

Figure 9. Gene changes at P2 after HC damage in the neonatal mouse cochlea. Left, Volcano plot of gene expression array data comparing Atoh1DTA and control cochlea. The dark grey, black, and red dots represent statistically significant genes that had a 1.5 fold change (p<0.05). In red Otof = Otoferlin. In black are the 2 other known HC genes. **Right,** Data from Atoh1DTA and control samples were correlated using a Pearson's linear correlation to Otoferlin expression to look for candidate co-regulated genes with this known marker. Genes in the Notch and Wnt pathways are listed. Each column is an individual sample and colors are the Z score.

To investigate the Notch signaling pathway during spontaneous HC regeneration, we performed real-time qPCR with whole cochlear samples obtained from Atoh1DTA mice. Controls without HC damage were obtained from littermates that lacked either the Cre or DTA allele. Using SYBR green and the ΔΔCt method of analysis, we measured changes in expression of Notch ligands (Delta1 (DLL1) and Jagged2 (Jag2)), the Notch receptor (Notch1), and Notch target genes (Hey1, HeyL, Hes1, and Hes5) at P2 and P4 (Figure 10). Decreased expression of the HC-specific gene Pou4f3 confirmed HC loss in Atoh1DTA (damaged) samples. There was a significant reduction in the

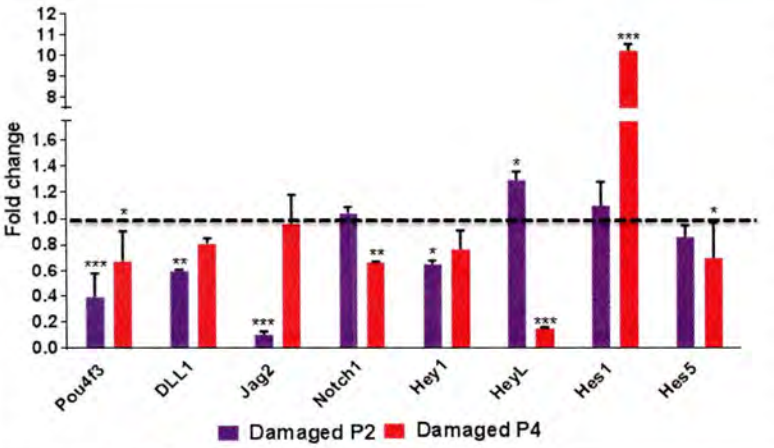

Figure 10: Decreased expression of genes in the Notch pathway after HC damage. Relative mRNA expression of genes in the Notch pathway was analyzed in whole cochlear samples from undamaged (control) and HC damaged (Atoh1DTA) mice at P2 and P4 using real-time qPCR. The HC-specific gene Pou4f3 was analyzed to confirm HC loss in damaged samples. Rpl19 was used as a housekeeping gene and samples are expressed as fold change compared to age-matched control samples (dashed line). (*p<0.05, **p <0.01, ***p<0.001 as determined by a two-way ANOVA with a Bonferroni post-hoc test) N=2-3.

expression of DLL1, Jag2, and Hey1 in the damaged cochlea at P2, and in Notch1, HeyL, and Hes5 at P4. There was also an increase in HeyL expression at P2, as well an increase in Hes1 at P4. These results suggest that regulation
of the Notch signaling pathway during the HC regeneration process is more complex than just downregulation.

We also used immunostaining to investigate the SC-specific ligand, Jagged1 (Jag1) in the cochlea of Atoh1DTA mice. In control samples Jag1 was expressed in the membranes of most SC subtypes (Figure 11A-F). However in Atoh1DTA (HC damaged) mice at both P2 and P4, Jag1 expression was lost in the vast majority of Deiter's cells, yet retained in pillar cells, inner phalangeal cells, and the GER through P4. (Figure 11G-L). This data demonstrates that different SC subtypes vary in their capacity to downregulate genes in the

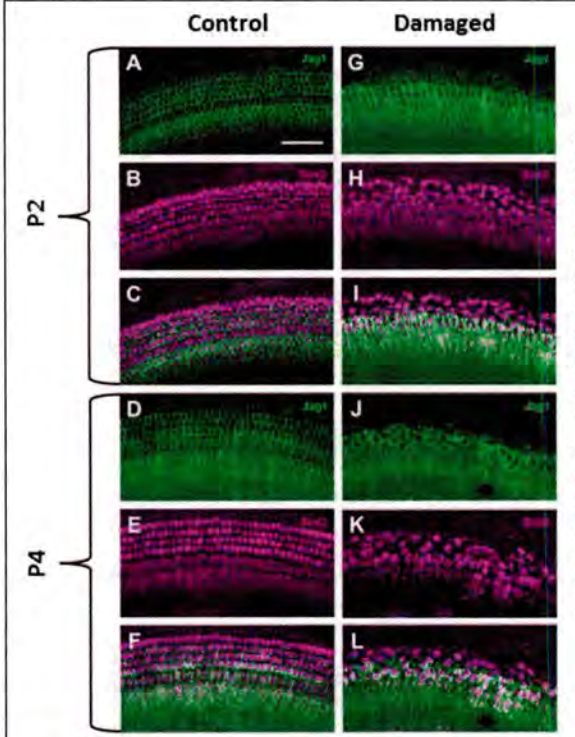

Figure 11: Decreased expression of Jag1 after HC damage in the neonatal mouse cochlea. Confocal images of Jag1 (green) and Sox2 (magenta) expression in control (**A-F**) and Atoh1DTA (damaged) mice (**G-L**) at P2 and P4. Scale bar = 50 µm

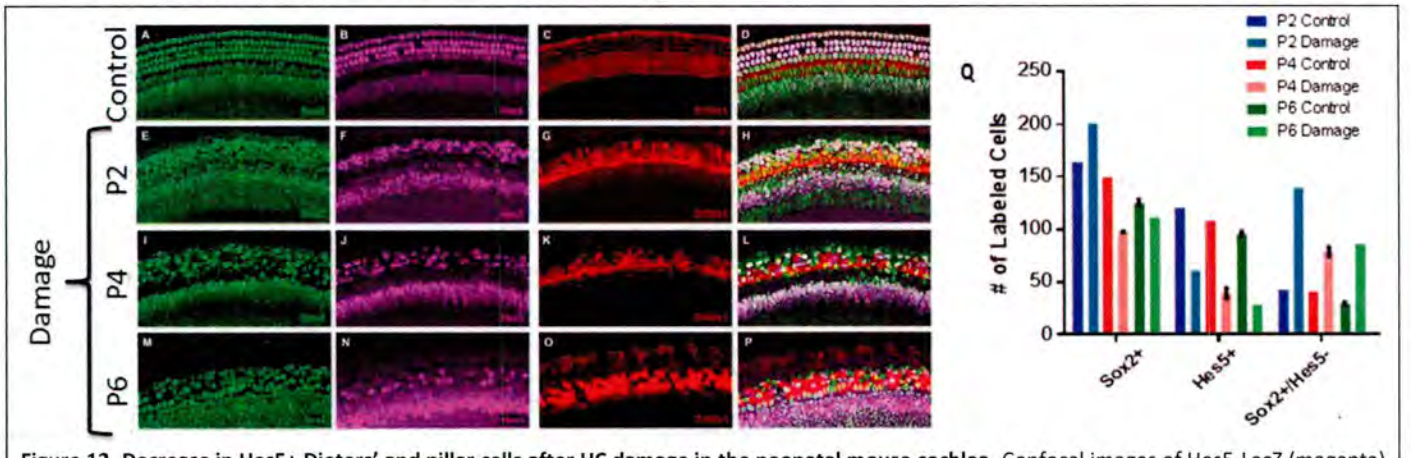

Figure 12. Decrease in Hes5+ Dieters' and pillar cells after HC damage in the neonatal mouse cochlea. Confocal images of Hes5-LacZ (magenta) and Sox2 (green) expression in control (**A-D**) and Atoh1DTA::Hes5-nlsLacZ (damaged) mice at P2 (**C-H**), P4 (**I-L**), and P6 (**M-P**). S100a1 (red) labeling was used to mark Deiter's and pillar cells. **Q**, Quantification of Hes5+, Sox2+, and Sox2+/Hes5-negative cells in 150 µm regions of the apical turn (N =1-2).

Notch signaling pathway after HC damage which may also suggest that different SC subtypes vary in their ability to form regenerated HCs.

We also measured changes in expression of the Notch target gene Hes5 at the cellular level. The Hes5-nlsLacZ mouse line can also be used as a reporter of Hes5 expression since the LacZ gene was knocked into the Hes5 locus and is controlled by the endogenous Hes5 promoter (Imayoshi et al., 2010). We used Sox2 to label all SC subtypes and S100a1 to label Deiter's and pillar cells. Cells expressing Hes5 and or Sox2 were quantified within the band of S100a1 labeling. There was a decrease in the number of Hes5+ cells at P2, P4, and P6 in Atoh1DTA::Hes5-nlsLacZ$^{+/-}$ (HC damaged) mice compared to control (Figure 12). To confirm that this decrease in Hes5+ cells was not caused by a loss of Deiter's and pillar cells, we quantified the number of these cells using Sox2 in the same region. At P2 there was an increase in the number of Sox2+ cells, followed by a small decrease at P4 and P6 (Figure 12). We also observed an increase in the number Deiter's and pillar cells that were Sox2+ but Hes5-negative in Atoh1DTA::Hes5-nlsLacZ$^{+/-}$ (damaged) mice compared to control (Figure 12). Taken together these data suggest that the Deiter's and pillar cells are still present, but have just lost Notch signaling. We predict this is the first step needed for SCs to convert into HCs.

VI. Work Plan

Not applicable.

VII. Major Problems if any

Funding was not started until April 2013 thus the grant period was only 2.3 years and not all components of the proposal were completed. We also experienced technical difficulties in the mouse genetic strategy proposed for Aim 1 as described in sections IV and V. However we have overcome these problem and will complete Aim 1 in 2016.

VIII. Technology Transfer

Data from this ONR award was used to apply for, and successfully obtain, a 3 year grant from the Department of Defense's Congressionally Directed Medical Research Program (CDMRP) under the Neurosensory and Rehabilitation Research Award. Grant #W81XWH-15-1-0475 entitled "Investigation of Notch signaling in during spontaneous regeneration of cochlear hair cells" will fund the Cox lab from 9/15/2015 – 9/14/2018.

IX. Foreign Collaborations and Supported Foreign Nationals

NA

X. Productivity

Peer-reviewed journal articles

Cox BC*, Chai R*, Lenoir A, Liu Z, Zhang L, Nguyen D, Chalasani K, Steigelman KA, Fang J, Rubel EW, Cheng AG, and Zuo J. (2014) Spontaneous hair cell regeneration in the neonatal mouse cochlea in vivo. *Development* 141:816-829. (Published)
*authors contributed equally

Cox, BC, Dearman JA, Brancheck J, Zindy F, Roussel MF, and Zuo J. (2014) Generation of Atoh1-rtTA transgenic mice: a tool for inducible gene expression in hair cells of the inner ear. *Sci Rep* 4:6885. (Published)

Brancheck J*, McGovern MM*, Grant AC, Graves-Ramsey KA, and Cox BC (submitted) Quantitative Analysis of Supporting Cell Subtype Specificity among CreER Lines in the Neonatal Mouse Cochlea. J *Ass Res Otolaryngol* (to be submitted by 12/31/2015)

Workshops & Conferences

Brancheck J and Cox BC. (2014) Using Cre-loxP Mouse Genetics to Target Specific Cochlear Supporting Cell Subtypes. *Association for Research in Otolaryngology: 37th annual midwinter research meeting,* 2014 February 2-26, San Diego, CA, #PS-351 (poster presentation)

Randle M, Zuo J, and Cox BC. (2014) Ablation of Different Quantities of Hair Cells in the Neonatal Mouse Cochlea to Examine Mechanisms of Regeneration. *Association for Research in Otolaryngology: 37th annual midwinter research meeting,* 2014 February 2-26, San Diego, CA, #PS-192 (poster presentation)

Trone, MM, Karmarkar, SW, Cox, BC (2015) Changes in the Notch Signaling Pathway during Spontaneous Hair Cell Regeneration in the Neonatal Mouse Cochlea. *Association for Research in Otolyrangology: 38th annual midwinter meeting*, 2015 February 21-25, Baltimore, MD (poster presentation)

Trone, MM, Karmarkar, SW, and Cox, BC. (2015) Dynamic changes in the Notch signaling pathway after hair cell ablation in the neonatal mouse cochlea. *Joint meeting of the Midwest Auditory Research Conference and the Midwest Auditory Neuroscience Symposium*. July 23-25, 2014, Omaha, NE (oral presentation)

Trone, MM, Brancheck J, Grant AC, Graves-Ramsey K, and, Cox, BC. (2015) Using Cre-loxP mouse genetics to target specific cochlear supporting cell subtypes. *Joint meeting of the Midwest Auditory Research Conference and the Midwest Auditory Neuroscience Symposium*. July 23-25, 2014, Omaha, NE (poster presentation)

Cox BC (2013) Spontaneous hair cell regeneration in the neonatal mouse cochlea and utricle in vivo. *Iowa Center for Molecular Auditory Neuroscience Symposium*, 2013 October 17, *University of Iowa, Iowa City (*Keynote speaker)

Cox, BC. Using mouse genetic models to investigate the mechanism of spontaneous hair cell regeneration in the neonatal mouse cochlea. *Department of Pharmacology & Physiology, Georgetown University*. November 20, 2014, Washington, DC. (seminar presentation)

Cox, BC. Using mouse genetic models to investigate the mechanism of spontaneous hair cell regeneration in the neonatal mouse cochlea. *Department of Physiology, Southern Illinois University Carbondale*. October 3, 2014, Carbondale, IL. (seminar presentation)

XI. Award Participants

Brandon C. Cox, PI	June 2013 - September 2014 @ 33% salary support October 2014 - September 2015 @ 28% salary support
Joe Brancheck, Technician	June 2013 - May 2014 @ 100% salary support
Sumedha Karmarkar, Postdoc	September 2013 – June 2014 – no salary support
Melissa McGovern-Trone, graduate student	June 2014 – September 2015 – no salary support
Kaley Ramsey, Technician	August 2014 - September 2015 @ 100% salary support

Cell Source and Mechanism of Hair Cell Regeneration in the Neonatal Mouse Cochlea

Brandon Cox, Southern Illinois University School of Medicine

Objective:

- Aim 1: To determine the cell source of regenerated hair cells in the neonatal mouse cochlea.
- Aim 2: To determine the molecular mechanism of spontaneous hair cell regeneration in the neonatal mouse cochlea.

Approach:

- Fate-map supporting cells and individual supporting cell subtypes during the hair cell regeneration process using mouse genetics.
- Perform gene expression arrays during the hair cell regeneration process and confirm these changes using real time PCR and immunohistochemistry.

Accomplishments:

- Published 2 papers related to Aim 1 and a 3rd paper was submitted for publication.
- Using data from Aim 2, successfully obtained a 3 year grant from DOD
- Demonstrated that supporting cells are the source of regenerated hair cells in the neonatal mouse cochlea.
- Validated the results of the gene expression arrays to show that changes in the Notch signaling pathway occur after hair cell damage.

Impact:

- The first evidence that hair cell regeneration can occur in mammals & that regenerated hair cells are derived from neighboring supporting cells.
- The Atoh1-rtTA mouse line is the first to specifically target hair cells using the tetracycline inducible system & provides a new tool for the field.

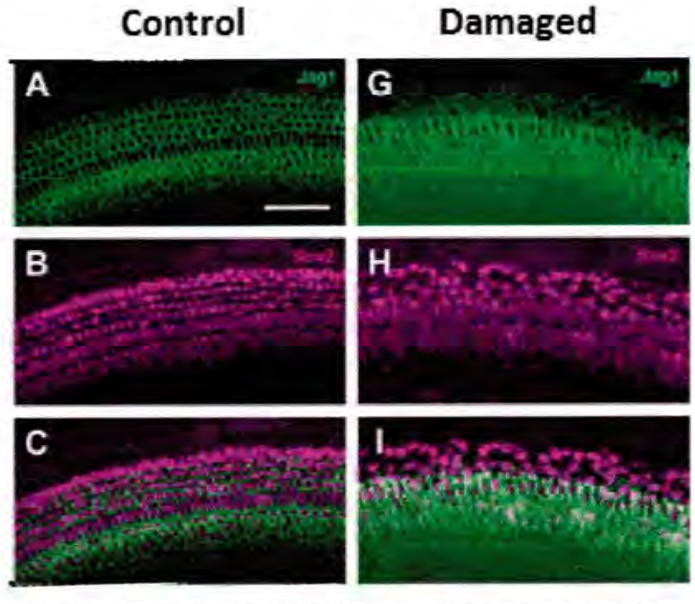

In the cochlea of Atoh1DTA (HC damaged) mice, there was a reduction in the expression of the Notch ligand Jagged1 (green) in the Deiter's cell region while many Sox2+ (magenta) Deiter's cells remain. Jagged1 expression appears to be maintained in pillar cells, interphalangeal cells, and cells in the greater epithelial ridge (GER) through postnatal day 4. Scale bar = 50 µm.

© 2014. Published by The Company of Biologists Ltd | Development (2014) 141, 1599 doi:10.1242/dev.109421

CORRECTION

Spontaneous hair cell regeneration in the neonatal mouse cochlea *in vivo*

Brandon C. Cox[1,2,*], Renjie Chai[3,4,*], Anne Lenoir[1,5], Zhiyong Liu[1,6], LingLi Zhang[1], Duc-Huy Nguyen[3], Kavita Chalasani[3], Katherine A. Steigelman[1,6], Jie Fang[1], Edwin W. Rubel[7], Alan G. Cheng[3,‡] and Jian Zuo[1,‡]

[1]Department of Developmental Neurobiology, St. Jude Children's Research Hospital, Memphis, TN 38105, USA. [2]Department of Pharmacology, Southern Illinois University School of Medicine, Springfield, IL 62702, USA. [3]Department of Otolaryngology-Head and Neck Surgery, Stanford University School of Medicine, Stanford, CA 94305, USA. [4]Key Laboratory for Developmental Genes and Human Disease, Ministry of Education, Institute of Life Sciences, Southeast University, Nanjing 210096, China. [5]Universite Paris-Diderot, UFR Sciences du vivant, Paris 7, Paris, France. [6]Department of Anatomy and Neurobiology, University of Tennessee Health Science Center, Memphis, TN 38163, USA. [7]Virginia Merrill Bloedel Hearing Research Center, Department of Otolaryngology-Head and Neck Surgery, University of Washington School of Medicine, Seattle, WA, 98195-7923, USA.
*These authors contributed equally to this work

‡Authors for correspondence (aglcheng@stanford.edu; jian.zuo@stjude.org)

There was an error published in *Development* **141**, 816-829.

Edwin W. Rubel was omitted from the authorship of the paper. The correct author list and affiliations appears above.

In addition the Acknowledgements and Author contributions sections should read as follows.

Acknowledgements
We thank L. Tong and R. Palmiter (University of Washington) for Pou4f3DTR/+ mice and discussion; S. Baker (St. Jude) for Atoh1-CreERTM mice and discussion; R. Kageyama (Kyoto University) for Hes5-nlsLacZ mice; P. Chambon (Institut Genetique Biologie Moleculaire Cellulaire) for the CreERT2 construct; S. Heller (Stanford University) for the anti-espin antibody and critical reading, J. Corwin, J. Burns and other members of the Corwin laboratory (University of Virginia) as well as members of our laboratories for discussion and critical comments; S. Connell, V. Frohlich, Y. Ouyang and J. Peters (St. Jude) for expertise in confocal imaging; A. Xue, V. Nookala, N. Pham, A. Vu, G. Huang and W. Liu (Stanford University) for excellent technical support; and L. Boykins (University of Memphis), R. Martens and J. Goodwin (University of Alabama) for assistance and expertise in scanning electron microscopy.

Author contributions
B.C.C., R.C., E.W.R., A.G.C. and J.Z. developed the concepts or approach; B.C.C., R.C., A.L., Z.L., L.Z., D.-H.N., K.C., K.A.S., J.F., A.G.C. and J.Z. performed experiments or data analysis; B.C.C., R.C., A.G.C. and J.Z. prepared or edited the manuscript prior to submission.

The authors apologise to readers for this mistake

© 2014. Published by The Company of Biologists Ltd | Development (2014) 141, 816-829 doi:10.1242/dev.103036

RESEARCH ARTICLE

STEM CELLS AND REGENERATION

Spontaneous hair cell regeneration in the neonatal mouse cochlea *in vivo*

Brandon C. Cox[1,2,*], Renjie Chai[3,4,*], Anne Lenoir[1,5], Zhiyong Liu[1,6], LingLi Zhang[1], Duc-Huy Nguyen[3], Kavita Chalasani[3], Katherine A. Steigelman[1,6], Jie Fang[1], Alan G. Cheng[3,‡] and Jian Zuo[1,‡]

ABSTRACT

Loss of cochlear hair cells in mammals is currently believed to be permanent, resulting in hearing impairment that affects more than 10% of the population. Here, we developed two genetic strategies to ablate neonatal mouse cochlear hair cells *in vivo*. Both *Pou4f3*$^{DTR/+}$ and *Atoh1-CreER*^{TM}*; ROSA26*$^{DTA/+}$ alleles allowed selective and inducible hair cell ablation. After hair cell loss was induced at birth, we observed spontaneous regeneration of hair cells. Fate-mapping experiments demonstrated that neighboring supporting cells acquired a hair cell fate, which increased in a basal to apical gradient, averaging over 120 regenerated hair cells per cochlea. The normally mitotically quiescent supporting cells proliferated after hair cell ablation. Concurrent fate mapping and labeling with mitotic tracers showed that regenerated hair cells were derived by both mitotic regeneration and direct transdifferentiation. Over time, regenerated hair cells followed a similar pattern of maturation to normal hair cell development, including the expression of prestin, a terminal differentiation marker of outer hair cells, although many new hair cells eventually died. Hair cell regeneration did not occur when ablation was induced at one week of age. Our findings demonstrate that the neonatal mouse cochlea is capable of spontaneous hair cell regeneration after damage *in vivo*. Thus, future studies on the neonatal cochlea might shed light on the competence of supporting cells to regenerate hair cells and on the factors that promote the survival of newly regenerated hair cells.

KEY WORDS: Lgr5, Direct transdifferentiation, Mitotic regeneration, Diphtheria toxin, Atoh1, Fate mapping

INTRODUCTION

Hair cells (HCs) regenerate in both the auditory and vestibular systems of non-mammalian vertebrates, leading to restoration of hearing and balance (Balak et al., 1990; Corwin and Cotanche, 1988; Lombarte et al., 1993; Ryals and Rubel, 1988). This process occurs by two mechanisms: direct transdifferentiation and mitotic regeneration. Direct transdifferentiation refers to a cell fate change when neighboring supporting cells (SCs) convert into HCs without cell division. Mitotic regeneration occurs when a SC first divides and, subsequently, one or both daughter cells becomes a HC (Adler and Raphael, 1996; Baird et al., 1996; Corwin and Cotanche, 1988; Jones and Corwin, 1996; Ryals and Rubel, 1988; Warchol and Corwin, 1996).

In mammals, limited HC regeneration occurs in the vestibular system (Burns et al., 2012; Forge et al., 1993; Golub et al., 2012; Kawamoto et al., 2009; Warchol et al., 1993), yet no spontaneous regeneration has been observed in the mature auditory system (Bohne et al., 1976; Hawkins et al., 1976; Oesterle et al., 2008). Recent studies demonstrate that SCs isolated from the neonatal cochlea are competent to form new HCs in culture (Chai et al., 2012; Doetzlhofer et al., 2006; Oshima et al., 2007; Savary et al., 2007; Shi et al., 2012; Sinkkonen et al., 2011; White et al., 2006). In addition, neonatal SCs can be induced to generate supernumerary HCs upon inhibition of the Notch pathway (Doetzlhofer et al., 2009; Yamamoto et al., 2006), ectopic expression of Atoh1 (Kelly et al., 2012; Liu et al., 2012a; Zheng and Gao, 2000) or overexpression of β-catenin (Shi et al., 2013). Similar manipulations failed to coerce a HC fate in the undamaged, adult cochlea, suggesting that the neonatal cochlea is a more permissive environment for the formation of new HCs.

To investigate possible HC regeneration in the embryonic cochlea, Kelley and colleagues laser ablated HCs in cultured explants and found rare regenerated HCs (Kelley et al., 1995). Whether the postnatal cochlea can regenerate lost HCs and the source of potential regenerated cells have not been clearly defined, in part because HCs in the neonatal cochlea are insensitive to damage *in vivo*. Aminoglycoside antibiotics are widely used to damage HCs *in vitro* but preferentially inflict damage in the basal turn and are ineffective *in vivo*.

Here, we present two strategies to kill neonatal HCs *in vivo* using mouse genetics. After HC death was induced at birth, fate-mapping studies showed that SCs acquire a HC fate. We also observed mitotic regeneration, with regenerated cells expressing five markers of HCs and exhibiting immature stereocilia bundles, although most new HCs failed to survive. In addition, we defined the time period when HC regeneration can occur, finding it to be limited to the first postnatal week. Together, these findings demonstrate that neonatal SCs have the intrinsic capacity to regenerate HCs after damage.

RESULTS

Hair cell ablation in the neonatal cochlea

The neonatal cochlea is resistant to HC damage caused by exposure to noise or ototoxic drugs *in vivo*. To circumvent this limitation, we developed two genetic methods to damage neonatal HCs *in vivo*. First, we used a knock-in mouse in which expression of the human diphtheria toxin receptor (DTR) is driven by the *Pou4f3* promoter (*Pou4f3*$^{DTR/+}$) (Golub et al., 2012; Mahrt et al., 2013; Tong et al., 2011) and selective HC death is induced by injection of diphtheria toxin (DT), as *Pou4f3* is exclusively expressed by HCs in the inner

[1]Department of Developmental Neurobiology, St. Jude Children's Research Hospital, Memphis, TN 38105, USA. [2]Department of Pharmacology, Southern Illinois University School of Medicine, Springfield, IL 62702, USA. [3]Department of Otolaryngology-Head and Neck Surgery, Stanford University School of Medicine, Stanford, CA 94305, USA. [4]Key Laboratory for Developmental Genes and Human Disease, Ministry of Education, Institute of Life Sciences, Southeast University, Nanjing 210096, China. [5]Universite Paris-Diderot, UFR Sciences du vivant, Paris 7, Paris, France. [6]Department of Anatomy and Neurobiology, University of Tennessee Health Science Center, Memphis, TN 38163, USA.
*These authors contributed equally to this work

‡Authors for correspondence (aglcheng@stanford.edu; jian.zuo@stjude.org)

Received 23 August 2013; Accepted 20 November 2013

Development (2014) doi:10.1242/dev.103036

ear (Erkman et al., 1996; Xiang et al., 1998). Progressive HC death was observed in *Pou4f3*$^{DTR/+}$ mice after DT injection at P1 (Fig. 1), consistent with previous reports (Golub et al., 2012; Mahrt et al., 2013; Tong et al., 2011).

Second, we used a HC-specific inducible Cre line, *Atoh1-CreER*^{TM}, to drive expression of diphtheria toxin fragment A (DTA). When tamoxifen was administrated at postnatal day (P) 0 and P1, Cre recombinase was activated in ~80-90% of HCs (Chow et al., 2006; Weber et al., 2008). In other organ systems, Cre-mediated excision of the floxed stop sequence in the *ROSA26-loxP-stop-loxP-DTA* (*ROSA26*^{DTA}) allele causes cell-autonomous ablation of Cre$^+$ cells (Abrahamsen et al., 2008; Ivanova et al., 2005). Beginning 2 days after tamoxifen administration, *Atoh1-CreER*^{TM}; *ROSA26*$^{DTA/+}$ (*Atoh1DTA*) mice show rapid and reproducible loss of both inner and outer HCs (Fig. 2A-O). There is also considerable disorganization in the organ of Corti, with Sox2$^+$ nuclei detected in the HC layer (Fig. 2P,Q).

Supporting cells acquire a hair cell fate

To determine how SCs respond to HC damage induced at birth and whether they could acquire a HC fate, we generated *Pou4f3*$^{DTR/+}$; *Lgr5*$^{CreER/+}$; *ROSA26*$^{CAG\text{-}tdTomato/+}$ transgenic mice. This strategy was designed to fate map SCs using the *Lgr5-EGFP-IRES-CreER*^{T2} allele (*Lgr5*^{CreER}) (Barker et al., 2007) and the *ROSA26*$^{CAG\text{-}tdTomato}$ reporter line (Madisen et al., 2010) after HC ablation. Lgr5 is expressed in a subset of SCs, so when control animals (*Pou4f3*$^{+/+}$; *Lgr5*$^{CreER/+}$; *ROSA26*$^{CAG\text{-}tdTomato/+}$ mice) were given tamoxifen at P1, tdTomato expression was detected at P7 in several SC subtypes, including cells in the greater epithelial ridge (GER). Specifically, tdTomato expression was detected in Deiters' cells (first row, 4.0±1.8%; second row, 5.0±0.3%; third row, 98.3±0.4%), pillar cells (outer pillar, 3.7±2.0%; inner pillar, 67.0±1.6%) and inner phalangeal/border cells (87.3±0.8%) (n=3). Also, we detected occasional tdTomato+/Myosin VIIa+ (Myo7a+) cells at P7 (apex, 12±1.5; middle, 2±0.7; base, 0.5±0.3; n=4; Fig. 3A,H-J; supplementary material Table S2A). These results are consistent with the previous report (Chai et al., 2012). Lgr5 expression decreased and remained limited to SCs in *Pou4f3*$^{DTR/+}$; *Lgr5*$^{CreER/+}$ mice 8, 24 and 48 hours after DT injection at P1 (supplementary material Fig. S1).

In *Pou4f3*$^{DTR/+}$; *Lgr5*$^{CreER/+}$; *ROSA26*$^{CAG\text{-}tdTomato/+}$ mice, tamoxifen was given at P1 to label Lgr5$^+$ SCs and DT ~8 hours later to kill HCs. At P7, we found a significant increase of tdTomato$^+$/Myo7a$^+$ cells in all three cochlear turns, with a nearly 10-fold increase in the apical and middle turns and a 5-fold increase in the basal turn (apex, 99.0±4.6; middle, 22.8±6.5; base, 2.3±0.9; n=4; Fig. 3B,H-J; supplementary material Table S2A) compared with undamaged controls lacking the *Pou4f3*$^{DTR/+}$ allele (P<0.001 for apical and middle turns and P<0.05 for base). In this experiment, we also stained for Sox2, which is transiently expressed in nascent HCs in the embryonic cochlea (Dabdoub et al., 2008; Hume et al., 2007; Kiernan et al., 2005; Mak et al., 2009) and becomes restricted to SCs after P1 (Hume et al., 2007; Oesterle et al., 2008). In addition, Myo7a$^+$ cells that formed from isolated SCs *in vitro* expressed Sox2 (Sinkkonen et al., 2011). Therefore, Sox2 and Myo7a co-expression can be viewed as a marker of immature HCs. After HC ablation, we found many Myo7a$^+$/Sox2$^+$ cells and Myo7a$^+$/Sox2$^+$/tdTomato$^+$ cells in the apical and middle turns of *Pou4f3*$^{DTR/+}$; *Lgr5*$^{CreER/+}$; *ROSA26*$^{CAG\text{-}tdTomato/+}$ mice at P7 (Fig. 3C-J; supplementary material Table S2A), whereas neither were observed in control samples lacking the *Pou4f3*$^{DTR/+}$ allele (n=4). In summary, these findings demonstrate that newly regenerated Myo7a$^+$ cells are derived from adjacent SCs after HC ablation in the neonatal mouse cochlea. This regenerative capacity was most robust in the apex and decreased towards the base.

Similarly, we performed fate-mapping studies of SCs in the *Atoh1DTA* model. Although fate mapping is primarily performed using the Cre/loxP system, we were already using this system to kill HCs and thus needed another mouse genetic tool to trace SCs (Stern

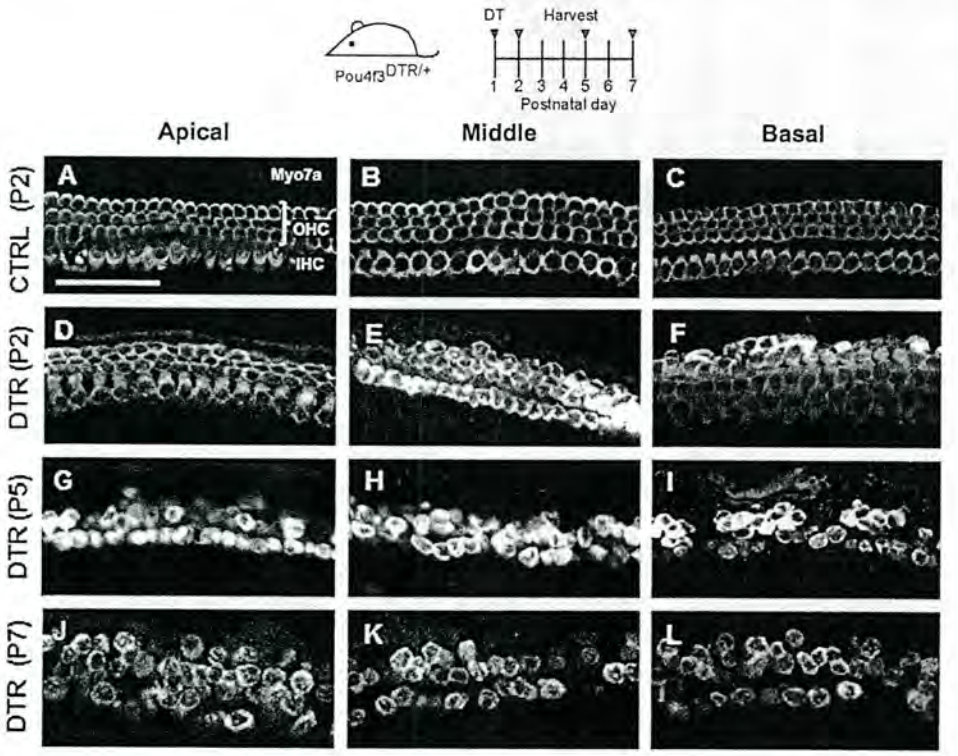

Fig. 1. Progressive HC death in the *Pou4f3*$^{DTR/+}$ model. Projection images of Myo7a immunofluorescence in cochlear whole-mounts of control wild-type mice at P2 (A-C) and *Pou4f3*$^{DTR/+}$ mice at P2 (D-F), P5 (G-I) and P7 (J-L) after diphtheria toxin (DT) injection at P1. Repopulation of HCs was most robust in the apical turn at P7 (J). OHC, outer hair cells; IHC, inner hair cells. Scale bar: 50 μm.

Development (2014) doi:10.1242/dev.103036

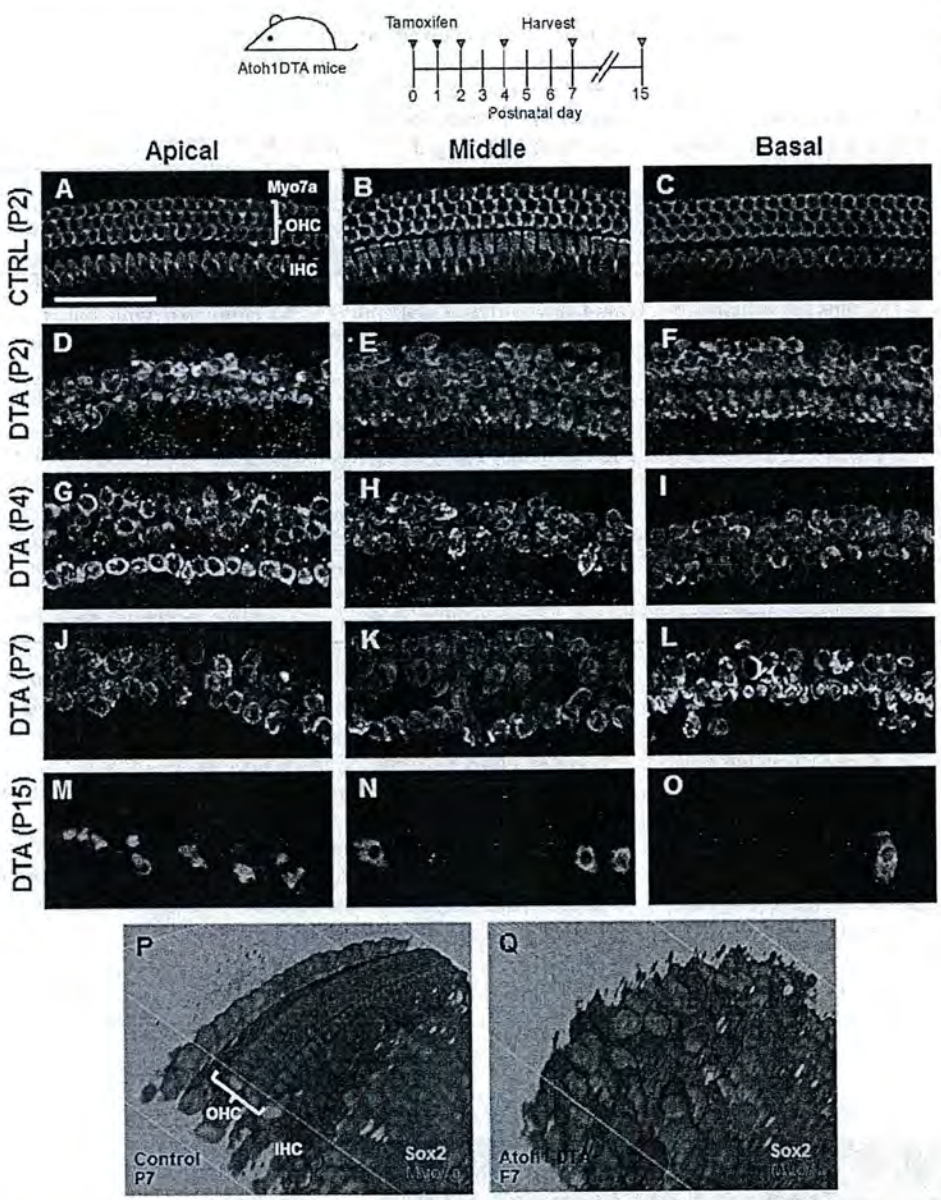

Fig. 2. Progressive HC death in the *Atoh1DTA* model. (A-O) Projection images of Myo7a immunofluorescence in cochlear whole-mounts from control mice (lacking either the *Cre* or *DTA* allele) at P2 (A-C) and *Atoh1DTA* mice at P2 (D-F), P4 (G-I), P7 (J-L) and P15 (M-O). Repopulation of HCs was most robust in the apical turn at P4 (G). (P,Q) 3D reconstruction of confocal *z*-stack images with SC nuclei labeled by Sox2 (green) and HCs labeled by Myo7a (magenta) in the middle turn of control (P) and *Atoh1DTA* (Q) cochleae at P7. Scale bar: 50 µm.

and Fraser, 2001). Since Hes5 is expressed in SCs of the postnatal cochlea (Hartman et al., 2009; Lanford et al., 2000; Li et al., 2008; Zine et al., 2001), we characterized a recently generated *Hes5-nlsLacZ* knock-in allele (Imayoshi et al., 2010). *lacZ* was strongly expressed throughout the P1 cochlea (Fig. 4A,B) and robustly labeled Deiters' cells and outer pillar cells, with mosaic weak labeling of inner phalangeal cells/border cells (Fig. 4C-H). *lacZ* expression was not detected in inner pillar cells or HCs. For fate mapping, we generated *Atoh1DTA; Hes5-nlsLacZ*$^{+/-}$ mice. After tamoxifen injection at P0/P1, we first observed Myo7a^{+}/*lacZ*$^{+}$ cells at P2 (Fig. 4I-L) in an apical-basal gradient (apex, 58.3±30.2; middle, 9.3±7.9; base, 1.3±1.3; n=3), whereas no *lccZ*$^{+}$ HCs were found in control samples that were lacking either the *Cre* or *DTA* allele (Fig. 4M; supplementary material Table S1B) (n=3) or at P1 in experimental or control cochleae (n=3). This finding is consistent with the fate-mapping experiments performed in the *Pou4f3*$^{DTR/+}$ model indicating that SCs have changed cell fate and differentiated into Myo7a^{+} cells *in vivo*.

Hair cell damage stimulates proliferation

Since mitotic HC regeneration has been described in non-mammalian vertebrates, we investigated whether cell division can occur after HC damage in the neonatal mouse cochlea. When the mitotic tracer 5-ethynyl-2′-deoxyuridine (EdU) was administered once per day from P3-P5 to control mice lacking the *Pou4f3*$^{DTR/+}$ allele (and DT given at P1), no EdU^{+} cells were observed in the organ of Corti at P7 (n=4), confirming previous findings that postnatal HCs and SCs are mitotically quiescent (Lee et al., 2006; Ruben, 1967). In *Pou4f3*$^{DTR/+}$ mice identically treated with DT and EdU, EdU^{+}/Sox2^{+} cells were observed in the P7 organ of Corti (apex, 13.2±3.7 cells per 225 µm cochlear length; middle, 5.8±1.6; base, 3.5±1.5; n=6; Fig. 5A-C; supplementary material Table S2C). We also observed EdU^{+}/Myo7a^{+} cells restricted to the apical turn, averaging 11.0±1.8 in this whole region (n=6) and suggesting mitotic HC regeneration (Fig. 5D-F; supplementary material Table S2C). Moreover, some cells that were double positive for EdU and Myo7a also had Sox2^{+} nuclei (4.7±1.3, n=6; Fig. 5G-I;

Development (2014) doi:10.1242/dev.103036

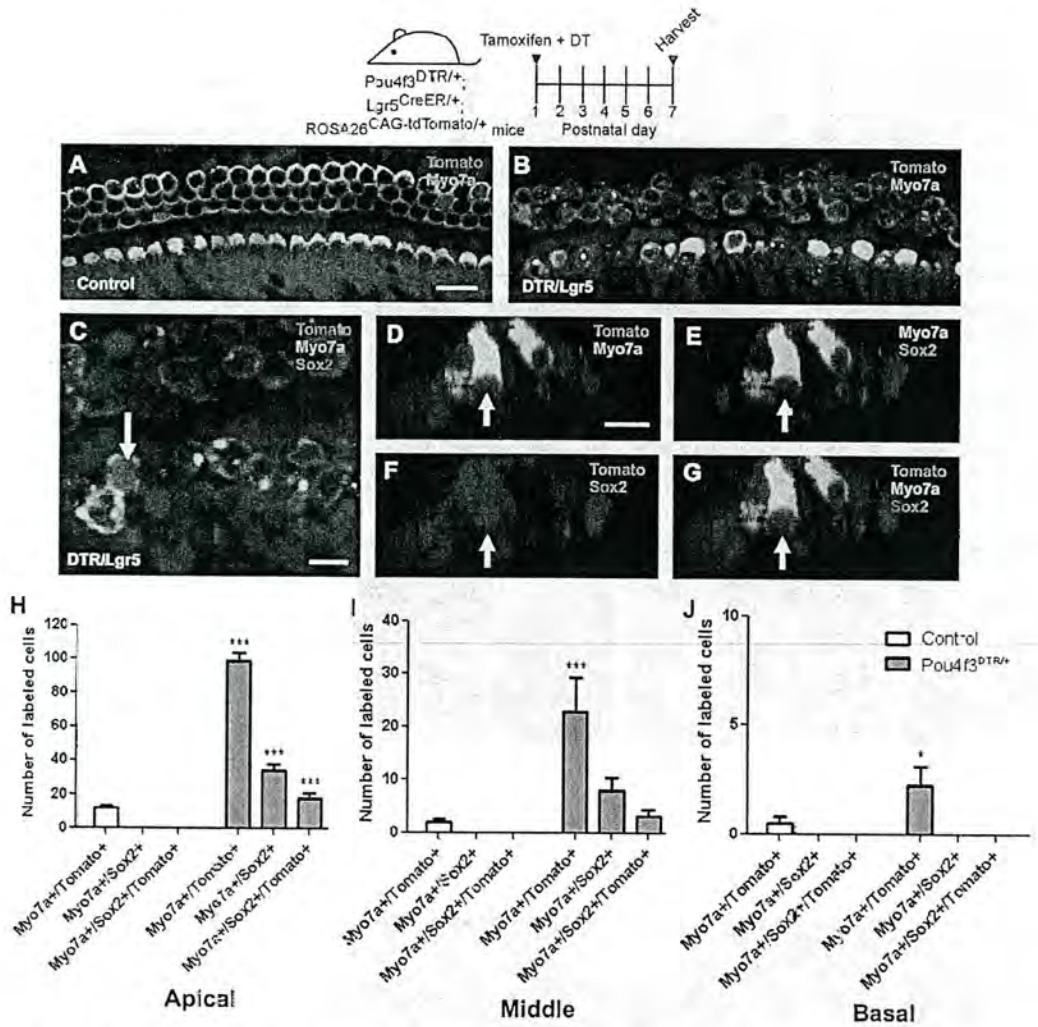

Fig. 3. Fate mapping of SCs in the *Pou4f3*$^{DTR/+}$ model. Confocal images of tdTomato$^+$ (magenta) HCs (Myo7a, green) in the apical cochlear turn of control (*Lgr5*$^{CreER/+}$; *ROSA26*$^{CAG\text{-}tdTomato/+}$) (A) and *Pou4f3*$^{DTR/+}$; *Lgr5*$^{CreER/+}$; *ROSA26*$^{CAG\text{-}tdTomato/+}$ (B) mice at P7. (C) Confocal image of tdTomato$^+$/Myo7a$^+$ HCs that also express Sox2 (blue) in the apical turn of *Pou4f3*$^{DTR/+}$; *Lgr5*$^{CreER/-}$; *ROSA26*$^{CAG\text{-}tdTomato/+}$ mice at P7. (D-G) Cross-section focused on the tdTomato$^+$/Sox2$^+$ HC indicated by the arrow in C. Note that GFP expression from the *Lgr5*$^{CreER/+}$ allele is much weaker than Sox2 labeling. Number of double (Myo7a$^+$/tdTomato$^+$ or Myo7a$^+$/Sox2$^+$) or triple (Myo7a$^+$/Sox2$^+$/tdTomato$^+$) labeled cells in the apical (H), middle (I) and basal (J) turns of *Pou4f3*$^{DTR/+}$; *Lgr5*$^{CreER/+}$; *ROSA26*$^{CAG\text{-}tdTomato/+}$ mice and control littermates. Data are expressed as mean ± s.e.m., n=3. *P<0.05, ***P<0.001 compared with control number of the corresponding turn as determined by a two-way ANOVA followed by a Student's t-test with a Bonferroni correction. Scale bars: A,B, 20 µm; C-G, 10 µm.

supplementary material Table S2C) suggesting that they were immature, regenerated HCs.

In parallel, we probed for proliferative cells after HC loss in *Atoh1DTA* mice by injecting EdU once at ages ranging from P2 to P5. Cochlear tissues were analyzed 24 hours after each injection when one round of cell division was presumably complete. Similar to the results obtained with *Pou4f3*$^{DTR/+}$ mice, this regimen also yielded no EdU$^+$ cells in the organ of Corti from control mice that lacked either the *Cre* or *DTA* allele (n=3). By contrast, EdU$^+$/Sox2$^+$ cells were found at the SC nuclear level in the damaged organ of Corti in all three turns between P2 and P5 (Fig. 5J,K; supplementary material Table S2D). In addition, we observed EdU$^-$/Myo7a$^-$ cells in the apical turn only from P2-P5 (P2, 2.0±2.0; P3, 3.3±0.9; P4, 3.7±2.3; P5, 1.0±0.6; Fig. 5L,M; supplementary material Table S2D; n=3). EdU$^+$/Myo7a$^+$ cells were found at the lumenal surface of the sensory epithelium where HCs normally reside (Fig. 5N,O). As in the *Pou4f3*$^{DTR/+}$ model, we also detected EdU$^+$/Myo7a$^+$/Sox2$^+$ cells (Fig. 5P-R). These data show that HC ablation results in proliferation in the normally mitotically quiescent organ of Corti in both the *Pou4f3*$^{DTR/+}$ and *Atoh1DTA* models. The majority of proliferation and all EdU$^+$/Myo7a$^+$ cells were observed in the apical turn, where the progression of cell cycle arrest first occurs (Lee et al., 2006; Ruben, 1967) and where HC differentiation is last observed during development (Lumpkin et al., 2003; Montcouquiol and Kelley, 2003).

Mitotic hair cell regeneration

To determine whether SCs can proliferate and differentiate into HCs, we next treated *Pou4f3*$^{DTR/+}$; *Lgr5*$^{CreER/+}$; *ROSA26*$^{CAG\text{-}tdTomato/+}$ mice with tamoxifen and DT at P1, followed by the mitotic tracer EdU at P3-P5. At P7, we observed 6.7±0.6 EdU$^+$/Myo7a$^+$/tdTomato$^+$ cells in the whole apical turn and none in the middle and basal turns (Fig. 6A-G; supplementary material Table S2E; n=3). In the same organs, there were also EdU$^-$/Myo7a$^+$/tdTomato$^+$ cells (apex, 106.3±14.8; middle,

Development (2014) doi:10.1242/dev.103036

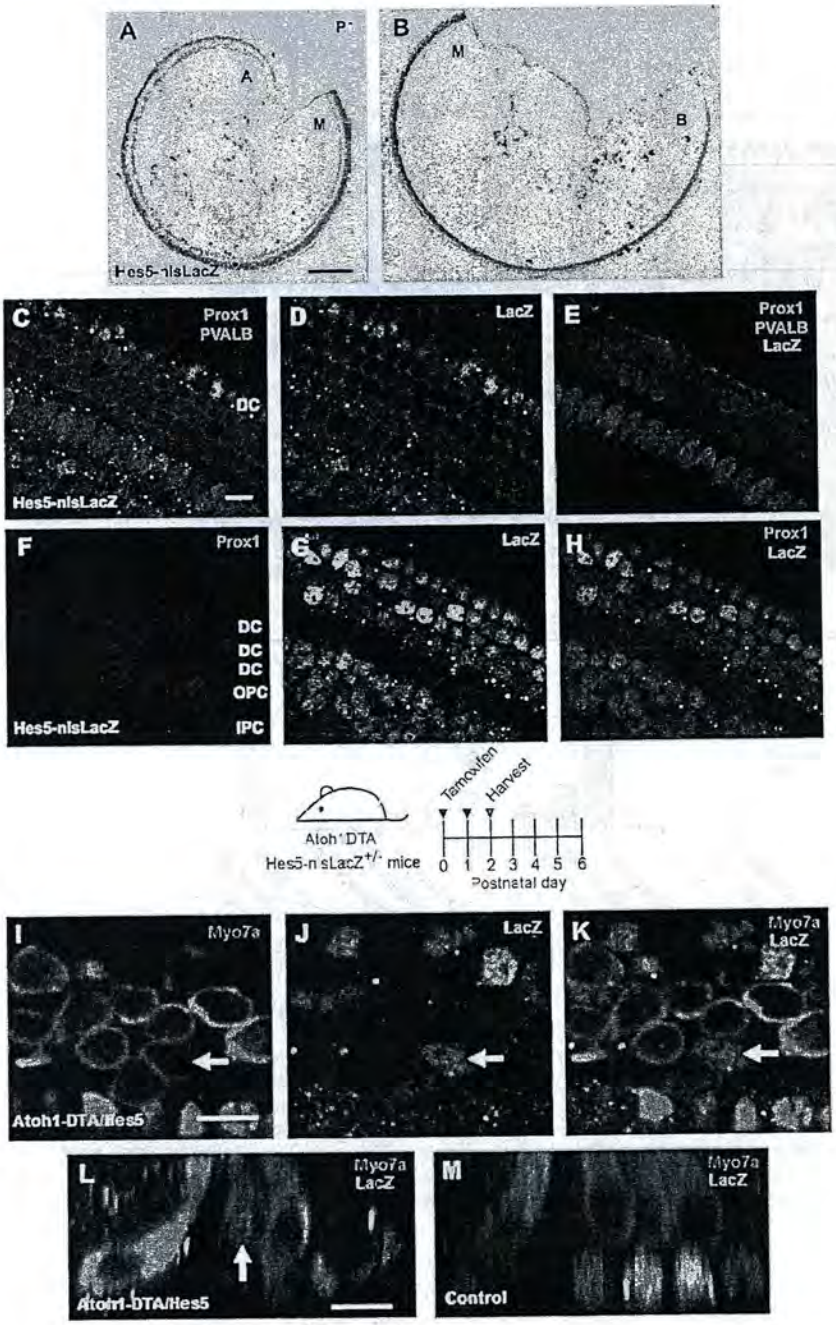

Fig. 4. Fate mapping of SCs in the *Atoh1DTA* model. (A,B) X-Gal staining (blue) in *Hes5-nlsLacZ* cochlea at P1. Cochlear turns are labeled as apical (A), middle (M) and basal (B). (C-H) Confocal images of the apical turn of *Hes5-nlsLacZ* mice at P1. *lacZ* expression is detected with anti-β-gal antibody (green) and is specific to SCs. HCs are labeled by parvalbumin (PVALB; magenta). No β-gal$^+$ cells were detected in control samples lacking the *Hes5-nlsLacZ* allele. Deiters' cells (DC), outer pillar cells (OPC) and inner pillar cells (IPC) are labeled by Prox1 (blue). (I-K) Confocal images of β-gal$^+$ (green) HCs (Myo7a, magenta) in the apical turn of *Atoh1DTA; Hes5-nlsLacZ*$^{+/-}$ mice at P2. (L) Cross-section focused on the β-gal$^+$ HC labeled by the arrow in I-K. (M) Transverse section of a littermate control (lacking either the *Cre* or *DTA* allele) at P2, in which all β-gal$^+$ cells are in the SC nuclear layer. Scale bars: 200 μm in A,B; 10 μm in C-M.

25.7±5.5; base, 2.7±1.5; Fig. 6H-I). Control animals (*Pou4f3*$^{+/-}$; *Lgr5*$^{CreER+}$; *RCSA26*$^{CAG\text{-}tdTomato/+}$) receiving the same drug regimen did not exhibit any EdU$^+$ cells and significantly fewer EdU$^-$/Myo7a$^+$/tdTomato$^+$ cells than in damaged organs (apex, 9.8±2.1; middle, 1.3±0.5; base, 0.3±0.5; n=6; supplementary material Table S2E), which is similar to the number of Myo7a$^+$/tdTomato$^+$ cells found in controls without EdU injection (Fig. 3A,H-J; supplementary material Table S2A). The finding of EdU$^+$/Myo7a$^+$/tdTomato$^+$ cells likely indicate that Lgr5$^+$ SCs proliferated prior to acquiring a HC fate, consistent with mitotic HC regeneration described previously in non-mammalian species (Baird et al., 1996; Corwin and Cotanche, 1988; Jones and Corwin, 1996; Ryals and Rubel, 1988; Warchol and Corwin, 1996). Although substantially more EdU$^+$/Sox2$^+$ cells were found in all three cochlear turns (supplementary material Table S2C), mitotic HC regeneration (EdU$^+$/Myo7a$^+$/tdTomato$^+$ cells) appears limited to the apical turn and represents 5.9% of total fate-mapped, regenerated HCs in this region.

We next sought to investigate whether original, differentiated HCs could also contribute to the observed EdU$^+$/Myo7a$^+$ cells. Based on reporter assays using the *ROSA26*^{lacZ} allele, ~80-90% of HCs in *Atoh1-CreER*^{TM} mice were *lacZ*$^+$ at P6 after tamoxifen injection at P0/P1 (Chow et al., 2006; Weber et al., 2008). Since the *ROSA26*^{DTA} allele uses the same promoter as the *ROSA26*^{lacZ} allele, ~80-90% of HCs in our model probably expressed DTA and thus ~10-20% of original, differentiated HCs might remain. To explore the possibility that these surviving HCs serve as a source of EdU$^+$/Myo7a$^+$ cells in

Development (2014) doi:10.1242/dev.103036

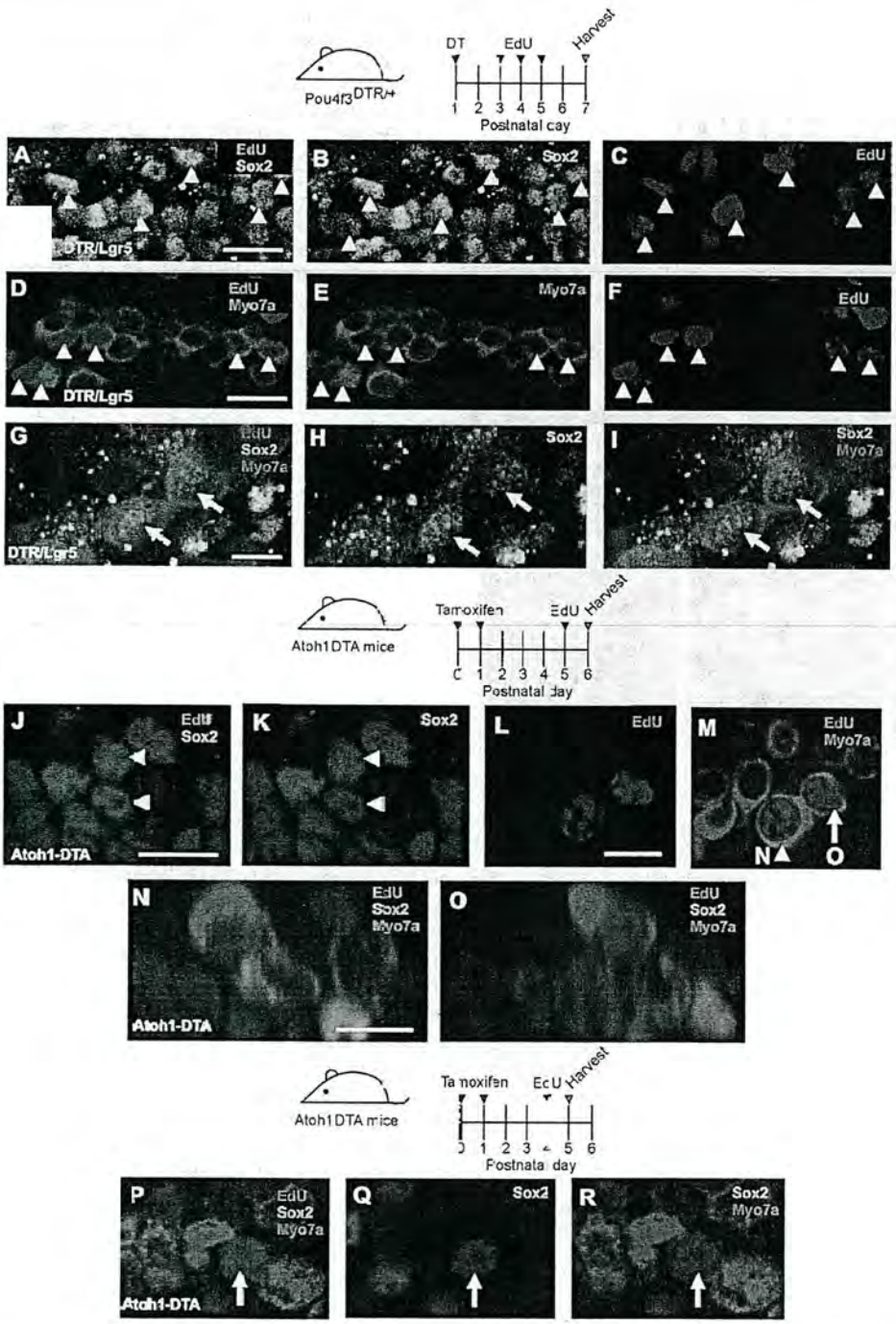

Fig. 5. Mitotic HC regeneration in the neonatal mouse cochlea. Confocal images of EdU (blue) incorporation in Sox2$^+$ SCs (green, A-C) and Myo7a$^+$ cells (magenta, D-F) in the apical turn of *Pou4f3*$^{DTR/+}$ mice at P7 after EdU injections at P3-P5. Some EdU$^+$ HCs (Myo7a$^+$) were also co-labeled with Sox2 (G-I). EdU$^+$ SCs (Sox2, J,K) and EdU$^+$/Myo7a$^+$ cells (L,M) were also observed in the apical turn of *Atoh1DTA* mice 24 hours after EdU injection at P5. (N-O) Cross-section focused on the EdU$^+$ nucleus of the cells indicated by the arrowhead and arrow in M. (P-R) Confocal images of EdU$^+$ (blue) HCs (Myo7a, magenta) co-labeled with Sox2 (green) in the apical turn of *Atoh1DTA* mice 24 hours after EdU injection at P4. Scale bars: 20 µm in A-F; 10 µm in G-O.

the *Atoh1DTA* cochleae, we traced HCs using the *ROSA26*$^{CAG\text{-}tdTomato}$ allele, which labels 99.5±0.2% of HCs at P6 in *Atoh1-CreER*^{TM} mice after tamoxifen injection at P0/P1 (Fig. 7A,B). We injected tamoxifen at P0/P1 and then EdU at P3 or P4 in *Atoh1-CreER*^{TM}; *ROSA26*$^{DTA\ CAG\text{-}tdTomato}$ mice and analyzed the cochlea 24 hours later. All EdU$^+$/Myo7a$^+$ cells (12 cells from six mice) were tdTomato$^-$ (Fig. 7C-E), suggesting that EdU$^+$/Myo7a$^+$ cells are likely to be derivatives of surrounding SCs and not surviving HCs, since they were not present when tamoxifen was injected at P0/P1 to turn on the tdTomato reporter.

During development, mitosis of HC precursors terminates by E14.5 (Lee et al., 2006; Ruben, 1967), and HC differentiation and maturation is a dynamic process that occurs over 3 perinatal weeks in mice. Based on our findings that HC loss stimulates SC proliferation, we investigated whether newly generated Myo7a$^+$ cells could also be active in the cell cycle. We analyzed cochleae just 4 hours after EdU injection at P4 in *Atoh1DTA* mice, as the mammalian cell cycle usually takes ~24 hours to complete (Alberts et al., 2002). We found 2±0.5 EdU$^+$/Myo7a$^+$ cells (n=4) in the apical turn (Fig. 8A-D). Moreover, we observed several Myosin VI+ (Myo6$^+$) cells that were co-labeled with the M-phase marker phospho-histone H3 (pH3) (Fig. 8E-H) and an EdU$^+$/calbindin$^+$ cell with mitotic figures (Fig. 8I-M), providing further evidence that rare Myo7a$^+$ cells can be active in the cell cycle. Likewise, in the

Development (2014) doi:10.1242/dev.103036

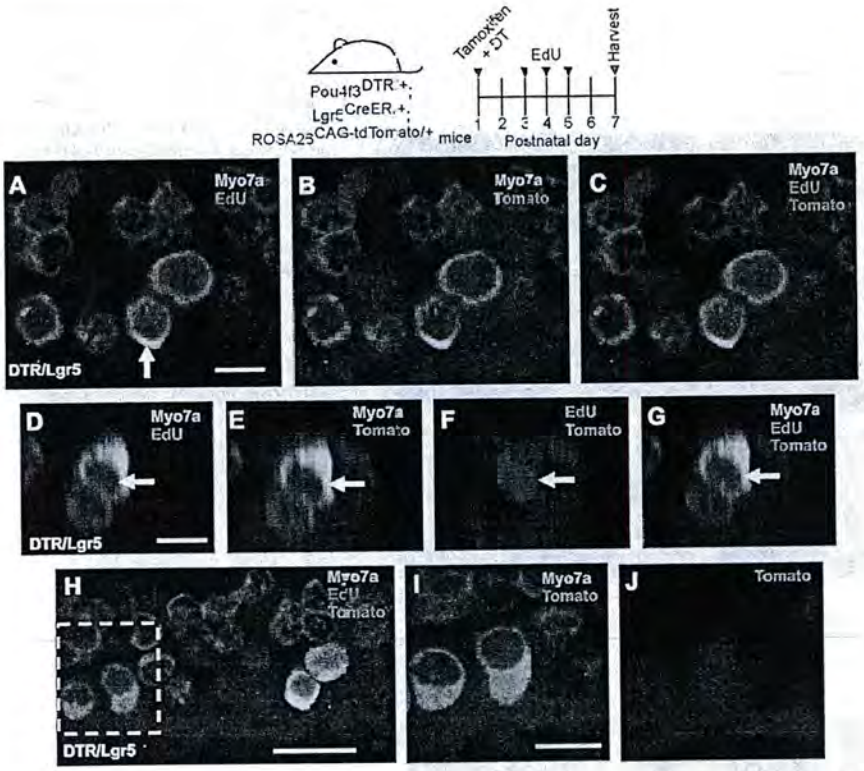

Fig. 6. Both mitotic regeneration and direct transdifferentiation occur in the neonatal mouse cochlea. (A-C) Confocal images of tdTomato$^+$ (magenta) HCs (Myo7a, green) that are labeled by EdU (blue) in the apical turn of *Pou4f3*$^{DTR/+}$; *Lgr5*$^{CreER/+}$; *ROSA26*$^{CAG\text{-}tdTomato/+}$ mice at P7 after EdU injections at P3-P5. (D-G) Cross-section focused on the tdTomato$^+$/EdU$^+$ HC indicated by the arrow in A. Note that GFP expression from the *Lgr5*$^{CreER/+}$ allele is much weaker than EdU labeling. In the apical turn of the same organs, there were also EdU$^-$/Myo7a$^+$/tdTomato$^+$ cells (H-J). (I,J) Higher magnification of the boxed region in H. Scale bars: 20 µm.

Pou4f3$^{DTR/+}$ model, we observed rare pH3$^+$/Myo7a$^+$ cells (Fig. 8N,O). pH3 labeling only marks cells that are active in M phase [which lasts ~1 hour (Alberts et al., 2002)] at the time of tissue collection, and therefore most likely underestimates the total number of dividing cells over the several days following HC ablation. To exclude the possibility that EdU$^+$/Myo7a$^-$ cells are in the process of dying, we performed terminal dUTP nick end labeling (TUNEL) staining in the *Atoh1DTA* model and failed to detect degenerating cells (Kuan et al. 2004) in any of the nine EdU$^+$/Myo7a$^+$ cells from seven mice (data not shown)

Taken together, these findings from the *Atoh1DTA* and *Pou4f3*$^{DTR/+}$ models suggest that it is possible for SCs acquiring a HC fate to be active in the cell cycle. Considering that the frequency of EdU labeling was higher in Sox2$^+$ cells than in Myo7a$^+$ cells, it is plausible that the proliferative capacity of SCs gradually diminishes as they convert to a HC fate.

Maturation of regenerated hair cells

To elucidate whether regenerated HCs can survive and mature, we used EdU to trace newly generated Myo7a$^+$ cells at longer recovery time points in the *Atoh1DTA* model. EdU$^+$/Myo7a$^-$ cells expressed other markers of HCs, including calbindin (Fig. 9A-C), parvalbumin (Fig. 9D-F) and prestin (Slc26a5 – Mouse Genome Informatics) (Fig. 9G-I). As precursor cells acquire a HC fate these markers are expressed in a stepwise fashion, with Myo7a and calbindin among the first proteins to be expressed (Dechesne and Thorniasset, 1988; Montcouquiol and Kelley, 2003), followed by parvalbumin (Zheng and Gao, 1997) and finally prestin, a marker of terminal differentiation of outer HCs (Belyantseva et al., 2000; Legendre et al., 2008; Zheng et al., 2000). Myo7a and calbindin were detected as early as 4 hours after EdU injection, whereas cells double positive for EdU and parvalbumin were not found until 2 days after EdU injection. At 6 days post EdU injection, 46.7±13.3% of EdU$^+$/Myo7a$^+$ cells also expressed prestin. We did not detect the inner HC marker VGlut3 (Slc17a8 – Mouse Genome Informatics) in any EdU$^+$/Myo7a$^+$ cells at P10 or P15 (supplementary material Fig. S2), suggesting that regenerated HCs preferentially feature an outer HC phenotype. Under scanning electron microscopy, all stereocilia bundles in the apical turn of P15 *Atoh1DTA* cochleae appeared short and tightly packed and thus immature (Fig. 9M-O). Some bundles contained a kinocilium (Fig. 9O), which normally regresses by P10 (Sobkowicz et al., 1995). We confirmed that newly formed HCs have stereocilia bundles using EdU as a tracer and detected EdU$^+$/Myo7a$^+$ cells with espin$^+$ stereocilia bundles at P15 (Fig. 9J-L). Together, these data support the notion that EdU$^+$/Myo7a$^+$ cells are regenerated HCs that acquire features of endogenous HCs. Furthermore, the timing of expression for these HC markers in EdU$^+$ cells closely follows that of developing HCs, supporting the notion that regenerated HCs mature in a similar pattern to that seen in development.

Some regenerated HCs survived for more than a week, as EdU$^+$/Myo7a$^+$ cells were still found at P10 and P15 after EdU injection at P4 (Fig. 9P-R). However, the majority of regenerated HCs died progressively, with only a small number remaining at P15 (Fig. 2M-O).

We investigated potential factors that might be linked to the death of regenerated HCs. Pou4f3 is crucial for HC survival. In mice with germline deletion of *Pou4f3*, HCs initially form but die 1-2 weeks later (Erkman et al., 1996; Xiang et al., 1998). In the apical turn of P6 *Atoh1DTA* mice, out of 81.3±4.5 Myo7a$^+$ HCs (per 200 µm region), only 11.0±1.8 expressed Pou4f3 (13.9±4.4%), whereas all 104.0±8.3 HCs in control mice (lacking either the *Cre* or *DTA* allele) were Myo7a$^+$/Pou4f3$^+$ (100%) (supplementary material Fig. S3; n=3). Since the *Atoh1DTA* model targets ~80-90% of HCs, our data suggest that the majority of regenerated HCs lack a key intrinsic survival factor.

Development (2014) doi:10.1242/dev.103036

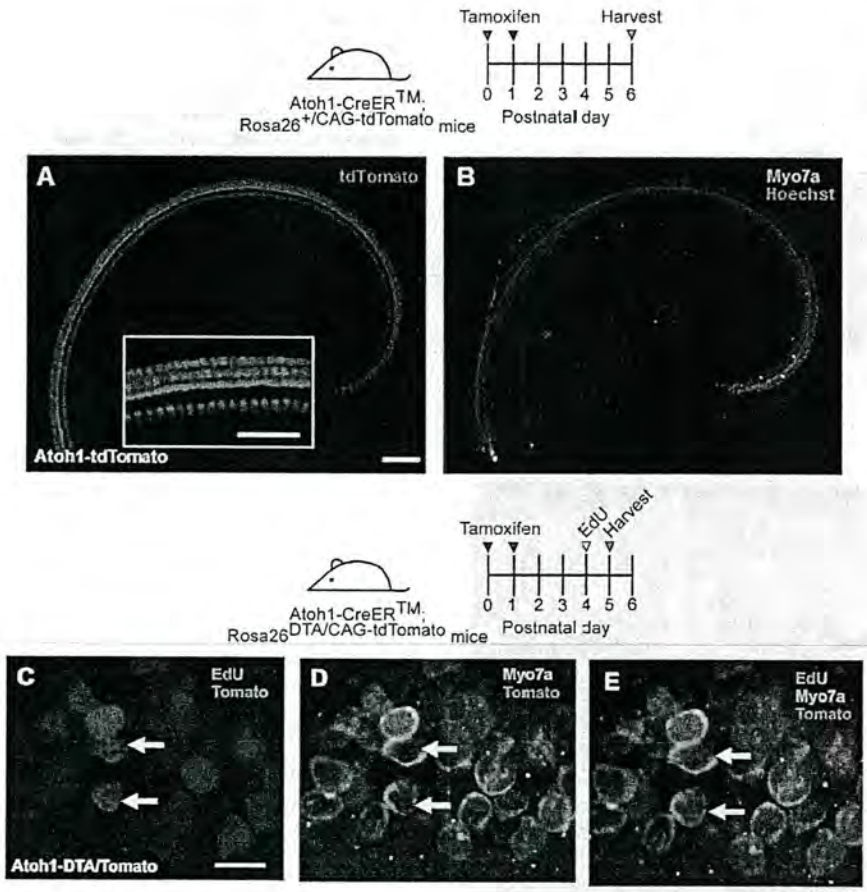

Fig. 7. Regenerated HCs are not derived from original, differentiated HCs. (A,B) Confocal images of tdTomato^{+} (magenta) HCs (Myo7a, green) in the apical turn of *Atoh1-CreER^{TM}; ROSA26$^{CAG\text{-}tdTomato}$* mice at P6 after tamoxifen injection at P0/P1. Nuclei are labeled by Hoechst (blue). Inset is a high- magnification image of tdTomato-labeled HCs. (C-E) Confocal images of EdU (blue) incorporation in Myo7a^{+} cells in the apical turn of *Atoh1-CreER^{TM}; ROSA26$^{DTA/CAG\text{-}tdTomato}$* mice 24 hours after EdU injection at P4. DTA^{-} HCs were traced with tdTomato (magenta). All EdU^{+}/Myo7a^{+} cells were tdTomato^{-}. Scale bars: 100 µm in A,B, 50 µm in inset; 10 µm in C-E.

Because a mosaic loss of SCs (<40% loss) also leads to HC death (Mellado Lagarde et al., 2013), we quantified fate-mapped SCs after HC ablation in *Pou4f3$^{DTR/+}$* mice to determine whether SC loss also occurs. After tamoxifen and DT were administrated to P1 *Pou4f3$^{DTR/+}$; Lgr5$^{CreER/+}$; ROSA26$^{CAG\text{-}tdTomato/+}$* mice, we noted at P7 significantly fewer tdTomato-labeled Sox2^{+} SCs in the organ of Corti in comparison with undamaged controls (*Pou4f3$^{+/+}$; Lgr5$^{CreER/+}$; ROSA26$^{CAG\text{-}tdTomato/+}$* mice) (supplementary material Table S2F; $P<0.01$). There were ~28-35% fewer SCs in all three cochlear turns and also a net loss of total traced organ of Corti cells (supplementary material Table S2F; $P<0.05$ in apex and $P<0.01$ in middle and base). As an additional control, we compared tdTomato^{+} cell counts in the GER, a region more remote from HC ablation, and did not observe any significant change (supplementary material Table S2F).

Last, we made auditory measurements of P30 *Atoh1DTA* mice and found them to exhibit elevated thresholds for auditory brainstem response across all frequencies tested (supplementary material Fig. S4). Prior work on HC ablation (at P2) using the *Pou4f3$^{DTR/+}$* allele similarly found elevated auditory thresholds in adult animals (Mahrt et al., 2013). In summary, the absence of Pou4f3 in HCs and/or the degeneration of surrounding SCs might have contributed to the poor survival of regenerating HCs and, consequently, to hearing loss.

Spontaneous hair cell regeneration can no longer occur after hair cell damage at 1 week

To determine when the neonatal cochlea loses the ability to spontaneously regenerate HCs, we ablated HCs and performed fate mapping of SCs using *Pou4f3$^{DTR/+}$; Lgr5$^{CreER/+}$; ROSA26$^{CAG\text{-}tdTomato/+}$* mice that were given tamoxifen at P1 and DT at P6, and found no significant difference in the number of Myo7a^{+}/tdTomato^{+} cells at P9 (apex, 15.3±0.9; middle, 0.3±0.3; base, 0±0; n=3) compared with control that lacked the *Pou4f3$^{DTR/+}$* allele (apex, 13.8±0.9; middle, 0.3±0.3; base, 0±0; n=4) (Fig. 10A-K).

In parallel, we induced DTA expression in HCs at P6. Since Atoh1 is rapidly downregulated after birth (Lumpkin et al., 2003), we instead used *Prestin-CreER^{T2}* mice (Fang et al., 2012). When injected with tamoxifen (once daily from P6-8), all outer HCs in *Prestin-CreER^{T2}; ROSA26$^{CAG\text{-}ZsGreen/+}$* mice expressed the reporter ZsGreen (Fig. 11A-C). When tamoxifen was administered in the same fashion, *Prestin-CreER^{T2}; ROSA26$^{DTA/+}$* (*PrestinDTA*) mice had progressive outer HC loss, whereas inner HCs remained intact (Fig. 11D-L). We also gave one EdU injection to *PrestinDTA* mice at ages ranging from P7 to P11 and analyzed the cochlea 24 hours after each injection (n=3). No EdU^{+} SCs or EdU^{+}/Myo7a^{+} cells were observed in the organ of Corti in any cochlear turn. Together, these data support the notion that proliferation and HC regeneration after HC loss only take place within a limited time window in the neonatal mouse cochlea.

DISCUSSION

Previous studies in mice have reported that isolated, postmitotic SCs can divide and generate HCs *in vitro* (Chai et al., 2012; Doetzlhofer et al., 2006; Savary et al., 2007; Shi et al., 2012; Sinkkonen et al., 2011; White et al., 2006) and that HC regeneration occurs in embryonic cochlear explants *in vitro* after laser ablation of HCs, with regeneration ending ~48 hours after HC fate commitment (Kelley et al., 1995). In other studies, HCs were damaged in the neonatal rat cochlea using antibiotic treatment *in vivo* and *in vitro*

Development (2014) doi:10.1242/dev.103036

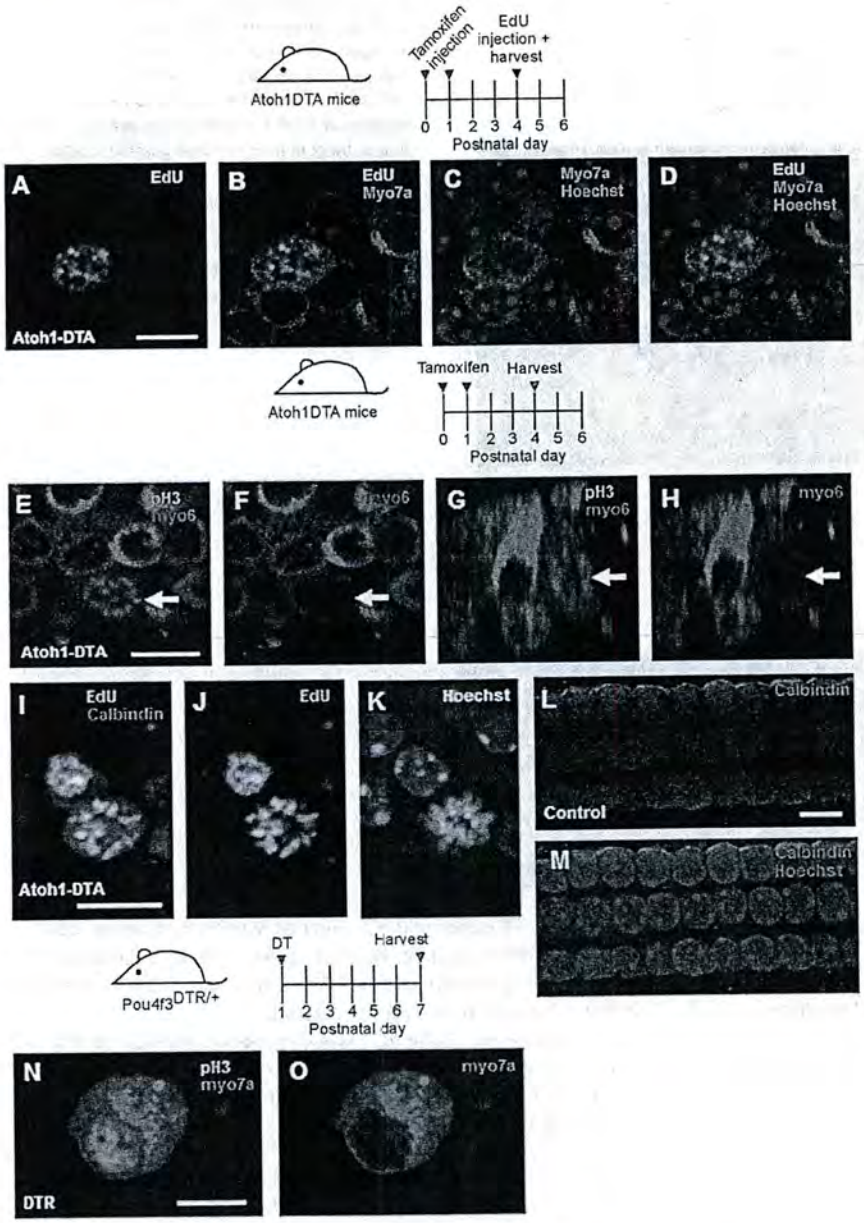

Fig. 8. Myo7a$^+$ cells are active in the cell cycle. (A-D) Confocal image of EdU incorporation (green) in Myo7a$^+$ cells (magenta) in the *Atoh1DTA* model 4 hours after EdU injection at P4. (E-H) A pH3$^+$ (green) HC (Myo6, magenta) was observed at P4 in the *Atoh1DTA* model. (G-H) Cross-section focused on the pH3$^+$ HC indicated by the arrow in E. Note that Myo6 expression of this cell is less robust than in adjacent cells. (I-K) An EdU$^+$ (green) HC (calbindin, magenta) with mitotic figures (Hoechst, grayscale) was observed in the *Atoh1DTA* model 24 hours after EdU injection at P4. (L,M) Control tissue (lacking either the *Cre* or *DTA* allele) shows expression of calbindin (magenta) in HC nuclei in tissues that were processed for EdU staining. (N,O) A pH3$^+$ (green) HC (Myo7a, magenta) was observed at P7 in the *Pou4f3*$^{DTR/+}$ model. Scale bars: 10 µm.

and transient 'atypical cells' were found that resembled immature HCs, with tufts of microvilli in the damaged regions (Daudet et al., 1998; Lenoir and Vago, 1997; Parietti et al., 1998; Romand et al., 1996; Zine and de Ribaupierre, 1998). However, it is unclear whether these cells expressed HC markers or if mitotic regeneration occurred. Moreover, the ototoxic antibiotic treatments were unable to damage HCs in the apical turn of the cochlea and most analyses were undertaken many days after HC damage. In our experiments using an effective method to eliminate neonatal HCs throughout the cochlea, we observed spontaneous HC regeneration during the first postnatal week. Fate-mapping experiments using a SC-specific CreER line and the *Hes5-nlsLacZ* allele reveal SCs as the source of newly regenerated HCs.

In experiments in which the *Hes5-nlsLacZ* allele was used to fate map SCs, the *lacZ*$^+$/Myo7a$^+$ cells observed are most likely to be regenerated HCs derived from Hes5-expressing SCs, particularly when interpreted in conjunction with the fate-mapping results obtained using the Cre-loxP system in the *Pou4f3*^{DTR} model. It is possible, but unlikely, that Myo7a$^+$ cells de-differentiated and upregulated Hes5, considering the antagonistic effect of Hes5 on the HC differentiation factor Atoh1 (Doetzlhofer et al., 2009; Kelley, 2006).

HC regeneration in non-mammalian vertebrates occurs by two mechanisms: mitotic regeneration and direct transdifferentiation. During mitotic regeneration, a SC first divides and then several days later one or both daughter cells changes fate to become a HC (Adler and Raphael, 1996; Baird et al., 1996; Corwin and Cotanche, 1988; Jones and Corwin, 1996; Ryals and Rubel, 1988; Warchol and Corwin, 1996). Fate mapping of SCs in our models revealed traced Myo7a$^+$ cells; thus, HC loss led SCs towards a HC fate in all turns of the cochlea, albeit predominantly in the apex. By applying mitotic tracers, we detected EdU$^+$ SCs and fate-mapped EdU$^+$/Myo7a$^+$ cells, indicating that the neonatal mouse cochlea can, to a limited extent, proliferate in response to HC loss and that some of these

Development (2014) doi:10.1242/dev.103036

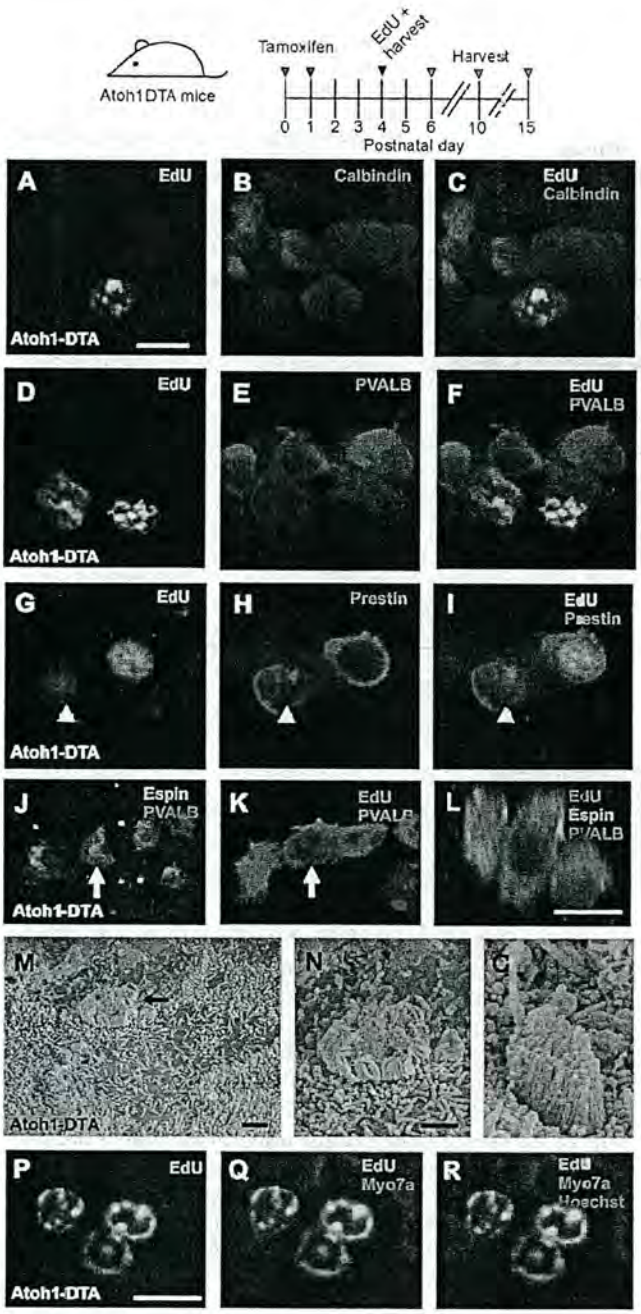

Fig. 9. Regenerated HCs are similar to endogenous HCs. Confocal images of EdU$^+$ (green) cells co-labeled with HC markers in the apical turn of *Atoh1DTA* mice. (A-C) Four hours after EdU injection at P5. EdU$^+$ cells also express calbindin (magenta). (D-F) Two days after EdU injection at P4 (at P6), EdU$^+$ cells express parvalbumin (PVALB; magenta). (G-I) Six days after EdU injection at P4 (at P10), EdU$^+$ cells express prestin (magenta). Note that prestin is expressed in the cytoplasm of the EdU$^+$ HC indicated by the arrowhead, which is characteristic of a young HC (Mahendrasingam et al., 2010). (J-L) Eleven days after EdU injection at P4 (at P15). EdU$^+$ cells (blue) have espin$^+$ (green) stereocilia bundles. (L) Cross-section focused on the EdU$^+$ HCs indicated by the arrow in J and K. (M-O) Scanning electron micrographs of the apical turn in *Atoh1DTA* mice at P15. (N) High-magnification image of M, showing an immature stereocilia bundle. The immature bundle in O still has a kinocilium. (P-R) Confocal images of EdU$^+$ (green) HCs (Myo7a, magenta) in the apical turn of *Atoh1DTA* mice at P10 after EdU injection at P4. Scale bars: 10 µm in A-L,P-R; 1 µm in M-O.

proliferating SCs can acquire a HC fate. Interestingly, we observed the expression of the mitotic markers EdU and pH3 in Myo7a$^+$ and Myo7a$^+$/Sox2$^+$ cells, which likely represent a differentiating SC or an immature HC. We postulate that the processes of cell cycle entry and that of differentiation towards a HC fate might overlap. Future studies using time-lapse imaging would be useful in investigating these steps further.

The other reported mechanism for HC regeneration is direct transdifferentiation, in which a SC directly acquires a HC phenotype without mitotic division (Adler and Raphael, 1996; Baird et al., 1996; Jones and Corwin, 1996). The experiments reported here did not directly address this mechanism because of the limited labeling efficiency of the mitotic tracers used. However, the number of EdU$^-$/Myo7a$^+$/tdTomato$^+$ cells observed in *Pou4f3*$^{DTR/+}$; *Lgr5*$^{CreER/+}$; *ROSA26*$^{CAG\text{-}tdTomato/+}$ mice was ~15-fold greater than the number of EdU$^+$/Myo7a$^+$/tdTomato$^+$ cells detected, which suggests that some of these cells were derived from direct transdifferentiation. The avian auditory epithelium regenerates via direct transdifferentiation 1-2 days after ototoxic antibiotic exposure (Cafaro et al., 2007; Roberson et al., 2004), and this mechanism has been reported to be the primary mode of HC regeneration in the adult mouse utricle (Forge et al., 1993; Forge et al., 1998; Golub et al., 2012; Kawamoto et al., 2009). In addition, Lgr5$^+$ SCs can generate HCs via both mechanisms *in vitro* (Chai et al., 2012). Of note, both methods of fate mapping might underestimate the total number of regenerated HCs resulting from direct transdifferentiation because of the incomplete labeling with the Cre-loxP system or *Hes5-nlsLacZ* allele and the possibility of other progenitor cell types.

The vast majority of regenerated HCs were observed in the apical turn of the cochlea. Our results are in agreement with previous findings that *in vitro* HC regeneration after laser ablation of embryonic HCs decreased in a basal-apical gradient (Kelley et al., 1995). Both HCs and SCs continue to mature during the first postnatal weeks, with cytoskeletal, morphological and functional changes detected in cells from the basal turn 2-3 days before cells in the apex (Hallworth et al., 2000; Jensen-Smith et al., 2003; Legendre et al., 2008; Lelli et al., 2009; Szarama et al., 2012). Thus, cells in the apical turn are less mature, which might provide a permissive environment for HC regeneration. Alternatively, the presence of two different HC regeneration mechanisms working in concert in the apex might indicate the presence of undifferentiated progenitor cells. It is worth noting that the apical turn of the cochlea is the first to exit the cell cycle and the last to acquire a HC or SC fate during embryonic development (Lee et al., 2006; Lumpkin et al., 2003; Montcouquiol and Kelley, 2003; Ruben, 1967).

Previous studies characterized an age-dependent decrease in stem/progenitor cells isolated from the cochlea (Oshima et al., 2007; White et al., 2006). This decline correlates well with our finding that the ability of the cochlea to spontaneously regenerate HCs diminished 1 week after birth, suggesting the loss of either progenitor cell competence or a corresponding niche. In support of this theory, there is an age-dependent decline in the ability of the cochlea to respond to Atoh1-mediated conversion of SCs into HCs (Kelly et al., 2012; Liu et al., 2012a) and Sox2/p27^{Kip1} control of SC proliferation (Liu et al., 2012b). Such an age-dependent decline in the ability to self-repair has been observed in other organ systems: hearts from P1 mice can regenerate after damage and this regenerative capacity is lost in P7 mice (Porrello et al., 2011). Interestingly, heart regeneration correlated with the endogenous proliferative capacity of cardiac tissue, whereas we found regeneration capacity in the cochlea more than a week after the cells in the organ of Corti had become quiescent.

Development (2014) doi:10.1242/dev.103036

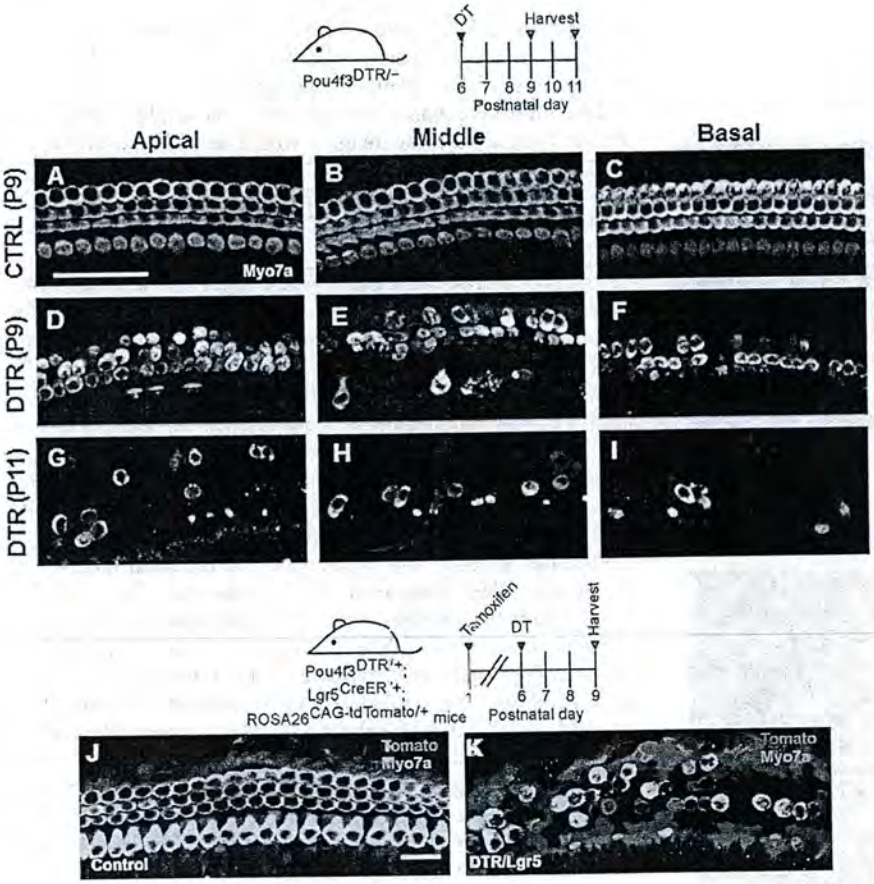

Fig. 10. No signs of HC regeneration when HC loss occurs 1 week after birth in the *Pou4f3*$^{DTR/+}$ model. Projection images of Myo7a immunofluorescence in cochlear whole-mounts of control wild-type mice at P9 (A-C) and *Pou4f3*$^{DTR/+}$ mice at P9 (D-F) and P11 (G-I) after DT injection at P6. Confocal images of tdTomato^{+} (magenta) HCs (Myo7a, green) in the apical turn of control (*Lgr5*$^{CreER/+}$; *ROSA26*$^{CAG\text{-}tdTomato/+}$) (J) and *Pou4f3*$^{DTR/+}$; *Lgr5*$^{CreER/+}$; *ROSA26*$^{CAG\text{-}tdTomato/+}$ (K) mice that were given tamoxifen at P1, DT at P6, and analyzed at P9. Scale bars: 50 µm in A-I; 20 µm in J,K.

Based on the timing of expression for various HC markers, we conclude that regenerated HCs follow a similar pattern of maturation to normal HC development. Interestingly, the *Atoh1DTA* model retains conditions favorable for the expression of prestin, a terminal outer HC marker that is not expressed in SC-derived HCs generated from ectopic expression of Atoh1 (Liu et al., 2012a). Unfortunately, regenerated HCs only contributed to a modest and transient degree of repopulation of the organ of Corti, and most regenerated HCs died by P15. The inability of regenerated HCs to survive could be caused by the lack of the survival factor Pou4f3 and/or loss of SCs, which normally provide structural and trophic support. In the described HC damage models, 80-90% of HCs regenerate and more than 100 SCs per cochlea change fate to become HCs, with a small amount of proliferation that is evidently insufficient to compensate for the overall cell loss. As a result, the regenerating organ of Corti is not only disarrayed, but contains an abnormal composition of HCs and SCs, which might affect the survival of regenerated HCs. In addition, the endocochlear potential normally develops between P11 and P17 (Rybak et al., 1992) and might play a role in the death of regenerated HCs by causing excitotoxicity. It is probable that these factors, individually or in combination, contribute to the demise of regenerated HCs. Identification of factors capable of promoting the survival and functional maturation of regenerated HCs could have significant therapeutic benefits.

Finally, regenerated HCs in our models come from unmanipulated SCs; thus, the regeneration process we observed is their natural response to HC death. The *Atoh1DTA* and *Pou4f3*$^{DTR/+}$ models likely induce HC death by reactive oxygen species-induced apoptosis (Abrahamsen et al., 2008; Ivanova et al., 2005), which is similar to the major cell death pathway implicated in noise- or drug-induced HC death (Clerici et al., 1996; Henderson et al., 2006). Thus, our observations are likely to have implications for HC regeneration in response to various insults.

In summary, our data demonstrate that the postnatal mammalian cochlea has the intrinsic capacity to spontaneously regenerate HCs after damage, which was believed to occur only in non-mammalian vertebrates. These models are applicable to the further study of the molecular mechanisms of mammalian HC regeneration, which could lead to the identification of drug targets for the treatment of hearing loss in humans and improve our understanding of factors that promote the survival of regenerated HCs and factors that limit HC regeneration in the maturing cochlea.

MATERIALS AND METHODS

Mouse models and treatments

ROSA26^{DTA} (Ivanova et al., 2005), *Lgr5*$^{CreER/+}$ (Barker et al., 2007), *ROSA26*$^{CAG\text{-}tdTomato/+}$ (Madisen et al., 2010) and *ROSA26*$^{CAG\text{-}ZsGreen/+}$ (Madisen et al., 2010) mice were purchased from The Jackson Laboratory (Bar Harbor, ME, USA). *Atoh1-CreER*^{TM} (Chow et al., 2006), *Pou4f3*$^{DTR/+}$ (Golub et al., 2012; Tong et al., 2011) and *Hes5-nlsLacZ* (Imayoshi et al., 2010) mice were kind gifts from S. Baker (St. Jude Children's Research Hospital, Memphis, TN, USA), E. Rubel, L. Tong and R. Palmiter (University of Washington, Seattle, WA, USA) and R. Kageyama at (Kyoto University, Kyoto, Japan). *Prestin-CreER*^{T2} mice were generated in our lab (Fang et al., 2012). Genotyping for *Lgr5*$^{CreER/+}$, *ROSA26*$^{CAG\text{-}tdTomato/+}$, *ROSA26*$^{CAG\text{-}ZsGreen/+}$, *Atoh1-CreER*^{TM} and *Prestin-CreER*^{T2} mice was described previously (Barker et al., 2007; Chow et al., 2006; Fang et al., 2012; Madisen et al., 2010). Genotyping for *ROSA26*^{DTA} mice, *Hes5-nlsLacZ* mice and *Pou4f3*$^{DTR/+}$ mice is described in supplementary material Table S1. Tamoxifen [3 mg/40 g body weight,

Development (2014) doi:10.1242/dev.103036

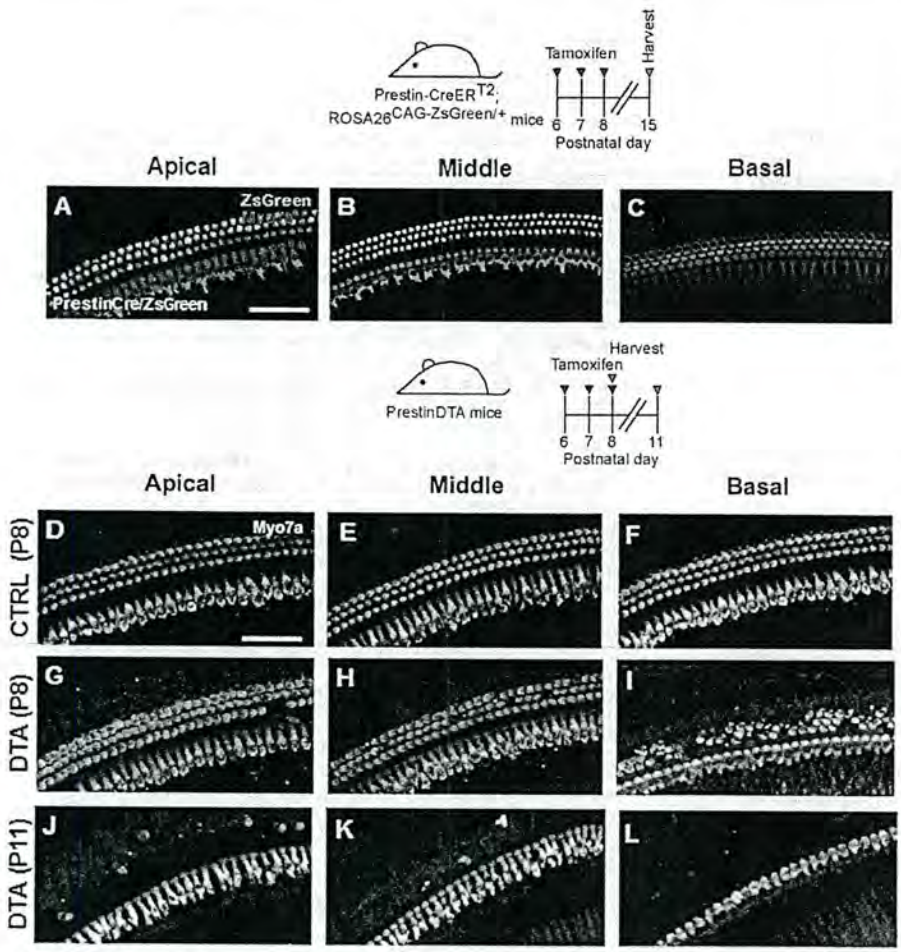

Fig. 11. No signs of HC regeneration when HC loss occurs 1 week after birth in the *PrestinDTA* model. (A-C) *Prestin-CreER^{T2}; ROSA26$^{CAG\text{-}ZsGreen/+}$* mice induced with tamoxifen from P6-P8 and analyzed at P15 have robust Cre activity in all outer HCs. HCs are labeled with Myo7a (magenta). Projection images of Myo7a immunofluorescence in cochlear whole-mounts of control mice (lacking the *Cre* or *DTA* allele) at P8 (D-F) and *PrestinDTA* mice at P8 (G-I) and P11 (J-L) given tamoxifen from P6-P8. Scale bars: 50 µm.

intraperitoneal injection (IP); Sigma] was injected once at P0 and P1 for *Atoh1-CreER^{TM}* mice and once at P6, P7 and P8 for *Prestin-CreER^{T2}* mice. Tamoxifen (0.75 mg/g) was given by gavage to *Lgr5$^{CreER/+}$* mice. DT (6.25 ng/g, IP, List Biological Laboratories) was injected at either P1 or P6 into *Pou4f3$^{DTR/-}$* mice. EdU (Click-iT EdU Imaging Kit, Invitrogen) was injected (50 µg/g, IP) once daily at P3-P5 into *Pou4f3$^{DTR/+}$* and *Atoh1DTA* mice; EdU was injected (10 µg/g, IP) once at the designated ages. Mice of both genders were used in this study. The *n* value throughout the paper reflects the number of animals analyzed per experiment. All animal work was approved by the Institutional Animal Care and Use Committees at St. Jude Children's Research Hospital and Stanford University.

Immunostaining

Cochlear samples were fixed in 4% paraformaldehyde overnight and standard immunohistochemistry was performed (Mellado Lagarde et al., 2013). For Sox2 staining, 0.02% sodium azide was added during the blocking and antibody incubation steps. TUNEL staining was performed using the *In Situ* Cell Death Detection Kit, TMR Red (Roche Applied Science) following the manufacturer's instructions, except for increasing the sodium citrate concentration in the permeabilization step to 1%. The following primary antibodies were used: anti-β-gal (1:500, AB9361 Abcam), anti-calbindin (1:500, AB1778 Millipore), anti-espin (1:5000, a gift from Dr S. Heller, Stanford University, Palo Alto, CA, USA), anti-Myo6 conjugated to Alexa 647 (1:40, specific request Proteus BioSciences), anti-Myo7a (1:200, 25-6790 Proteus BioSciences), anti-pH3 conjugated to Alexa 555 (1:50, 3475 Cell Signaling), anti-Prox1 (1:500, AB5475 Millipore), anti-parvalbumin (1:1000, P3088 Sigma), anti-VGlut3 (1:500, 135203 Synaptic Systems, Goettingen, Germany), anti-prestin (1:200, sc-22692 Santa Cruz Biotechnology), anti-Sox2 (1:1000, sc-17320 Santa Cruz Biotechnology) and anti-Pou4f3 (1:500, sc-81980 Santa Cruz Biotechnology). Nuclear staining employed Hoechst 33342 (1:2000, Invitrogen). EdU staining was performed using the Click-iT EdU Imaging Kit (Invitrogen) following the manufacturer's instructions. All secondary antibodies were Alexa conjugated (Invitrogen) and were used at 1:500 or 1:1000. Images were taken using a Zeiss LSM 700 confocal microscope and 3D reconstruction was performed using Imaris 7.1 software (Bitplane).

Cell counts

For counts of traced HCs in the *Pou4f3$^{DTR/+}$; Lgr5$^{CreER/+}$; ROSA26$^{CAG\text{-}tdTomato/+}$* and *Atoh1DTA; Hes5-nlsLacZ* samples, we imaged the entire cochlea using a 40× objective and counted Myo7a$^+$ or Sox2$^+$/Myo7a$^-$ cells that co-expressed *lacZ* or tdTomato. The same procedure was used to quantify EdU$^+$/Myo7a$^+$ cells, while EdU$^+$ or traced SC counts were obtained from counting 225 µm regions of each turn. For Pou4f3$^+$ HC counts, two 200 µm regions of the apical turn were analyzed.

Scanning electron microscopy

Samples were prepared as previously described (Steigelman et al., 2011) and were imaged using a JEOL 7000 field emission gun scanning electron microscope (University of Alabama, Tuscaloosa, AL, USA).

Auditory brainstem response

Animals were anesthetized with Avertin (0.6 mg/g, IP) and frequency-specific auditory responses were measured using the Tucker-Davis Technology System III System (Alachua, FL, USA) as previously described (Mellado Lagarde et al., 2013).

Statistical analysis

All data are presented as mean ± s.e.m. Statistical analyses were conducted using GraphPad Prism 5.0 software.

Acknowledgements
We thank E. Rubel, L. Tong and R. Palmiter (University of Washington) for *Pou4f3*$^{DTR/+}$ mice and discussion; S. Baker (St. Jude) for *Atoh1-CreER*^{TM} mice and discussion; R. Kageyama (Kyoto University) for *Hes5-nlsLacZ* mice; P. Chambon (Institut Genetique Biologie Moleculaire Cellulaire) for the CreER^{T2} construct; S. Heller (Stanford University) for the anti-espin antibody and critical reading, J. Corwin, J. Burns and other members of the Corwin laboratory (University of Virginia) as well as members of our laboratories for discussion and critical comments; S. Connell, V. Frohlich, Y. Ouyang and J. Peters (St. Jude) for expertise in confocal imaging; A. Xue, V. Nookala, N. Pham, A. Vu, G. Huang and W. Liu (Stanford University) for excellent technical support; and L. Boykins (University of Memphis), R. Martens and J. Goodwin (University of Alabama) for assistance and expertise in scanning electron microscopy.

Competing interests
The authors declare no competing financial interests.

Author contributions
B.C.C., R.C., A.G.C. and J.Z. developed the concepts or approach; B.C.C., R.C., A.L., Z.L., L.Z., D.-H.N., K.C., K.A.S., J.F., A.G.C. and J.Z. performed experiments or data analysis; B.C.C., R.C., A.G.C. and J.Z. prepared or edited the manuscript prior to submission.

Funding
This work was supported by grants from the National Institutes of Health [DC006471 (J.Z.), DC008800 (J.Z.), DC009393 (K.A.S.), DC010310 (B.C.C.), DC011043 (A.G.C.), CA21765 (St. Jude) and P30DC010363 (Stanford University)], Office of Naval Research [N000140911014, N000141210191 and N000141210775 to J.Z.], Stanford Dean's Fellowship (R.C.), Hearing Health Foundation (R.C.), National Organization for Hearing Research Foundation [J.F. and A.G.C.], Stanford Children's Health Research Institute Akiko Yamazaki and Jerry Yang Faculty Scholar Fund (A.G.C.), California Institute for Regenerative Medicine [RN3-06529 to A.G.C.] and American Lebanese Syrian Associated Charities (ALSAC) of St. Jude Children's Research Hospital. We thank the St. Jude/University of Paris Diderot/Paris 7 graduate student program for support of A.L. J.Z. is a recipient of The Hartwell Individual Biomedical Research Award. Deposited in PMC for release after 12 months.

Supplementary material
Supplementary material available online at
http://dev.biologists.org/lookup/suppl/doi:10.1242/dev.103036/-/DC1

References

Abrahamsen, B., Zhao, J., Asante, C. O., Cendan, C. M., Marsh, S., Martinez-Barbera, J. P., Nassar, M. A., Dickenson, A. H. and Wood, J. N. (2008). The cell and molecular basis of mechanical, cold, and inflammatory pain. *Science* **321**, 702-705.

Adler, H. J. and Raphael, Y. (1996). New hair cells arise from supporting cell conversion in the acoustically damaged chick inner ear. *Neurosci. Lett.* **205**, 17-20.

Alberts, B., Johnson, A., Lewis, J., Raff, M., Roberts, K. and Walter, P. (2002). *Molecular Biology of the Cell*. New York, NJ: Garland Science.

Baird, R. A., Steyger, P. S. and Schuff, N. R. (1996). Mitotic and nonmitotic hair cell regeneration in the bullfrog vestibular otolith organs. *Ann. N. Y. Acad. Sci.* **781**, 59-70.

Balak, K. J., Corwin, J. T. and Jones, J. E. (1990). Regenerated hair cells can originate from supporting cell progeny: evidence from phototoxicity and laser ablation experiments in the lateral line system. *J. Neurosci.* **10**, 2502-2512.

Barker, N., van Es, J. H., Kuipers, J., Kujala, P., van den Born, M., Cozijnsen, M., Haegebarth, A., Korving, J., Begthel, H., Peters, P. J. et al. (2007). Identification of stem cells in small intestine and colon by marker gene Lgr5. *Nature* **449**, 1003-1007.

Belyantseva, I. A., Adler, H. J., Curi, R., Frolenkov, G. I. and Kachar, B. (2000). Expression and localization of prestin and the sugar transporter GLUT-5 during development of electromotility in cochlear outer hair cells. *J. Neurosci.* **20**, RC116.

Bohne, B. A., Ward, P. H. and Fernández, C. (1976). Irreversible inner ear damage from rock music. *Trans. Sect. Otolaryngol. Am. Acad. Ophthalmol. Otolaryngol.* **82**, ORL50-ORL59.

Burns, J. C., Cox, B. C., Thiede, B. R., Zuo, J. and Corwin, J. T. (2012). In vivo proliferative regeneration of balance hair cells in newborn mice. *J. Neurosci.* **32**, 6570-6577.

Cafaro, J., Lee, G. S. and Stone, J. S. (2007). Atoh1 expression defines activated progenitors and differentiating hair cells during avian hair cell regeneration. *Dev. Dyn.* **236**, 156-170.

Chai, R., Kuo, B., Wang, T., Liaw, E. J., Xia, A., Jan, T. A., Liu, Z., Taketo, M. M., Oghalai, J. S., Nusse, R. et al. (2012). Wnt signaling induces proliferation of sensory precursors in the postnatal mouse cochlea. *Proc. Natl. Acad. Sci. USA* **109**, 8167-8172.

Chow, L. M., Tian, Y., Weber, T., Corbett, M., Zuo, J. and Baker, S. J. (2006). Inducible Cre recombinase activity in mouse cerebellar granule cell precursors and inner ear hair cells. *Dev. Dyn.* **235**, 2991-2998.

Clerici, W. J., Hensley, K., DiMartino, D. L. and Butterfield, D. A. (1996). Direct detection of ototoxicant-induced reactive oxygen species generation in cochlear explants. *Hear. Res.* **98**, 116-124.

Corwin, J. T. and Cotanche, D. A. (1988). Regeneration of sensory hair cells after acoustic trauma. *Science* **240**, 1772-1774.

Dabdoub, A., Puligilla, C., Jones, J. M., Fritzsch, B., Cheah, K. S., Pevny, L. H. and Kelley, M. W. (2008). Sox2 signaling in prosensory domain specification and subsequent hair cell differentiation in the developing cochlea. *Proc. Natl. Acad. Sci. USA* **105**, 18396-18401.

Daudet, N., Vago, P., Ripoll, C., Humbert, G., Pujol, R. and Lenoir, M. (1998). Characterization of atypical cells in the juvenile rat organ of corti after aminoglycoside ototoxicity. *J. Comp. Neurol.* **401**, 145-162.

Dechesne, C. J. and Thomasset, M. (1988). Calbindin (CaBP 28 kDa) appearance and distribution during development of the mouse inner ear. *Brain Res.* **468**, 233-242.

Doetzlhofer, A., White, P., Lee, Y. S., Groves, A. and Segil, N. (2006). Prospective identification and purification of hair cell and supporting cell progenitors from the embryonic cochlea. *Brain Res.* **1091**, 282-288.

Doetzlhofer, A., Basch, M. L., Ohyama, T., Gessler, M., Groves, A. K. and Segil, N. (2009). Hey2 regulation by FGF provides a Notch-independent mechanism for maintaining pillar cell fate in the organ of Corti. *Dev. Cell* **16**, 58-69.

Erkman, L., McEvilly, R. J., Luo, L., Ryan, A. K., Hooshmand, F., O'Connell, S. M., Keithley, E. M., Rapaport, D. H., Ryan, A. F. and Rosenfeld, M. G. (1996). Role of transcription factors Brn-3.1 and Brn-3.2 in auditory and visual system development. *Nature* **381**, 603-606.

Fang, J., Zhang, W. C., Yamashita, T., Gao, J., Zhu, M. S. and Zuo, J. (2012). Outer hair cell-specific prestin-CreERT2 knockin mouse lines. *Genesis* **50**, 124-131.

Forge, A., Li, L., Corwin, J. T. and Nevill, G. (1993). Ultrastructural evidence for hair cell regeneration in the mammalian inner ear. *Science* **259**, 1616-1619.

Forge, A., Li, L. and Nevill, G. (1998). Hair cell recovery in the vestibular sensory epithelia of mature guinea pigs. *J. Comp. Neurol.* **397**, 69-88.

Golub, J. S., Tong, L., Ngyuen, T. B., Hume, C. R., Palmiter, R. D., Rubel, E. W. and Stone, J. S. (2012). Hair cell replacement in adult mouse utricles after targeted ablation of hair cells with diphtheria toxin. *J. Neurosci.* **32**, 15093-15105.

Hallworth, R., McCoy, M. and Polan-Curtain, J. (2000). Tubulin expression in the developing and adult gerbil organ of Corti. *Hear. Res.* **139**, 31-41.

Hartman, B. H., Basak, O., Nelson, B. R., Taylor, V., Bermingham-McDonogh, O. and Reh, T. A. (2009). Hes5 expression in the postnatal and adult mouse inner ear and the drug-damaged cochlea. *J. Assoc. Res. Otolaryngol.* **10**, 321-340.

Hawkins, J. E., Jr, Johnsson, L. G., Stebbins, W. C., Moody, D. B. and Coombs, S. L. (1976). Hearing loss and cochlear pathology in monkeys after noise exposure. *Acta Otolaryngol.* **81**, 337-343.

Henderson, D., Bielefeld, E. C., Harris, K. C. and Hu, B. H. (2006). The role of oxidative stress in noise-induced hearing loss. *Ear Hear.* **27**, 1-19.

Hume, C. R., Bratt, D. L. and Oesterle, E. C. (2007). Expression of LHX3 and SOX2 during mouse inner ear development. *Gene Expr. Patterns* **7**, 798-807.

Imayoshi, I., Sakamoto, M., Yamaguchi, M., Mori, K. and Kageyama, R. (2010). Essential roles of Notch signaling in maintenance of neural stem cells in developing and adult brains. *J. Neurosci.* **30**, 3489-3498.

Ivanova, A., Signore, M., Caro, N., Greene, N. D., Copp, A. J. and Martinez-Barbera, J. P. (2005). In vivo genetic ablation by Cre-mediated expression of diphtheria toxin fragment A. *Genesis* **43**, 129-135.

Jensen-Smith, H. C., Eley, J., Steyger, P. S., Ludueña, R. F. and Hallworth, R. (2003). Cell type-specific reduction of beta tubulin isotypes synthesized in the developing gerbil organ of Corti. *J. Neurocytol.* **32**, 185-197.

Jones, J. E. and Corwin, J. T. (1996). Regeneration of sensory cells after laser ablation in the lateral line system: hair cell lineage and macrophage behavior revealed by time-lapse video microscopy. *J. Neurosci.* **16**, 649-662.

Kawamoto, K., Izumikawa, M., Beyer, L. A., Atkin, G. M. and Raphael, Y. (2009). Spontaneous hair cell regeneration in the mouse utricle following gentamicin ototoxicity. *Hear. Res.* **247**, 17-26.

Kelley, M. W. (2006). Hair cell development: commitment through differentiation. *Brain Res.* **1091**, 172-185.

Kelley, M. W., Talreja, D. R. and Corwin, J. T. (1995). Replacement of hair cells after laser microbeam irradiation in cultured organs of corti from embryonic and neonatal mice. *J. Neurosci.* **15**, 3013-3026.

Kelly, M. C., Chang, Q., Pan, A., Lin, X. and Chen, P. (2012). Atoh1 directs the formation of sensory mosaics and induces cell proliferation in the postnatal mammalian cochlea in vivo. *J. Neurosci.* **32**, 6699-6710.

Kiernan, A. E., Pelling, A. L., Leung, K. K., Tang, A. S., Bell, D. M., Tease, C., Lovell-Badge, R., Steel, K. P. and Cheah, K. S. (2005). Sox2 is required for sensory organ development in the mammalian inner ear. *Nature* **434**, 1031-1035.

Kuan, C. Y., Schloemer, A. J., Lu, A., Burns, K. A., Weng, W. L., Williams, M. T., Strauss, K. I., Vorhees, C. V., Flavell, R. A., Davis, R. J. et al. (2004). Hypoxia-ischemia induces DNA synthesis without cell proliferation in dying neurons in adult rodent brain. *J. Neurosci.* **24**, 10763-10772.

Lanford, P. J., Shailam, R., Norton, C. R., Gridley, T. and Kelley, M. W. (2000). Expression of Math1 and HES5 in the cochleae of wildtype and Jag2 mutant mice. *J. Assoc. Res. Otolaryngol.* **1**, 161-171.

Lee, Y. S., Liu, F. and Segil, N. (2006). A morphogenetic wave of p27Kip1 transcription directs cell cycle exit during organ of Corti development. *Development* **133**, 2817-2826.

Legendre, K., Safieddine, S., Küssel-Andermann, P., Petit, C. and El-Amraoui, A. (2008). alphaII-betaV spectrin bridges the plasma membrane and cortical lattice in the lateral wall of the auditory outer hair cells. *J. Cell Sci.* **121**, 3347-3356.

Lelli, A., Asai, Y., Forge, A., Holt, J. R. and Géléoc, G. S. (2009). Tonotopic gradient in the developmental acquisition of sensory transduction in outer hair cells of the mouse cochlea. *J. Neurophysiol.* **101**, 2961-2973.

Lenoir, M. and Vago, P. (1997). Does the organ of Corti attempt to differentiate new hair cells after antibiotic intoxication in rat pups? *Int. J. Dev. Neurosci.* **15**, 487-495.

Li, S., Mark, S., Radde-Gallwitz, K., Schlisner, R., Chin, M. T. and Chen, P. (2008). Hey2 functions in parallel with Hes1 and Hes5 for mammalian auditory sensory organ development. *BMC Dev. Biol.* **8**, 20.

Liu, Z., Dearman, J. A., Cox, B. C., Walters, B. J., Zhang, L., Ayrault, O., Zindy, F., Gan, L., Roussel, M. F. and Zuo, J. (2012a). Age-dependent in vivo conversion of mouse cochlear pillar and Deiters' cells to immature hair cells by Atoh1 ectopic expression. *J. Neurosci.* **32**, 6600-6610.

Liu, Z., Walters, B. J., Owen, T., Brimble, M. A., Steigelman, K. A., Zhang, L., Mellado Lagarde, M. M., Valentine, M. B., Yu, Y., Cox, B. C. et al. (2012b). Regulation of p27Kip1 by Sox2 maintains quiescence of inner pillar cells in the murine auditory sensory epithelium. *J. Neurosci.* **32**, 10530-10540.

Lombarte, A., Yan, H. Y., Popper, A. N., Chang, J. S. and Platt, C. (1993). Damage and regeneration of hair cell ciliary bundles in a fish ear following treatment with gentamicin. *Hear. Res.* **64**, 166-174.

Lumpkin, E. A., Collisson, T., Parab, P., Omer-Abdalla, A., Haeberle, H., Chen, P., Doetzlhofer, A., White, P., Groves, A., Segil, N. et al. (2003). Math1-driven GFP expression in the developing nervous system of transgenic mice. *Gene Expr. Patterns* **3**, 389-395.

Madisen, L., Zwingman, T. A., Sunkin, S. M., Oh, S. W., Zariwala, H. A., Gu, H., Ng, L. L., Palmiter, R. D., Hawrylycz, M. J., Jones, A. R. et al. (2010). A robust and high-throughput Cre reporting and characterization system for the whole mouse brain. *Nat. Neurosci.* **13**, 133-140.

Mahendrasingam, S., Beurg, M., Fettiplace, R. and Hackney, C. M. (2010). The ultrastructural distribution of prestin in outer hair cells: a post-embedding immunogold investigation of low-frequency and high-frequency regions of the rat cochlea. *Eur. J. Neurosci.* **31**, 1595-1605.

Mahrt, E. J., Perkel, D. J., Tong, L., Rubel, E. W. and Portfors, C. V. (2013). Engineered deafness reveals that mouse courtship vocalizations do not require auditory experience. *J. Neurosci.* **33**, 5573-5583.

Mak, A. C., Szeto, I. Y., Fritzsch, B. and Cheah, K. S. (2009). Differential and overlapping expression pattern of SOX2 and SOX9 in inner ear development. *Gene Expr. Patterns* **9**, 444-453.

Mellado Lagarde, M. M., Cox, B. C., Fang, J., Taylor, R., Forge, A. and Zuo, J. (2013). Selective ablation of pillar and deiters' cells severely affects cochlear postnatal development and hearing in mice. *J. Neurosci.* **33**, 1564-1576.

Montcouquiol, M. and Kelley, M. W. (2003). Planar and vertical signals control cellular differentiation and patterning in the mammalian cochlea. *J. Neurosci.* **23**, 9469-9478.

Oesterle, E. C., Campbell, S., Taylor, R. R., Forge, A. and Hume, C. R. (2008). Sox2 and JAGGED1 expression in normal and drug-damaged adult mouse inner ear. *J. Assoc. Res. Otolaryngol.* **9**, 65-89.

Oshima, K., Grimm, C. M., Corrales, C. E., Senn, P., Martinez Monedero, R., Géléoc, G. S., Edge, A., Holt, J. R. and Heller, S. (2007). Differential distribution of stem cells in the auditory and vestibular organs of the inner ear. *J. Assoc. Res. Otolaryngol.* **8**, 18-31.

Parietti, C., Vago, P., Humbert, G. and Lenoir, M. (1998). Attempt at hair cell neodifferentiation in developing and adult amikacin intoxicated rat cochleae. *Brain Res.* **813**, 57-66.

Porrello, E. R., Mahmoud, A. I., Simpson, E., Hill, J. A., Richardson, J. A., Olson, E. N. and Sadek, H. A. (2011). Transient regenerative potential of the neonatal mouse heart. *Science* **331**, 1078-1080.

Roberson, D. W., Alosi, J. A. and Cotanche, D. A. (2004). Direct transdifferentiation gives rise to the earliest new hair cells in regenerating avian auditory epithelium. *J. Neurosci. Res.* **78**, 461-471.

Romand, R., Chardin, S. and Le Calvez, S. (1996). The spontaneous appearance of hair cell-like cells in the mammalian cochlea following aminoglycoside ototoxicity. *Neuroreport* **8**, 133-137.

Ruben, R. J. (1967). Development of the inner ear of the mouse: a radioautographic study of terminal mitoses. *Acta Otolaryngol.* **220**, 1-44.

Ryals, B. M. and Rubel, E. W. (1988). Hair cell regeneration after acoustic trauma in adult Coturnix quail. *Science* **240**, 1774-1776.

Rybak, L. P., Whitworth, C. and Scott, V. (1992). Development of endocochlear potential and compound action potential in the rat. *Hear. Res.* **59**, 189-194.

Savary, E., Hugnot, J. P., Chassigneux, Y., Travo, C., Duperray, C., Van De Water, T. and Zine, A. (2007). Distinct population of hair cell progenitors can be isolated from the postnatal mouse cochlea using side population analysis. *Stem Cells* **25**, 332-339.

Shi, F., Kempfle, J. S. and Edge, A. S. (2012). Wnt-responsive Lgr5-expressing stem cells are hair cell progenitors in the cochlea. *J. Neurosci.* **32**, 9639-9648.

Shi, F., Hu, L. and Edge, A. S. (2013). Generation of hair cells in neonatal mice by β-catenin overexpression in Lgr5-positive cochlear progenitors. *Proc. Natl. Acad. Sci. USA* **110**, 13851-13856.

Sinkkonen, S. T., Chai, R., Jan, T. A., Hartman, B. H., Laske, R. D., Gahlen, F., Sinkkonen, W., Cheng, A. G., Oshima, K. and Heller, S. (2011). Intrinsic regenerative potential of murine cochlear supporting cells. *Sci. Rep.* **1**, 26.

Sobkowicz, H. M., Slapnick, S. M. and August, B. K. (1995). The kinocilium of auditory hair cells and evidence for its morphogenetic role during the regeneration of stereocilia and cuticular plates. *J. Neurocytol.* **24**, 633-653.

Steigelman, K. A., Lelli, A., Wu, X., Gao, J., Lin, S., Piontek, K., Wodarczyk, C., Boletta, A., Kim, H., Qian, F. et al. (2011). Polycystin-1 is required for stereocilia structure but not for mechanotransduction in inner ear hair cells. *J. Neurosci.* **31**, 12241-12250.

Stern, C. D. and Fraser, S. E. (2001). Tracing the lineage of tracing cell lineages. *Nat. Cell Biol.* **3**, E216-E218.

Szarama, K. B., Gavara, N., Petralia, R. S., Kelley, M. W. and Chadwick, R. S. (2012). Cytoskeletal changes in actin and microtubules underlie the developing surface mechanical properties of sensory and supporting cells in the mouse cochlea. *Development* **139**, 2187-2197.

Tong, L., Hume, C., Palmiter, R. and Rubel, E. (2011). Ablation of mouse cochlea hair cells by activating the human diphtheria toxin receptor (DTR). Gene targeted to the Pou4f3 locus. In *Abstracts of the 34th Annual Midwinter Research Meeting of the Association for Research in Otolaryngology* (ed. P. A. Santi), Abs. 836, p. 280. Mount Royal, NJ: ARO.

Warchol, M. E. and Corwin, J. T. (1996). Regenerative proliferation in organ cultures of the avian cochlea: identification of the initial progenitors and determination of the latency of the proliferative response. *J. Neurosci.* **16**, 5466-5477.

Warchol, M. E., Lambert, P. R., Goldstein, B. J., Forge, A. and Corwin, J. T. (1993). Regenerative proliferation in inner ear sensory epithelia from adult guinea pigs and humans. *Science* **259**, 1619-1622.

Weber, T., Corbett, M. K., Chow, L. M., Valentine, M. B., Baker, S. J. and Zuo, J. (2008). Rapid cell-cycle reentry and cell death after acute inactivation of the retinoblastoma gene product in postnatal cochlear hair cells. *Proc. Natl. Acad. Sci. USA* **105**, 781-785.

White, P. M., Doetzlhofer, A., Lee, Y. S., Groves, A. K. and Segil, N. (2006). Mammalian cochlear supporting cells can divide and trans-differentiate into hair cells. *Nature* **441**, 984-987.

Xiang, M., Gao, W. Q., Hasson, T. and Shin, J. J. (1998). Requirement for Brn-3c in maturation and survival, but not in fate determination of inner ear hair cells. *Development* **125**, 3935-3946.

Yamamoto, N., Tanigaki, K., Tsuji, M., Yabe, D., Ito, J. and Honjo, T. (2006). Inhibition of Notch/RBP-J signaling induces hair cell formation in neonate mouse cochleas. *J. Mol. Med.* **84**, 37-45.

Zheng, J. L. and Gao, W. Q. (1997). Analysis of rat vestibular hair cell development and regeneration using calretinin as an early marker. *J. Neurosci.* **17**, 8270-8282.

Zheng, J. L. and Gao, W. Q. (2000). Overexpression of Math1 induces robust production of extra hair cells in postnatal rat inner ears. *Nat. Neurosci.* **3**, 580-586.

Zheng, J., Shen, W., He, D. Z., Long, K. B., Madison, L. D. and Dallos, P. (2000). Prestin is the motor protein of cochlear outer hair cells. *Nature* **405**, 149-155.

Zine, A. and de Ribaupierre, F. (1998). Replacement of mammalian auditory hair cells. *Neuroreport* **9**, 263-268.

Zine, A., Aubert, A., Qiu, J., Therianos, S., Guillemot, F., Kageyama, R. and de Ribaupierre, F. (2001). Hes1 and Hes5 activities are required for the normal development of the hair cells in the mammalian inner ear. *J. Neurosci.* **21**, 4712-4720.

© 2014. Published by The Company of Biologists Ltd | Development (2014) 141, 1599 doi:10.1242/dev.109421

CORRECTION

Spontaneous hair cell regeneration in the neonatal mouse cochlea *in vivo*

Brandon C. Cox[1,2,*], Renjie Chai[3,4,*], Anne Lenoir[1,5], Zhiyong Liu[1,6], LingLi Zhang[1], Duc-Huy Nguyen[3], Kavita Chalasani[3], Katherine A. Steigelman[1,6], Jie Fang[1], Edwin W. Rubel[7], Alan G. Cheng[3,‡] and Jian Zuo[1,‡]

[1]Department of Developmental Neurobiology, St. Jude Children's Research Hospital, Memphis, TN 38105, USA. [2]Department of Pharmacology, Southern Illinois University School of Medicine, Springfield, IL 62702, USA. [3]Department of Otolaryngology-Head and Neck Surgery, Stanford University School of Medicine, Stanford, CA 94305, USA. [4]Key Laboratory for Developmental Genes and Human Disease, Ministry of Education, Institute of Life Sciences, Southeast University, Nanjing 210096, China. [5]Universite Paris-Diderot, UFR Sciences du vivant, Paris 7, Paris, France. [6]Department of Anatomy and Neurobiology, University of Tennessee Health Science Center, Memphis, TN 38163, USA. [7]Virginia Merrill Bloedel Hearing Research Center, Department of Otolaryngology-Head and Neck Surgery, University of Washington School of Medicine, Seattle, WA, 98195-7923, USA.
*These authors contributed equally to this work

‡Authors for correspondence (aglcheng@stanford.edu; jian.zuo@stjude.org)

There was an error published in *Development* **141**, 816-829.

Edwin W. Rubel was omitted from the authorship of the paper. The correct author list and affiliations appears above.

In addition the Acknowledgements and Author contributions sections should read as follows.

Acknowledgements
We thank L. Tong and R. Palmiter (University of Washington) for Pou4f3DTR/+ mice and discussion; S. Baker (St. Jude) for Atoh1-CreERTM mice and discussion; R. Kageyama (Kyoto University) for Hes5-nlsLacZ mice; P. Chambon (Institut Genetique Biologie Moleculaire Cellulaire) for the CreERT2 construct; S. Heller (Stanford University) for the anti-espin antibody and critical reading, J. Corwin, J. Burns and other members of the Corwin laboratory (University of Virginia) as well as members of our laboratories for discussion and critical comments; S. Connell, V. Frohlich, Y. Ouyang and J. Peters (St. Jude) for expertise in confocal imaging; A. Xue, V. Nookala, N. Pham, A. Vu, G. Huang and W. Liu (Stanford University) for excellent technical support; and L. Boykins (University of Memphis), R. Martens and J. Goodwin (University of Alabama) for assistance and expertise in scanning electron microscopy.

Author contributions
B.C.C., R.C., E.W.R., A.G.C. and J.Z. developed the concepts or approach; B.C.C., R.C., A.L., Z.L., L.Z., D.-H.N., K.C., K.A.S., J.F., A.G.C. and J.Z. performed experiments or data analysis; B.C.C., R.C., A.G.C. and J.Z. prepared or edited the manuscript prior to submission.

The authors apologise to readers for this mistake.

SCIENTIFIC REPORTS

OPEN

SUBJECT AREAS:
HAIR CELL
INNER EAR
GENE REGULATION

Received
18 August 2014

Accepted
13 October 2014

Published
3 November 2014

Correspondence and requests for materials should be addressed to J.Z. (jian.zuo@stjude.org)

Generation of *Atoh1-rtTA* transgenic mice: a tool for inducible gene expression in hair cells of the inner ear

Brandon C. Cox[1,2,3], Jennifer A. Dearman[3], Joseph Brancheck[1], Frederique Zindy[4], Martine F. Roussel[4] & Jian Zuo[3]

[1]Department of Pharmacology, Southern Illinois University, School of Medicine, Springfield, IL 62702, [2]Department of Surgery, Division of Otolaryngology, Southern Illinois University, School of Medicine, Springfield, IL 62702, [3]Department of Developmental Neurobiology, St. Jude Children's Research Hospital, Memphis, TN 38105, [4]Department of Tumor Cell Biology. St. Jude Children's Research Hospital, Memphis, TN 38105.

Atoh1 is a basic helix-loop-helix transcription factor that controls differentiation of hair cells (HCs) in the inner ear and its enhancer region has been used to create several HC-specific mouse lines. We generated a transgenic tetracycline-inducible mouse line (called *Atoh1-rtTA*) using the *Atoh1* enhancer to drive expression of the reverse tetracycline transactivator (rtTA) protein and human placental alkaline phosphatase. Presence of the transgene was confirmed by alkaline phosphatase staining and rtTA activity was measured using two tetracycline operator (TetO) reporter alleles with doxycycline administered between postnatal days 0–3. This characterization of five founder lines demonstrated that *Atoh1-rtTA* is expressed in the majority of cochlear and utricular HCs. Although the tetracycline-inducible system is thought to produce transient changes in gene expression, reporter positive HCs were still observed at 6 weeks of age. To confirm that *Atoh1-rtTA* activity was specific to *Atoh1*-expressing cells, we also analyzed the cerebellum and found rtTA-driven reporter expression in cerebellar granule neuron precursor cells. The *Atoh1-rtTA* mouse line provides a powerful tool for the field and can be used in combination with other existing Cre recombinase mouse lines to manipulate expression of multiple genes at different times in the same animal.

Conditional gene expression enables the temporal study of genes during development and in adulthood. This method also allows for cell-type specific gene manipulation and alleviates embryonic lethality which can occur when certain genes are overexpressed or deleted in the germline. The Cre-mediated recombination system (Cre/loxP) is the most common method to delete or ectopically express genes in a cell-type specific manner, with temporal control of gene expression achieved by fusion of Cre recombinase with a modified tamoxifen-inducible estrogen receptor ($CreER^{TM}$ or $CreER^{T2}$) (reviewed in[1]). Tetracycline-inducible mouse models (Tet-On or Tet-Off) can also be used for conditional gene expression and in contrast to Cre/loxP, gene expression changes are transient[2,3]. In some cases one needs to manipulate expression of multiple genes in two different cell types or in the same cell type but at different ages. This can be achieved by combining Cre/loxP and tetracycline-inducible mouse models. Unfortunately there are few tetracycline-inducible mouse lines with cell-type specific expression available, thus warranting the development of new models.

The Tet-On system uses a reverse tetracycline transactivator (rtTA) protein that binds to the promoter and activates transcription of a second transgene which contains a tetracycline operator (TetO). The rtTA protein can only bind to TetO and activate transcription in the presence of doxycycline (a more potent analogue of tetracycline). Once doxycycline is removed, transcription will cease since rtTA can no longer bind to TetO, allowing for transient control of gene expression (Figure 1A)[2,3]. Cell-type specific expression can be achieved using specific promoters or enhancers to express the rtTA protein. This mechanism is distinct from the Cre/loxP system, and thus the two methods of conditional gene expression can be combined.

Atoh1, also called *Math1* in mice, is the mammalian homolog of the Drosophila gene, *atonal*, and is a basic helix-loop-helix transcription factor that controls differentiation of hair cells (HCs) in the inner ear[4] and proliferation of granule neuron precursor cells in the cerebellum[5]. The 1.7 kb enhancer element located in the 3′ untranslated region of *Atoh1*[6] has been used to generate several mouse lines: *Atoh1-Cre*[7], *Atoh1-*$CreER^{TM}$[8], *Atoh1-*$CreER^{T2}$[9], and *Atoh1-eGFP*[10]. Because each of these mouse models has Cre or eGFP expression in HCs and

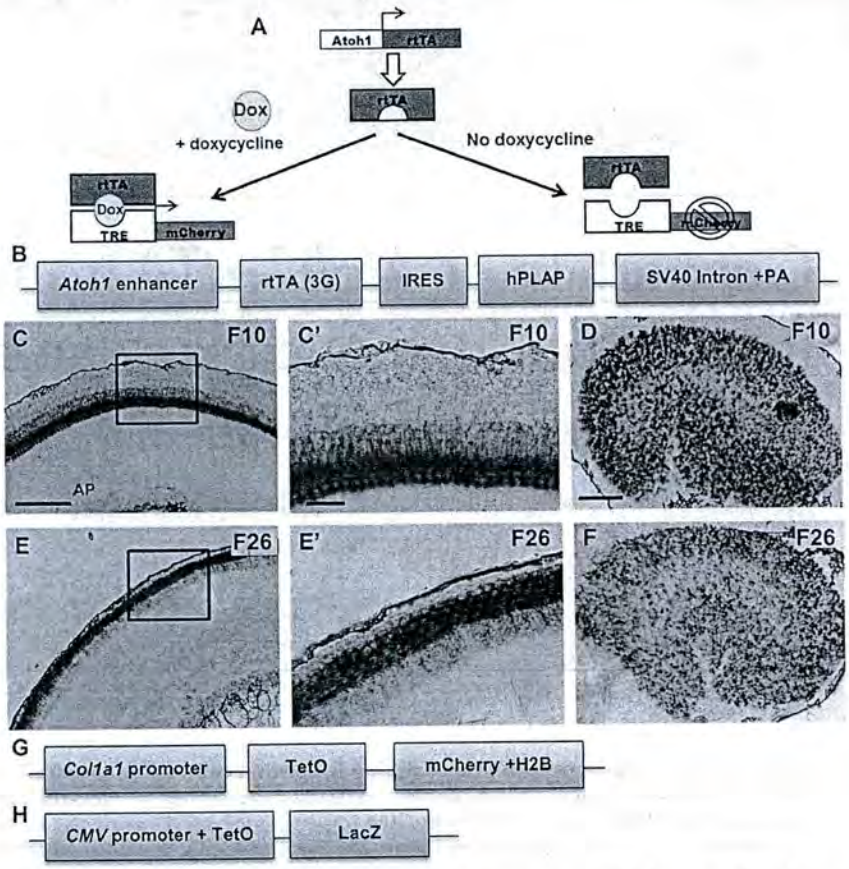

Figure 1 | Components of the Tet-On system and alkaline phosphatase staining. (A) Diagram explaining the Tet-On system. (B) Modified *Atoh1-CreER-IRES-hPLAP-SV40* Intron- polyadenylation construct[8] showing replacement of the *CreER* sequence with the *3G rtTA* sequence. Representative alkaline phosphatase (AP) staining images of F10 and F26 showing the presence of the *Atoh1-rtTA* transgene in the apical turn of the P0 cochlea (C, E) and utricle (D, F). (C′ and E′) High magnification images of region labeled by the black squares in (C) and (E). Scale bars: 100 μm in (C–F) and 20 μm in (C′) and (E′). Schematic of the *TetO-mCherry* (G) and *TetO-LacZ* (H) reporter alleles.

cerebellar granule cells, we used the same enhancer element to generate a HC-specific Tet-On mouse model. Here, we describe the generation and characterization of an *Atoh1-rtTA* mouse line in the inner ear.

Results

The *CreER* sequence in the *Atoh1-CreER-internal ribosome entry site (IRES)-human placental alkaline phosphatase (hPLAP)-SV40* intron-polyadenylation construct *(Atoh1-CreER-IRES-hPLAP-SV40-polyA)* was replaced with a *3G rtTA* (Figure 1B). This 3rd generation rtTA has reduced levels of basal expression and increased sensitivity to doxycycline compared to Tet-On and Tet-On Advanced systems[11]. After pronuclear injection, seven founders were produced and the presence of the transgene was confirmed by Southern blot and PCR analysis. All founders went through germline transmission. However, two founder lines did not breed well; thus we assessed rtTA activity in five founder lines (F7, F10, F12, F23, and F26), each of them showing expression of hPLAP in HCs of the cochlea and utricle at postnatal day (P) 0 (Figure 1C–F).

We used two rtTA reporter alleles since their reporter activity varied. The *TetO-mCherry* reporter is a knock-in allele where the TetO element and *mCherry* coding sequence fused to histone H2B were inserted downstream of the endogenous *collagen type 1, alpha 1* (*Col1a1*) promoter (Figure 1G)[12]. This reporter is robust since the *Col1a1* promoter is strongly expressed in epithelial cells[13], and the mCherry molecule provides bright endogenous fluorescence that is photostable[14]. In contrast, the *TetO-LacZ* reporter is a transgenic allele where *LacZ* is under the control of the human cytomegalovirus early promoter (CMV) fused to the TetO element (Figure 1H)[15]. *LacZ* expression is variable, requiring X-gal staining or an anti-βgalactosidase (βgal) antibody for detection.

Reporter alleles were first tested for basal activity at P3 with *TetO-reporter*$^{+ve}$ mice administered doxycycline between P0–P3, but in the absence of the *rtTA* allele. In *TetO-mCherry*$^{+ve}$ mice, no mCherry^{+ve} cells were seen in the sensory region of the cochlea or utricle (Figure 2A, B). However there was an apical-to-basal gradient of increasing mCherry^{+ve} cells in the spiral ganglion (SGN) region of the cochlea (Figure 2A–A′) as well as several mCherry^{+ve} cells in the utricular stroma (Figure 2B′). In *TetO-LacZ*$^{+ve}$ mice, no LacZ^{+ve} cells were observed in the cochlea or SGN; however, in the utricle, several LacZ^{+ve} supporting cells (SCs) were observed, but no HCs or stromal cells were labeled (Figure 2C–C″). The presence of reporter^{+ve} cells in the absence of the rtTA protein has been reported previously in other organ systems[15].

We also tested for leakiness of rtTA activity in the absence of doxycycline using *Atoh1-rtTA*$^{+ve}$; *TetO-mCherry*$^{+ve}$ or *Atoh1-rtTA*$^{+ve}$; *TetO-LacZ*$^{+ve}$ mice from the F7 lineage analyzed at P3. No mCherry^{+ve} cells were observed in the sensory regions of the cochlea or utricle; however, there was an apical-to-basal gradient of increasing mCherry^{+ve} cells in the SGN region (Figure 2D–D′) and mCherry^{+ve} cells in the utricular stroma (Figure 2E–E′), similar to the basal activity seen in *TetO-mCherry*$^{+ve}$ controls that received doxycycline but lacked the *rtTA* allele (Figure 2A–B′). No LacZ^{+ve} cells were detected in *Atoh1-rtTA*$^{+ve}$; *TetO-LacZ*$^{+ve}$ cochleae

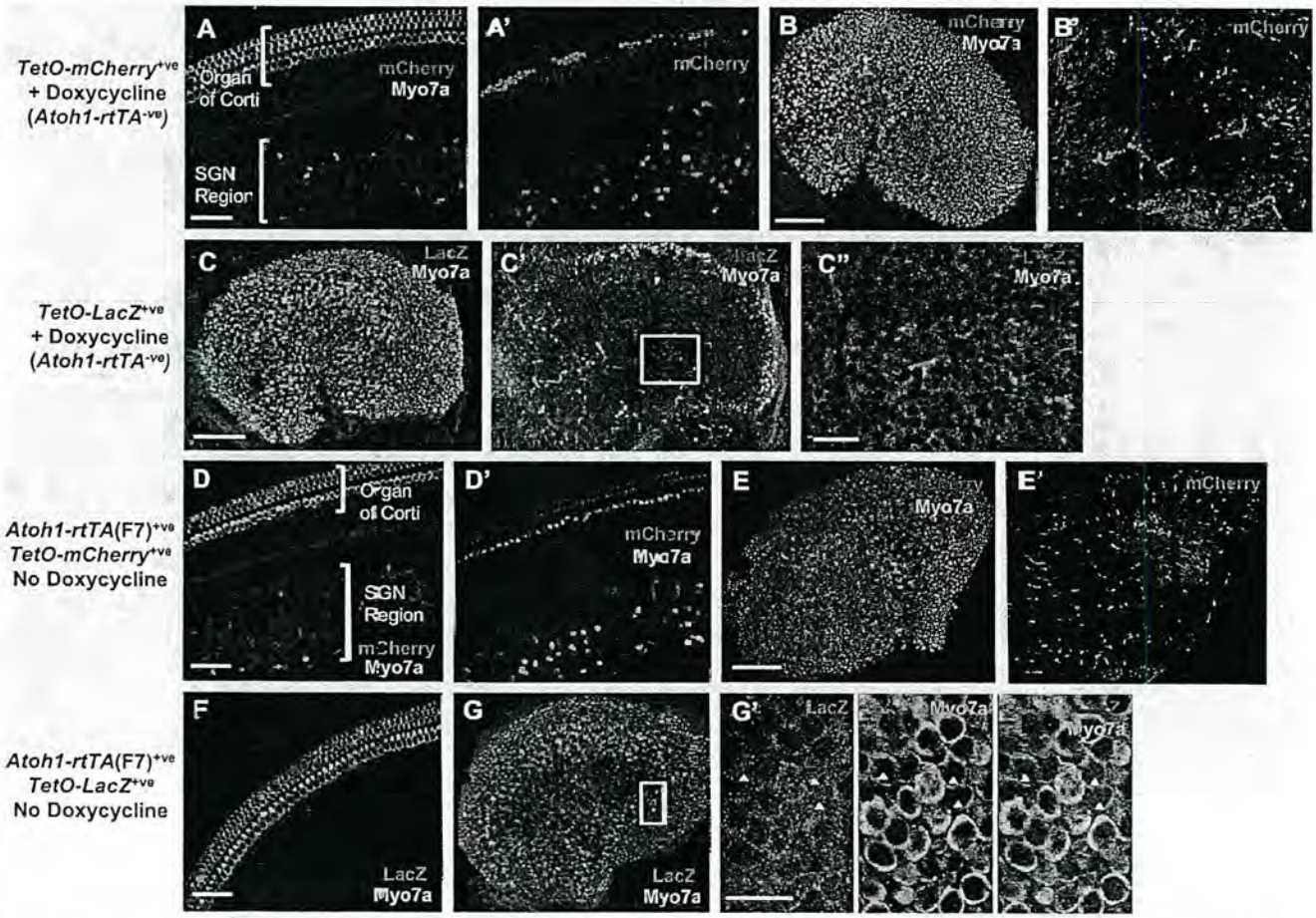

Figure 2 | Basal activity of *TetO-reporters* and *Atoh1-rtTA*(F7) activity in the absence of doxycycline. Representative confocal images of a *TetO-mCherry*$^{+ve}$ (*Atoh1-rtTA*$^{-ve}$) control cochlea (A–A′) and utricle (B–B′) at P3 from mice that were administered doxycycline to test for basal expression of the *TetO-mCherry* reporter. mCherry^{+ve} cells were detected in the SGN region of the cochlea (A–A′) and in the utricular stroma (B–B′). Note in A′ the labeled cells in the organ of Corti are red blood cells. No mCherry^{+ve} cells were detected in the sensory region of either the cochlea or utricle. (C–C′) Representative confocal images of a *TetO-LacZ*$^{+ve}$ (*Atoh1-rtTA*$^{-ve}$) control utricle at P3 from mice that were administered doxycycline to test for basal expression of the *TetO-LacZ* reporter. Some LacZ^{+ve} SCs but no LacZ^{+ve} HCs were detected. (C″) High magnification images of the region outlined by the white square in C′. Representative confocal images of an un-induced *Atoh1-rtTA*(F7)$^{+ve}$; *TetO-mCherry*$^{+ve}$ control cochlea (D–D′) and utricle (E–E′) at P3 that did not receive doxycycline. mCherry^{+ve} (red) cells were detected in the SGN region of the basal turn of the cochlea (D–D′) and in the utricular stroma (E–E′). No mCherry^{+ve} cells were detected in the sensory region of either the cochlea or utricle. Representative confocal image of an un-induced *Atoh1-rtTA*(F7)$^{+ve}$; *TetO-LacZ*$^{+ve}$ control cochlea (F) and utricle (G–G′) at P3 that did not receive doxycycline. Several HCs (myo7a^{+ve}, green) expressed LacZ (red) in the medial region of the utricle (G–G′) and no LacZ^{+ve} cells were detected in the cochlea (F). (G′) High magnification image of the region outlined by the white square in (G). Arrowheads denote LacZ^{+ve} HCs. Myo7a (green) was used to label HCs in most panels. Scale bar: 50 μm in (A–A′), (D–D′), and (F), 100 μm in (B–C′), (E), and (G), and 20 μm in (C″) and (G′).

(Figure 2F), while in the utricle some LacZ^{+ve} SCs were observed and a small percentage of HCs in the medial region were LacZ^{+ve} (Figure 2G–G′).

Each of the *Atoh1-rtTA* founder lines was bred with a *TetO-mCherry* or a *TetO-LacZ* reporter mouse and double-transgenic offspring (*Atoh1-rtTA*$^{+ve}$; *TetO-reporter*$^{+ve}$) administered doxycycline between P0–P3 were evaluated at P3 for rtTA activity. The five *Atoh1-rtTA* founders bred with the *TetO-mCherry* reporter showed robust expression of mCherry^{+ve} cochlear HCs: F7 = 99.6 ± 0.1%, F10 = 99.7 ± 0.2%, F12 = 98.2 ± 0.4%, F23 = 69.6 ± 11.5%, and F26 = 94.4 ± 1.6% (mCherry^{+ve} HCs expressed as a percentage of total HCs, n = 3, Figure 3A–E′, K). There was no significant difference in the number of mCherry^{+ve} cells between inner and outer HCs or across cochlea turns for any founder line. In addition, the intensity of the mCherry reporter was very consistent across all turns of the cochlea and in all founders (Figure 3A–E′). However, there were variations in the cell type-specificity of mCherry expression (Table 1). F26 was the only founder in which mCherry expression was specific to HCs. F7, F10, and F23 each had mCherry^{+ve} HCs in all turns of the cochlea. In apical and middle turns, mCherry expression was only observed in HCs. However in the basal turn of these founders, there were some mCherry^{+ve} inner phalangeal cells (IPhCs) (a SC subtype that surrounds inner HCs) and a few mCherry^{+ve} cells in the greater epithelial ridge (GER). Lastly, F12 had HC-specific mCherry labeling only in the apex. In addition to mCherry^{+ve} HCs, the middle turn had few mCherry^{+ve} IPhCs, which increased in number in the basal turn.

The cochlea of *Atoh1-rtTA; TetO-LacZ* mice also showed variability among the five founders: F7 = 77.0 ± 11.0%, F10 = 85.8 ± 3.3%, F12 = 84.1 ± 4.6%, F23 = 63.5 ± 6.8%, and F26 = 78.7 ± 2.8% (LacZ^{+ve} HCs expressed as a percentage of total HCs, n = 3–4, Figure 3F–J′, L). There was no significant difference in the number of LacZ^{+ve} cells between inner and outer HCs or across cochlear turns in any founder. All founders had LacZ expression in other cells besides HCs (Table 1). In F7 and F26, LacZ expression was the most

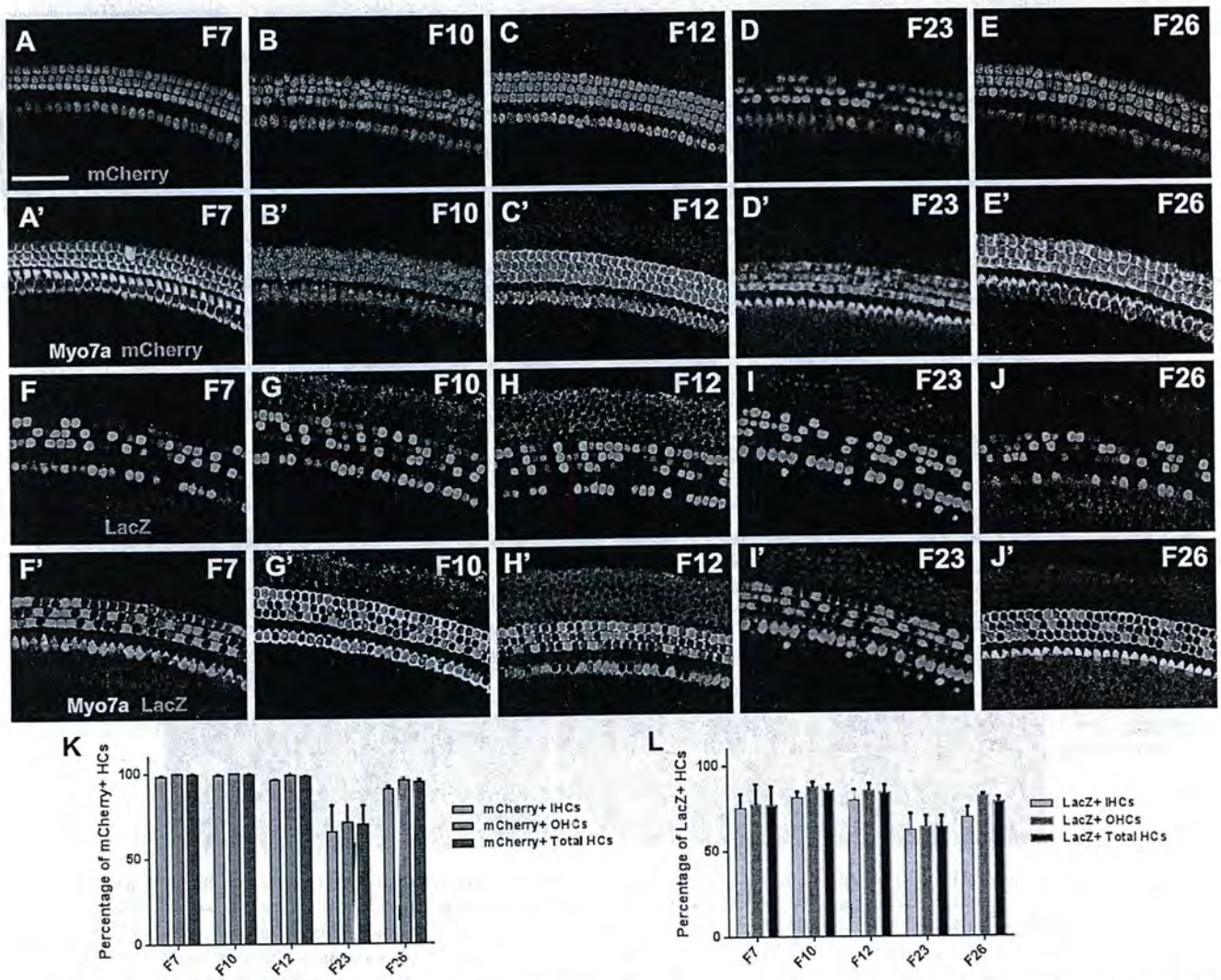

Figure 3 | *Atoh1-rtTA* activity in the cochlea. Representative confocal images of mCherry^{+ve} (red) cells in the middle turn of each founder line breed with the *TetO-mCherry* reporter at P3 (A–E) and corresponding merged images where HCs were labeled with myosin VIIa (Myo7a, green) (A′–E′). Representative confocal images of LacZ^{+ve} (red) cells in the middle turn of each founder line breed with the *TetO-LacZ* reporter at P3 (F–J) and corresponding merged images where HCs were labeled with Myo7a (green) (F′–J′). (K) Percentage of Myo7a^{+ve} cells that express mCherry in each founder line, normalized to the number of total Myo7a^{+ve} cells in the same region. (L) Percentage of Myo7a^{+ve} cells that express LacZ in each founder line, normalized to the number of total Myo7a^{-ve} cells in the same region. Data are expressed as mean ± S.E.M for an *n* of 3–4. IHC, inner hair cells; OHC, outer hair cells. Scale bar: 50 μm.

specific to HCs with both lines having few LacZ^{+ve} IPhCs in the basal turn. There were also some LacZ^{+ve} cells in the SGN region of the basal turn for F26. In F23, LacZ expression was specific to HCs only in the apical turn with a moderate amount of LacZ^{+ve} IPhCs and cells in the GER in the middle turn that increased in the basal turn. Lastly, F10 had some LacZ^{+ve} IPhCs and GER cells in all three cochlear turns, while F12 had an apical-to-basal gradient of increasing quantities of LacZ^{+ve} IPhCs. In contrast to the consistent mCherry intensity, LacZ intensity varied from cell to cell across all founders (Figure 3F–J′).

In *Atoh1-rtTA; TetO-mCherry* utricles, the percentage of total mCherry^{+ve} HCs were: F7 = 78.2 ± 0.6%, F10 = 85.6 ± 0.5%, F12 = 73.7 ± 4.1%, F23 = 48.6 ± 6.4%, and F26 = 79.4 ± 3.6% (mCherry^{+ve} HCs expressed as a percentage of total HCs, n = 3, Figure 4A–E, K). Several of the *Atoh1-rtTA; TetO-mCherry* founders showed a significant difference in the percentage of mCherry^{+ve} HCs

Table 1 | Summary of Atoh1-rtTA activity in non-hair cells of the cochlea

	F7	F10	F12	F23	F26
TetO-mCherry	Base = Few GER, Several IPhC	Base = Few GER, Several IPhC	Middle = Few IPhC Base = Moderate IPhC	Base = Few GER, Several IPhC	N/A
TetO-LacZ	Base = Few IPhC	Apex, Middle, and Base = Few IPhC and GER	Apical to basal gradient of increasing IPhCs	Middle = Few IPhC and GER Base = Moderate IPhC and GER	Base = Few IPhC, Few SGC

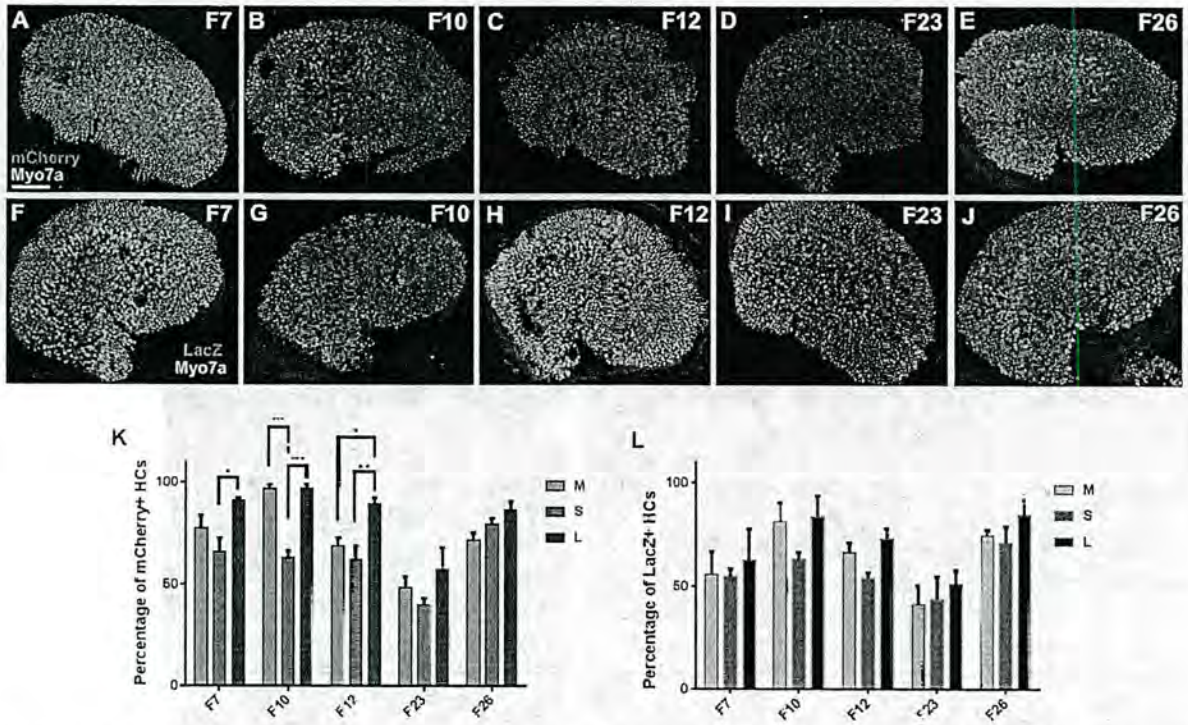

Figure 4 | *Atoh1-rtTA* activity in the utricle. (A–E) Representative confocal images of mCherry^{+ve} (red) cells and Myo7a-labeled HCs (green) in the utricle for each founder line breed with the *TetO-mCherry* reporter at P3. (F–J) Representative confocal images of LacZ^{+ve} (red) cells and Myo7a-labeled HCs (green) in the utricle for each founder line breed with the *TetO-LacZ* reporter at P3. (K) Percentage of Myo7a^{+ve} cells that express mCherry in utricular regions of each founder line, normalized to the number of total Myo7a^{+ve} cells in the same region. (L) Percentage of Myo7a^{+ve} cells that express LacZ in utricular regions of each founder line, normalized to the number of total Myo7a^{+ve} cells in the same region. Data are expressed as mean ± S.E.M for an *n* of 3. Statistical differences between regions were obtained using a two-way ANOVA followed by a Tukey's posthoc test. *$p < 0.05$, **$p < 0.01$, ***$p < 0.001$. M, medial; S, striolar; L, lateral Scale bar: 100 μm.

in different regions of the utricle (Figure 4K). This included a difference between striolar and lateral regions in F7, F10, and F12 and a difference between medial and striolar regions in F10. All founders had varying numbers of mCherry^{+ve} SCs that were found across all regions of the utricle with F7 and F10 having the fewest and F12 having the most. Lastly, the mCherry intensity varied from cell to cell across all founders (Figure 4A–E). We also observed mCherry^{+ve} HCs in the lateral and superior cristae.

In contrast, fewer numbers of labeled cells were detected in *Atoh1-rtTA; TetO-LacZ* utricles: F7 = 57.7 ± 9.9%, F10 = 76.0 ± 7.3%, F12 = 64.5 ± 0.6%, F23 = 45.4 ± 8.8%, and F26 = 76.8 ± 5.8% (LacZ^{+ve} HCs expressed as a percentage of total HCs, $n = 3$, Figure 4F–J, L). There was no significant difference in the number of LacZ^{+ve} HCs among utricular regions, however all founder lines had LacZ^{-ve} SCs with F7 and F26 having the fewest and F23 and F12 having the most. LacZ intensities also varied with all founders having a mosaic expression pattern throughout the utricle (Figure 4F–J). We also observed LacZ^{+ve} HCs in the lateral and superior cristae.

During postnatal development of the cerebellum, *Atoh1* is expressed in proliferating granule neuron precursors (GNPs) of the external granule layer[5]. We therefore assessed mCherry expression in cerebella of the five *Atoh1-rtTA; TetO-mCherry* transgenic lines at P3, after doxycycline treatment was administered from P0–P3. We observed mCherry^{+ve} GNPs in all transgenic lines with F7, F12, and F26 having the most labeled cells (Figure 5A–J′). In uninduced negative controls, which did not receive doxycycline, no mCherry^{+ve} cells were observed in the cerebellum (Figure 5P–P′). This finding confirms that *Atoh1-rtTA* activity occurs in *Atoh1*-expressing cells in the cerebellum. We also examined the rest of the brain and only observed mCherry^{+ve} cells in the hippocampus of F12, F23, and F26 (Figure 5K–O′). No other brain region had mCherry expression. This misexpression of mCherry in the hippocampus of three founder lines matches the eGFP expression seen in *Atoh1-eGFP* mice which also use the *Atoh1* enhancer element to drive expression of eGFP[16]. However *Atoh1-eGFP* mice have eGFP expression in the cortex which was not observed in our model[16].

Additional control experiments were performed with *Atoh1-rtTA* mice of the F7 lineage which showed strong and consistent rtTA activity in cochlear and utricular HCs and was HC-specific in apical and middle turns of the cochlea. These included measuring transient expression of TetO reporters in inner ear tissues and the hearing ability of mice containing the newly generated Atoh1-rtTA allele.

The Tet-On system is designed to produce transient changes in gene expression since the rtTA protein can no longer bind to TetO and activate transcription once doxycycline is removed[2,3]. To measure transient effects in our system, we used *Atoh1-rtTA* mice of the F7 lineage bred with *TetO-mCherry* or *TetO-LacZ* reporter mice and administered doxycycline from P0–P3. The cochlea and utricle were analyzed at P7, P21, and 6 weeks of age. In *Atoh1-rtTA*$^{+ve}$; *TetO-LacZ*$^{+ve}$ mice, the majority of cochlear and utricular HCs retained expression of LacZ at all ages tested and no HC loss was detected (Figure 6A–B). A similar expression pattern of mCherry^{+ve} HCs was seen in *Atoh1-rtTA*$^{+ve}$; *TetO-mCherry*$^{+ve}$ mice. However outer HC loss was detected at P21 which worsened at 6 weeks of age, but inner HCs and utricular HCs remained intact (Figure 6C–E). Since the Tet-On system requires the presence of both the rtTA protein and doxycycline for gene expression to occur (Figure 1A) and the *Atoh1-rtTA* transgene we generated uses the *Atoh1* enhancer element to drive expression of both rtTA and hPLAP (Figure 1B), we performed alkaline phosphatase staining in the cochlea and utricle at 6 weeks

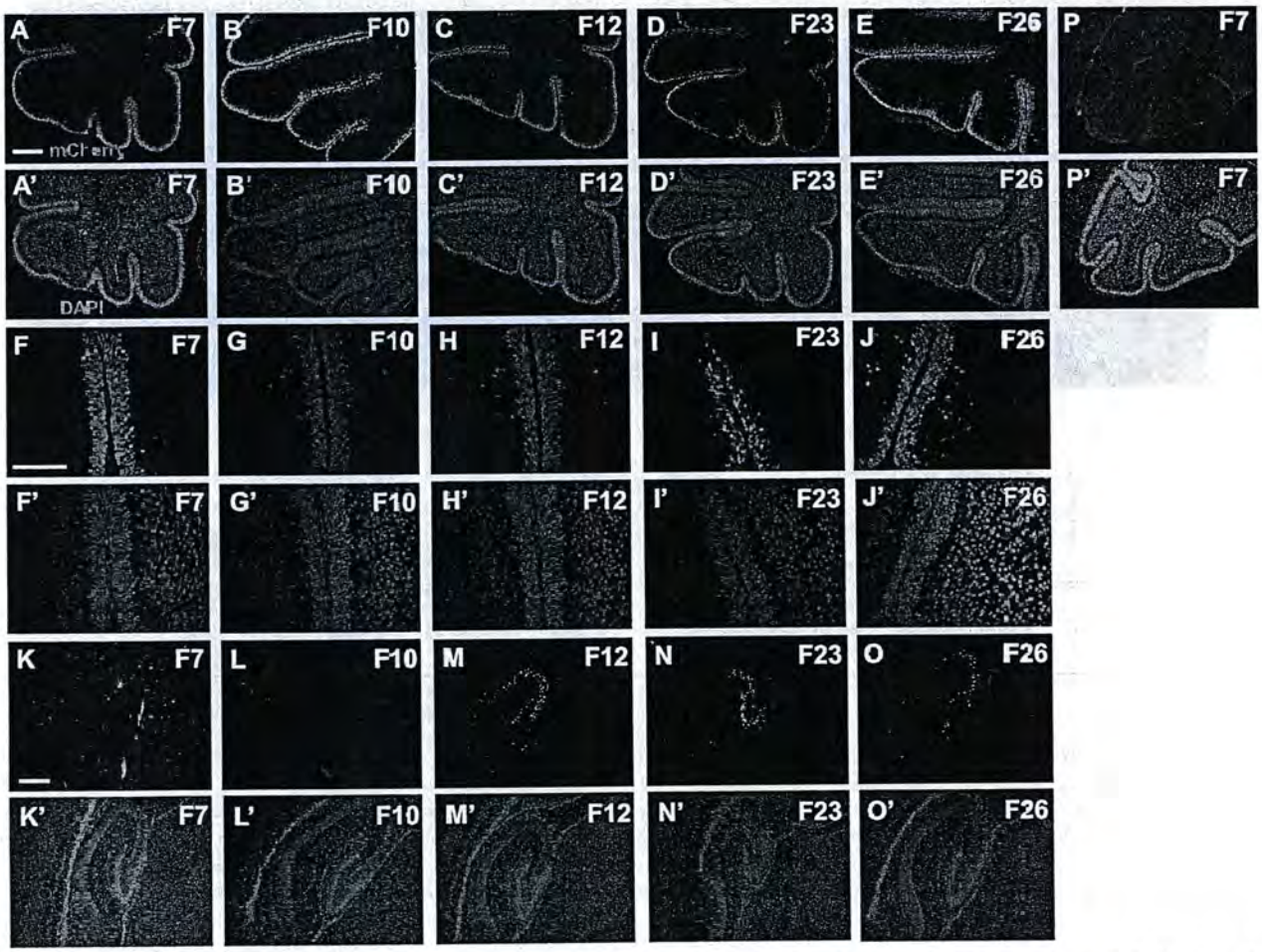

Figure 5 | *Atoh1-rtTA* activity in the cerebellum and hippocampus. Representative images of mCherry^{+ve} (red) cells in the cerebella (A–J′) and hippocampus (K–O′) of each founder line at P3 after doxycycline administration from P0–P3. (P–P′) un-induced control images of *Atoh1-rtTA*(F7)$^{+ve}$; *TetO-LacZ*$^{+ve}$ cerebella without doxycycline induction. Nuclei are labeled by DAPI (blue). Scale bars: 200 μm.

of age to determine whether expression of the transgene persists. Faint alkaline phosphatase staining was present in the utricle of *Atoh1-rtTA*$^{+ve}$ mice from the F7 lineage (Figure 6G) suggesting that the transgene is still expressed at 6 weeks of age. However no staining was observed in the cochlea (Figure 6F).

Finally we measured the hearing ability of *Atoh1-rtTA* mice using evoked auditory brainstem response (ABR) to investigate whether the *Atoh1-rtTA* transgene had any negative effects on cochlear function. ABR was performed on 3 month old *Atoh1-rtTA*$^{+ve}$; *TetO-mCherry*$^{+ve}$ mice of the F7 lineage without administration of doxycycline and littermate controls that lacked both the *rtTA* and *mCherry* alleles. There was no significant difference in ABR responses between groups at any of the frequencies tested (Figure 7). Thus we conclude that *Atoh1-rtTA* mice have normal hearing and the *Atoh1-rtTA* transgene had no effect on genes required for hearing function.

Discussion

We have created a new transgenic mouse model using the tetracycline-inducible system to target HCs in the inner ear and provided a thorough characterization of rtTA activity in five founder lines using two *TetO-reporter* alleles. Differences in rtTA activity among founders were expected since the *Atoh1-rtTA* mouse lines are transgenics. Thus each founder likely has a different insertion site and a different copy number of the transgene. In summary, F7, F10, F12, and F26 showed rtTA activity in the majority of cochlear HCs (94–99% with *TetO-mCherry* and 77–85% with *TetO-LacZ*), while F23 was less robust, labeling 70% of HCs with *TetO-mCherry* and 64% with *TetO-LacZ*. F26 was the most specific to HCs, but had highly variable LacZ intensity levels which may suggest a lower level of rtTA expression. LacZ intensity levels were more robust in F7, F10, and F12, but *Atoh1-rtTA* activity was also detected in other cell types. F7 showed non-HC reporter expression only in the basal turn, while F10 and F12 labeled other cells in all turns of the cochlea. Therefore F7 provides strong and consistent rtTA activity in cochlear HCs and was HC-specific in apical and middle turns of the cochlea.

In control experiments for basal activity of the reporter lines and leakiness of the un-induced *Atoh1-rtTA* allele, there was a similar expression pattern of mCherry^{+ve} cells in the SGN of the cochlea, mCherry^{+ve} cells in the utricular stroma, as well as some LacZ^{+ve} SCs in the utricle. The presence of reporter^{+ve} cells in the absence of the rtTA protein has been reported previously in other organ systems[15] and thus these reporter^{+ve} cells can be ignored in the characterization of the founder lines since they are not related to *Atoh1-rtTA*. The *TetO-mCherry* and *TetO-LacZ* reporter lines are still useful to measure *Atoh1-rtTA*-driven activity since no HCs were labeled in the cochlea or utricle and only a few SCs were labeled by LacZ in the utricle. However we observed a small percentage of LacZ^{+ve} HCs in the medial region of the utricle in un-induced *Atoh1-rtTA*$^{+ve}$; *TetO-LacZ*$^{+ve}$ mice from the founder 7 lineage suggesting that a few utricular HCs can express LacZ without doxycycline. Yet no labeled HCs were observed when the *TetO-mCherry* reporter was used in un-induced negative control experiments. Taken together this data

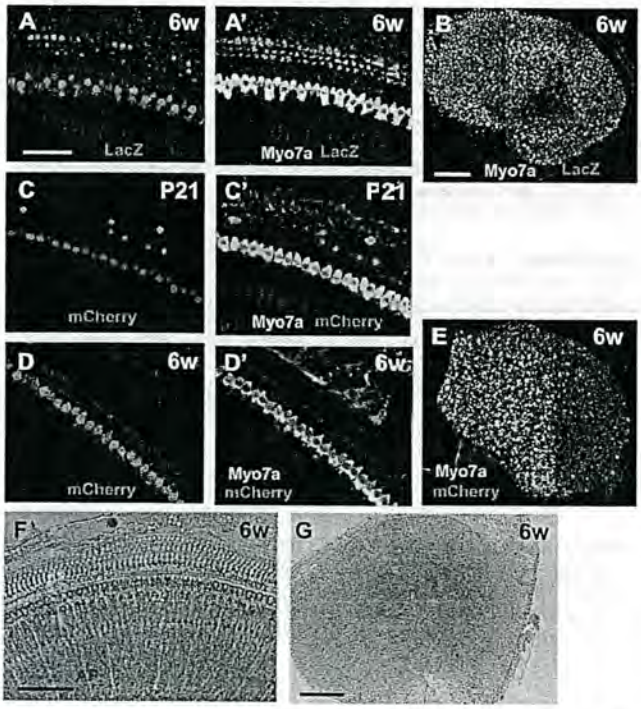

Figure 6 | TetO-reporter expression was still present at 6 weeks of age. Representative confocal images of LacZ^{+ve} (red) cells in the middle cochlear turn (A) and utricle (B) of *Atoh1-rtTA*(F7)$^{+ve}$; *TetO-LacZ*$^{+ve}$ mice at 6 weeks of age after doxycycline treatment ended at P3. (A') is a merged image with HCs labeled by myosin VIIa (Myo7a, green). Representative confocal images of mCherry^{+ve} (red) cells in the middle cochlear turn of *Atoh1-rtTA*(F7)$^{+ve}$; *TetO-mCherry*$^{+ve}$ mice at P21 (C) and 6 weeks of age (D) and in the utricle at 6 weeks of age (E) after doxycycline treatment ended at P3. (C', D') are merged images with HCs labeled by myosin VIIa (Myo7a, green). Representative alkaline phosphatase (AP) staining images at 6 weeks of age in the cochlea (F) and utricle (G) of *Atoh1-rtTA* mice from the F7 lineage. Scale bars: 50 μm in (A–A'), (C–D) and 100 μm in (B, E–G).

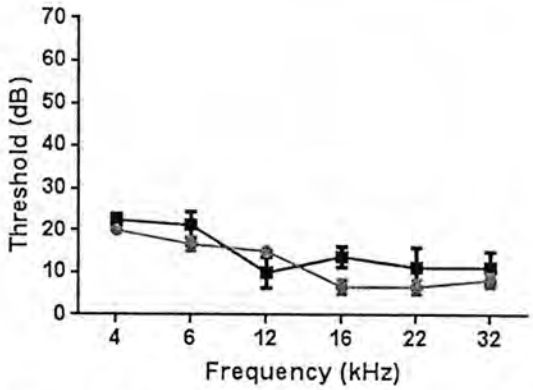

Figure 7 | Hearing ability of *Atoh1-rtTA*(F7) mice. ABR was performed on 3 month old *Atoh1-rtTA(F7)*$^{+ve}$; *TetO-mCherry*$^{+ve}$ mice without administration of doxycycline (grey circles) and littermate controls that lacked both the *rtTA* and *mCherry* alleles (black squares). Data are expressed as mean ± S.E.M for an *n* of 3–4. There were no statistical differences between groups.

illustrates the importance of using more than one reporter line to characterize a new Tet-On mouse line.

In the cochlea, several founder lines showed mCherry or LacZ expression in cells other than HCs including IPhCs and cells in the GER. This may have been caused by a low level of *Atoh1* expression when doxycycline was administered or by transgene insertion effects. Others have shown that *Atoh1* is expressed in SCs, although this expression becomes undetectable by embryonic day 17[17,18]. Therefore, some IPhCs at P0–P3 may still have *Atoh1* expression that is below the level of detection. However the cochlea matures in a gradient from base to apex[19–22] with *Atoh1* expression persisting for the longest period of time in the apex. In contrast we observed more mCherry^{+ve} and LacZ^{+ve} IPhCs in middle and basal turns which does not match this pattern. In addition not all founder lines showed mCherry^{+ve} IPhCs with the same doxycycline induction paradigm. Thus a more likely explanation is that local regulatory elements located near the *Atoh1-rtTA* transgene insertion site could have caused expression of rtTA in IPhCs.

In addition several of the founders showed a significant difference in the percentage of mCherry^{+ve} HCs in different regions of the utricle. These regional differences may have been caused by differences in the timing of cell cycle exit and subsequent HC differentiation[23], by differences in postnatal addition of HCs among regions[24], or by transgene insertion effects. However no regional differences were observed when using the *TetO-LacZ* reporter making transgene insertion effects the most likely explanation. Similarly three of the five founder lines had mCherry^{+ve} cells in the hippocampus where *Atoh1* is not normally expressed. This was also observed in the *Atoh1-eGFP* transgenic line[16] and was likely caused by transgene insertion effects.

Since the tetracycline-inducible system is designed to produce transient changes in gene expression and the half-life of LacZ is 24–48 hours in mammalian cells[25], it is surprising that both reporters remained robustly expressed at 6 weeks of age when doxycycline treatment ended at P3. (The half-life of mCherry is unknown.) The Tet-On system requires the presence of both the rtTA protein and doxycycline for expression of TetO-driven genes. Others have demonstrated that endogenous *Atoh1* is rapidly downregulated in the inner ear during the first postnatal week[4]. However expression of eGFP was observed in cochlear HCs at 6 weeks of age in the *Atoh1-eGFP* mouse[26] which uses the same *Atoh1* enhancer element to drive expression of *eGFP* as our *Atoh1-rtTA* transgene. Using alkaline phosphatase staining, we detected weak expression of the *Atoh1-rtTA* transgene in utricular HCs at 6 weeks of age, but not in cochlear HCs. In the *Atoh1-rtTA* transgene, hALAP expression is controlled by IRES-mediated translation while rtTA expression is controlled by 5′ cap-dependent translation. Others have shown that IRES-mediated translation is less efficient[27] thus it is possible that rtTA is expressed in cochlear HCs when hALAP is below the level of detection. Another possible explanation for the persistent expression of the TetO-reporters is that the rtTA/doxycycline/TetO complex may be very stable and resistant to degradation.

In support of our findings for persistent TetO-reporter expression, a *Sox10-rtTA* allele was recently characterized in the inner ear using the *TetO-LacZ* reporter and LacZ expression was also observed at 8 weeks of age after cessation of doxycycline treatment at P2[28]. Analogous to the blood-brain barrier, the blood-labyrinth barrier functions to protect the inner ear from substances circulating in the blood. Since the blood-labyrinth barrier develops in rodents during the first two postnatal weeks[29], it is possible that a large amount of doxycycline entered the cochlear and vestibular systems before it was formed and then became trapped. In addition doxycycline is heavily protein bound (>90%)[30] which could contribute to a long half-life in inner ear tissues and other drugs have been shown to remain in the inner ear for a much longer time than in serum, brain, or other organs[31]. In support of our hypothesis, doxycycline treatment administered at P14 failed to induce rtTA-driven gene expression in the inner ear using the *Rosa26-loxP-stop-loxP-rtTA-IRES-eGFP* mouse line[32]. While the *Sox10-rtTA* model showed decreased rtTA-driven activity when doxycycline was administered at P14, no effect was observed at P28 unless doxycycline was combined with the loop diuretic furosemide, which alters the properties of the blood-laby-

rinth barrier[28]. In addition others have shown that tetracycline, which is structurally similar to doxycycline, cannot cross the blood-brain barrier[31]. Taken together, these data suggest that doxycycline has limited ability to cross the blood-labyrinth barrier and supports our hypothesis that the persistent expression of rtTA-driven reporter expression in *Atoh1-rtTA* mice is caused by sequestration of doxycycline in inner ear tissues. In light of our observations, it is uncertain whether transient gene expression occurred when other *rtTA* alleles were used in inner ear studies such as the *Rosa26-loxP-stop-loxP-rtTA-IRES-eGFP* allele[32–34] and the *Pax2-rtTA* allele[35]. To determine if similar long lasting effects occur, each *rtTA* allele should be tested with a *TetO-reporter* line specifically in inner ear tissues using the same doxycycline induction paradigm used in experimental studies.

It was also surprising that outer HC loss occurred in *Atoh1-rtTA*$^{+ve}$; *TetO-mCherry*$^{+ve}$ mice at P21 and 6 weeks of age. Outer HCs are known to be more susceptible to death than inner HCs when exposed to multiple types of insults including noise or ototoxic drugs[36–40]. However to our knowledge the death of outer HCs by expression of a reporter gene has not been previously reported. This cell death may have occurred due to a large amount of mCherry mRNA or protein that accumulated in the cell between P3 and P21 which overwhelmed the transcriptional/translational machinery at the detriment of genes required for outer HC survival. Alternatively the mCherry protein could directly induce cell death pathways in outer HCs. In addition, in the *TetO-mCherry* allele, *mCherry* was knocked into the endogenous *Col1a1* locus[12] and thus only one copy of *Col1a1* is expressed which may contribute to the outer HC death we observed. However no outer HC loss was observed in *TetO-mCherry* mice without doxycycline induction at 3 months of age as demonstrated by the normal ABR measurements we obtained. Thus one copy of *Col1a1* is not toxic but the combination of one copy of *Col1a1* with mCherry expression could be.

In conclusion, the *Atoh1-rtTA* mouse produces rtTA activity in the majority of HCs in the cochlea and utricle and in GNP cells of the cerebellum during neonatal ages. Therefore it is a valuable tool for future experiments especially when used in combination with existing Cre and CreER mouse models to modulate expression of multiple genes in two distinct cell types or in the same cell type at different times. While transient control of gene expression was not achieved with the *Atoh1-rtTA* mouse model, this is likely a property of the inner ear's inability to remove doxycycline efficiently and has implications for other tetracycline-inducible mouse models used in inner ear research. Our studies also highlight potential problems with long term expression of the mCherry reporter in outer HCs.

Methods

Generation of *Atoh1-rtTA* transgenic mice. The *Atoh1-CreER-IRES-hPLAP-SV40-polyA* construct[8] was modified to replace the *CreER* sequence with a *Tet-On 3G rtTA* sequence (Clontech, cat# 631159). Founder lines were obtained and Southern blot was performed as previously described[8]. Briefly, Southern blot analysis used the XbaI restriction enzyme and a probe that recognizes the *Atoh1* enhancer sequence. Genotyping primers were designed with the forward primer in the *Atoh1* enhancer element and the reverse primer in the *rtTA* sequence (5′ TCGTCAAGGGCGTCGGTCGGC 3′ and 5′ CTGGCAGAGGCTCCTGGCC 3′).

Characterization of *Atoh1-rtTA* transgenic mice. Expression of the transgene was detected at P0 using alkaline phosphatase staining (NBT/BCIP ready to use tablets (Roche cat#11697471001)). Temporal bones were post-fixed for 1 hour in 4% paraformaldehyde, then transferred to 10 mM PBS. After dissection, samples were heated at 65°C for 1 hour in 10 mM PBS then cooled to room temperature before the addition of the alkaline phosphatase staining reagent (1 NBT/BCIP tablet dissolved in 10 ml double-distilled water). The enzymatic reaction occurred at room temperature in the dark for 30 to 90 minutes followed by washes in PBS and mounting to slides.

To characterize rtTA activity, we bred five founder lines with two different TetO-reporter lines: *TetO-mCherry* (The Jackson Laboratory, stock #14592) and *TetO-lacZ* (The Jackson Laboratory, stock #2621). TetO reporter expression was induced with doxycycline administered in the food (2000 mg/kg, Harlan Laboratories) to the nursing mother from P0–P3 as well as an injection of doxycycline (100 mg/kg, intraperitoneal (IP), Fisher) administered to the pups at P1. Samples were collected at P3 and post-fixed overnight in 4% paraformaldehyde. Routine immunostaining procedures[41] were used with the following primary antibodies: anti-βgal (1 : 500, cat #AB9361 Abcam) and anti-myosin VIIa (1 : 200, cat #25-6790 Proteus BioSciences). All secondary antibodies were Alexa-conjugated from Invitrogen and were used at a 1 : 1000 dilution. mCherry was directly visualized on 12 μm brain cryosections stained with DAPI (1 : 1000, Invitrogen). Images of the cochlea and utricle were taken using a Zeiss LSM 700 or a Leica SP5 confocal microscope. Images of the brain were taken using a Zeiss Axioskop 2 plus with an AxioCanHRc camera. All animal work was performed in accordance with the guidance and approval from the Institutional Animal Care and Use Committee at St. Jude Children's Research Hospital and Southern Illinois University, School of Medicine.

Quantification. Inner ear HCs were identified by myosin VIIa labeling. In the cochlea, the number of LacZ^{+ve} HCs was counted in two, 200 μm regions, randomly chosen from each cochlear turn. Since the mCherry reporter had more robust expression, the entire cochlea was scanned and mCherry negative HCs were counted. For the utricle, the number of labeled HCs in 50 μm × 50 μm squares was counted at nine locations spaced along the anterior/posterior axis of the medial, striolar, and lateral regions as previously described[42]. Reporter^{+ve} cells were averaged across turns or utricle regions and expressed as a percentage of total HCs per organ. The *n* value throughout the paper refers to one ear per animal.

Auditory Brainstem Response. Mice were anesthetized using Avertin (600 mg/kg, IP) and ABR was performed as previously described[41].

Statistical Analysis. All data are presented as mean ± S.E.M. Statistical analyses were performed using Graphpad Prism 6.02 (Graphpad Software Inc.). Comparison of labeled HCs from different groups (i.e. inner vs. outer HCs, across cochlear turns, and among utricle regions) and ABR threshold values across frequencies were determined using a two-way ANOVA followed by either Sidak's or Tukey's multiple comparisons test.

1. Cox, B. C., Liu, Z., Lagarde, M. M. & Zuo, J. Conditional gene expression in the mouse inner ear using Cre-loxP. *J Assoc Res Otolaryngol* **13**, 295–322 (2012).
2. Gossen, M. *et al.* Transcriptional activation by tetracyclines in mammalian cells. *Science* **268**, 1766–1769 (1995).
3. Mansuy, I. M. *et al.* Inducible and reversible gene expression with the rtTA system for the study of memory. *Neuron* **21**, 257–265 (1998).
4. Bermingham, N. A. *et al.* Math1: an essential gene for the generation of inner ear hair cells. *Science* **284**, 1837–1841 (1999).
5. Ben-Arie, N. *et al.* Math1 is essential for genesis of cerebellar granule neurons. *Nature* **390**, 169–172 (1997).
6. Helms, A. W., Abney, A. L., Ben-Arie, N., Zoghbi, H. Y. & Johnson, J. E. Autoregulation and multiple enhancers control Math1 expression in the developing nervous system. *Development* **127**, 1185–1196 (2000).
7. Matei, V. *et al.* Smaller inner ear sensory epithelia in Neurog 1 null mice are related to earlier hair cell cycle exit. *Dev Dyn* **234**, 633–650 (2005).
8. Chow, L. M. *et al.* Inducible Cre recombinase activity in mouse cerebellar granule cell precursors and inner ear hair cells. *Dev Dyn* **235**, 2991–2998 (2006).
9. Machold, R. & Fishell, G. Math1 is expressed in temporally discrete pools of cerebellar rhombic-lip neural progenitors. *Neuron* **48**, 17–24 (2005).
10. Chen, P., Johnson, J. E., Zoghbi, H. Y. & Segil, N. The role of Math1 in inner ear development: Uncoupling the establishment of the sensory primordium from hair cell fate determination. *Development* **129**, 2495–2505 (2002).
11. Jacques, B. E., Montcouquiol, M. E., Layman, E. M., Lewandoski, M. & Kelley, M. W. Fgf8 induces pillar cell fate and regulates cellular patterning in the mammalian cochlea. *Development* **134**, 3021–3029 (2007).
12. Egli, D., Rosains, J., Birkhoff, G. & Eggan, K. Developmental reprogramming after chromosome transfer into mitotic mouse zygotes. *Nature* **447**, 679–685 (2007).
13. Hochedlinger, K., Yamada, Y., Beard, C. & Jaenisch, R. Ectopic expression of Oct-4 blocks progenitor-cell differentiation and causes dysplasia in epithelial tissues. *Cell* **121**, 465–477 (2005).
14. Rizzo, M. A., Davidson, M. W. & Piston, D. W. Fluorescent protein tracking and detection: applications using fluorescent proteins in living cells. *Cold Spring Harb Protoc* **2009**, pdb top64 (2009).
15. Furth, P. A. *et al.* Temporal control of gene expression in transgenic mice by a tetracycline-responsive promoter. *Proc Natl Acad Sci U S A* **91**, 9302–9306 (1994).
16. Lumpkin, E. A. *et al.* Math1-driven GFP expression in the developing nervous system of transgenic mice. *Gene Expr Patterns* **3**, 389–395 (2003).
17. Yang, H., Xie, X., Deng, M., Chen, X. & Gan, L. Generation and characterization of Atoh1-Cre knock-in mouse line. *Genesis* **48**, 407–413 (2010).
18. Driver, E. C., Sillers, L., Coate, T. M., Rose, M. F. & Kelley, M. W. The Atoh1-lineage gives rise to hair cells and supporting cells within the mammalian cochlea. *Dev Biol* **376**, 86–98 (2013).
19. Hallworth, R., McCoy, M. & Polan-Curtain, J. Tubulin expression in the developing and adult gerbil organ of Corti. *Hear Res* **139**, 31–41 (2000).
20. Jensen-Smith, H. C., Eley, J., Steyger, P. S., Luduena, R. F. & Hallworth, R. Cell type-specific reduction of beta tubulin isotypes synthesized in the developing gerbil organ of Corti. *J Neurocytol* **32**, 185–197 (2003).
21. Legendre, K., Safieddine, S., Kussel-Andermann, P., Petit, C. & El-Amraoui, A. alphaII-betaV spectrin bridges the plasma membrane and cortical lattice in the lateral wall of the auditory outer hair cells. *J Cell Sci* **121**, 3347–3356 (2008).

22. Lelli, A., Asai, Y., Forge, A., Holt, J. R. & Geleoc, G. S. Tonotopic gradient in the developmental acquisition of sensory transduction in outer hair cells of the mouse cochlea. *J Neurophysiol* **101**, 2961–2973 (2009).
23. Jiang, T. in *Association for Research in Otolaryngology 37th Annual Midwinter Meeting* (San Diego, CA, 2014).
24. Burns, J. C., On, D., Baker, W., Collado, M. S. & Corwin, J. T. Over half the hair cells in the mouse utricle first appear after birth, with significant numbers originating from early postnatal mitotic production in peripheral and striolar growth zones. *J Assoc Res Otolaryngol* **13**, 609–627 (2012).
25. Smith, R. L., Geller, A. I., Escudero, K. W. & Wilcox, C. L. Long-term expression in sensory neurons in tissue culture from herpes simplex virus type 1 (HSV-1) promoters in an HSV-1-derived vector. *J Virol* **69**, 4593–4599 (1995).
26. Liu, Z. *et al.* Age-dependent in vivo conversion of mouse cochlear pillar and Deiters' cells to immature hair cells by Atoh1 ectopic expression. *J Neurosci* **32**, 6600–6610 (2012).
27. Kazadi, K. *et al.* Genomic determinants of the efficiency of internal ribosomal entry sites of viral and cellular origin. *Nucleic Acids Res* **36**, 6918–6925 (2008).
28. Walters, B. J. & Zuo, J. in *36th Annual MidWinter Meeting of the Association for Research in Otolaryngology* (Baltimore, MD, 2013).
29. Suzuki, M., Yamasoba, T. & Kaga, K. Development of the blood-labyrinth barrier in the rat. *Hear Res* **116**, 107–112 (1998).
30. Bidgood, T. L. & Papich, M. G. Comparison of plasma and interstitial fluid concentrations of doxycycline and meropenem following constant rate intravenous infusion in dogs. *Am J Vet Res* **64**, 1040–1046 (2003).
31. Stupp, H., Kupper, K., Lagler, F., Sous, H. & Quante, M. Inner ear concentrations and ototoxicity of different antibiotics in local and systemic application. *Audiology* **12**, 350–363 (1973).
32. Kelly, M. C., Chang, Q., Pan, A., Lin, X. & Chen, P. Atoh1 directs the formation of sensory mosaics and induces cell proliferation in the postnatal mammalian cochlea in vivo. *J Neurosci* **32**, 6699–6710 (2012).
33. Pan, W. *et al.* Ectopic expression of activated notch or SOX2 reveals similar and unique roles in the development of the sensory cell progenitors in the mammalian inner ear. *J Neurosci* **33**, 16146–16157 (2013).
34. Pan, W., Jin, Y., Stanger, B. & Kiernan, A. E. Notch signaling is required for the generation of hair cells and supporting cells in the mammalian inner ear. *Proc Natl Acad Sci U S A* **107**, 15798–15803 (2010).
35. Burger, A., Koesters, R., Schafer, B. W. & Niggli, F. K. Generation of a novel rtTA transgenic mouse to induce time-controlled, tissue-specific alterations in Pax2-expressing cells. *Genesis* **49**, 797–802 (2011).
36. Stebbins, W. C., Hawkins, J. E., Jr., Johnson, L. G. & Moody, D. B. Hearing thresholds with outer and inner hair cell loss. *Am J Otolaryng* **1**, 15–27 (1979).
37. Rydmarker, S. & Nilsson, P. Effects on the inner and outer hair cells. *Acta Otolaryngol Supp* **441**, 25–43 (1987).
38. Sha, S. H., Taylor, R., Forge, A. & Schacht, J. Differential vulnerability of basal and apical hair cells is based on intrinsic susceptibility to free radicals. *Hear Res* **155**, 1–8 (2001).
39. Li, G. *et al.* Salicylate protects hearing and kidney function from cisplatin toxicity without compromising its oncolytic action. *Lab Invest* **82**, 585–596 (2002).
40. Oesterle, E. C., Campbell, S., Taylor, R. R., Forge, A. & Hume, C. R. Sox2 and JAGGED1 expression in normal and drug-damaged adult mouse inner ear. *J Assoc Res Otolaryngol* **9**, 65–89 (2008).
41. Mellado Lagarde, M. M. *et al.* Selective ablation of pillar and deiters' cells severely affects cochlear postnatal development and hearing in mice. *J Neurosci* **33**, 1564–1576 (2013).
42. Burns, J. C., Cox, B. C., Thiede, B. R., Zuo, J. & Corwin, J. T. In vivo proliferative regeneration of balance hair cells in newborn mice. *J Neurosci* **32**, 6570–6577 (2012).

Acknowledgments

We thank Suzanne Baker, Shelly Wilkerson, and Kristen Correia (St. Jude Children's Research Hospital) for the *Atoh1-CreER-IRES-hPLAP-SV40-polyA* construct, for sectioning and staining the mouse brains, and for assistance with microinjection of the transgene, respectively. This work was supported in part by grants from the National Institute of Health (DC006471 (JZ), DC010310 (BCC), CA096832 (MFR), and Cancer Center Core Grant P30CA21765 (JZ, MFR)); the Office of Naval Research (N000140911014 (JZ), N000141210191 (JZ), N000141210775 (JZ), and N000141310569 (BCC)); and the American Lebanese Syrian Associated Charities (ALSAC) of St. Jude Children's Research Hospital. J. Zuo is a recipient of The Hartwell Individual Biomedical Research Award. The Southern Illinois University School of Medicine Research Imaging facility equipment was supported by Award Number S10RR027716 from the National Center for Research Resources-Health.

Author contributions

B.C.C., J.A.D., F.Z., M.F.R. and J.Z. developed the approach; B.C.C., J.A.D., J.B. and F.Z. performed experiments and data analysis; B.C.C., J.B., F.Z., M.F.R. and J.Z. wrote or edited the manuscript text. All authors reviewed the manuscript prior to submission.

Additional information

Competing financial interests: The authors declare no competing financial interests.

How to cite this article: Cox, B.C. *et al.* Generation of *Atoh1-rtTA* transgenic mice: a tool for inducible gene expression in hair cells of the inner ear. *Sci. Rep.* 4, 6885; DOI:10.1038/srep06885 (2014).

Using Cre-loxP Mouse Genetics to Target Specific Cochlear Supporting Cell Subtypes

Joseph Brancheck[1], Brandon C. Cox[1]

1. Department of Pharmacology, Southern Illinois University School of Medicine, Springfield, IL 62702.

Background: When compared to our knowledge of hair cell (HC) physiology, relatively little is known about the differences among supporting cell (SC) subtypes and the roles each subtype plays in normal and pathological conditions. The known SC subtypes in the cochlea include Claudius' cells, Hensen's cells, Deiters' cells (DC), pillar cells (PC), inner phalangeal cells (IPhC), and cells of the greater epithelial ridge. Development of SC subtype-specific CreER alleles would provide important tools for the field, allowing gene deletion, ectopic gene expression, and fate mapping of individual subtypes. Previously published CreER lines that target SCs have Cre expression in multiple subtypes and some even show Cre expression in HCs (Cox et al., 2012); however, these findings are based on tamoxifen induction paradigms (TIPs) that are quite robust. Altering the tamoxifen concentration and number of injections can decrease the Cre expression pattern and increase cell-type specificity. There are also several reporter alleles which have different expression patterns even when the same CreER line and TIP are used. I hypothesize that altering both the TIP and reporter allele will modify the Cre expression pattern in existing CreER mouse lines to become specific to certain SC subtypes.

Methods: We will use the following CreER alleles known to have expression in SCs at neonatal ages (FGFR3-iCreER, Prox1-CreER, Sox2-CreER, and Plp-CreER) in combination with one of three different reporter alleles (CAG-eGFP, $ROSA26^{CAG/tdTomato}$, or $ROSA26^{LacZ}$). We will alter previously published TIPs to decrease both the tamoxifen concentration and/or number of injections to increase specificity.

Results: When Plp-CreER; $ROSA26^{CAG/tdTomato}$ mice were injected with tamoxifen (3mg/40g) at postnatal day (P)0 and P1, tdTomato expression was present in 5-10% of DC and PC and 50% of IPhC (Cox et al., 2012). By instead using a Plp-CreER; CAG-eGFP mouse and giving tamoxifen (3mg/40g) at P0 only, we found GFP expression in approximately 2.5% of DC and 1.5% of PC while still labeling 32% of IPhC. Similar experiments using other reporter alleles and modified TIPs with FGFR3-iCreER, Prox1-CreER, and Sox2-CreER lines are underway.

Conclusions: Development of SC subtype-specific CreER mouse models would allow for fate mapping of individual subtypes, as well as targeting specific subtypes for gene deletion or ectopic gene expression. This would provide powerful tools to the hearing field to increase our knowledge of SC subtype roles and plasticity. More importantly, it would provide a means to exploit these differences through targeted gene modification.

Funding: Supported by the Office of Naval Research (N000141310569)

Ablation of Different Quantities of Hair Cells in the Neonatal Mouse Cochlea to Examine Mechanisms of Regeneration

Michelle Randle[1], Jian Zuo[2], and Brandon C. Cox[1]

1. Department of Pharmacology, Southern Illinois University School of Medicine, Springfield, IL 62702.
2. Department of Developmental Neurobiology, St. Jude Children's Research Hospital, Memphis, TN 38105

Background: Pancreatic beta cells regenerate via different mechanisms depending on their initial amount of death (Thorel et al., 2010 *Nature*; Nir et al., 2007 *J Clin Invest*). Our lab recently found that neonatal mice are capable of regenerating cochlear hair cells (HCs) after damage. In this model where ~80% of HCs are damaged, we have evidence of two mechanisms of HC regeneration. Supporting cells either underwent direct transdifferentiation or mitotic regeneration to produce new HCs (Cox et al., in revision). We hypothesize that HCs will regenerate using different mechanisms when the HC ablation model is modified to kill 50%, 25%, or 10% of HCs.
Methods: Atoh1-CreER^{TM} is specifically expressed in HCs when tamoxifen is given at neonatal ages. The commonly used ROSA26^{LacZ} reporter allele was used to measure the number of Cre+ HCs when different dosages of tamoxifen were given. Once we established a tamoxifen induction paradigm that targets 50%, 25%, and 10% of HCs, we used it in a similar mouse model (Atoh1-CreER^{TM}; ROSA26^{DTA}) that kills HCs by forced expression of diphtheria toxin, fragment A (DTA). To fate map supporting cells, we introduced the Hes5-nlsLacZ allele into the Atoh1-CreER^{TM}; ROSA26^{DTA} mouse since Hes5-nlsLacZ has LacZ expression in Deiters' cells, outer pillar cells, and inner phalangeal cells at neonatal ages (Cox et al., in revision) and analyzed samples at postnatal day (P) 2. To detect mitotic regeneration, we used BrdU injections (50mg/kg) given between P3-P6 (2 injections per day, ~6 hours apart) and analyzed samples 24hrs after the final injection. BrdU is incorporated into DNA during S phase and therefore will indicate which HCs were derived by supporting cell division.
Results: Atoh1-CreER^{TM}; ROSA26^{LacZ} mice given 3mg/40g tamoxifen at P0 only had ~50% LacZ+ HCs whereas those given 0.1mg/40g tamoxifen at P0 only had ~10% LacZ+ HCs. Using this new tamoxifen induction paradigm in Atoh1-CreER^{TM}; ROSA26^{DTA} mice, both mechanisms of HC regeneration were detected when ~50% of HCs were ablated and studies for the 10% HC death model are underway. Further research is in progress to obtain a tamoxifen induction paradigm that will target 25% of HCs.
Conclusion: Neonatal mice are capable of regenerating cochlear HCs using either direct transdifferentiation or mitotic regeneration mechanisms *in vivo*. Both mechanisms occur when ~80% or ~50% of HCs are killed.
Funding: This work was supported in part by NIH grant DC006471 (JZ) and the Office of Naval Research N000141310569 (BC) and N000140911014 (JZ).

Changes in the Notch Signaling Pathway during Spontaneous Hair Cell Regeneration in the Neonatal Mouse Cochlea

Melissa M. Trone, Sumedha W. Karmakar, Brandon C. Cox
Department of Pharmacology, Southern Illinois University, School Of Medicine, Springfield Illinois

The Notch signaling pathway has been implicated in the developmental regulation of the inner ear sensory epithelium as well as in non-mammalian hair cell regeneration. During development, Notch signaling mediates lateral inhibition which allows some progenitor cells to differentiate into hair cells while neighboring cells are inhibited from a hair cell fate and instead become supporting cells. Many studies have shown that inhibition of Notch signaling allows mammalian supporting cells to convert into hair cells in the normal, undamaged cochlea and in the drug damaged cochlear explant. This mechanism is also implicated during the spontaneous hair cell regeneration process in non-mammalian vertebrates. However, it is currently unknown whether the Notch pathway plays a role during spontaneous hair cell regeneration that was recently observed in the neonatal mouse cochlea *in vivo*. In this model, hair cells were killed *in vivo* using Atoh1-Cre^{ER}+;Rosa26-loxP-Stop-loxP-$DTA^{+/f}$ mice (Atoh1-DTA) and tamoxifen administration at postnatal day (P) 0 and P1. This produced hair cell ablation by Cre-mediated expression of diphtheria toxin fragment A (DTA) specifically in hair cells. Subsequently supporting cells were able to either directly transdifferentiate into hair cells or mitotically regenerate hair cells. We investigated the Notch signaling pathway in the Atoh1-DTA model as a potential mediator for the regenerative capacity observed with the hypothesis that Notch signaling is reduced in supporting cells of the Atoh1-DTA damaged cochlea, allowing them to transdifferentiate and regenerate hair cells. In a gene expression array from P2 cochlear tissue, the expression of Jagged1, a Notch ligand, and Hey1, a downstream Notch effector, were reduced in Atoh1-DTA cochleae compared to control cochleae. Using the Hes5-nlsLacZ reporter mouse, we also found that the number of cells expressing Hes5, another downstream Notch effector, was reduced in Atoh1-DTA cochleae at P2 while the supporting cell population was maintained. Additional studies are underway using *in situ* hybridization and real time qPCR to further investigate the Notch signaling pathway in the Atoh1-DTA model. From our preliminary data we expect to find that Notch signaling is reduced after hair cell damage in the neonatal mouse cochlea.

Funding: Supported by the Office of Naval Research (N000141310569) and the National Center for Research Resources-Health (S10RR027716).

No abstracts were submitted for the following:

Trone, MM, Karmarkar, SW, and Cox, BC. (2015) Dynamic changes in the Notch signaling pathway after hair cell ablation in the neonatal mouse cochlea. *Joint meeting of the Midwest Auditory Research Conference and the Midwest Auditory Neuroscience Symposium*. July 23-25, 2014, Omaha, NE (oral presentation)

Trone, MM, Brancheck J, Grant AC, Graves-Ramsey K, and, Cox, BC. (2015) Using Cre-loxP mouse genetics to target specific cochlear supporting cell subtypes. *Joint meeting of the Midwest Auditory Research Conference and the Midwest Auditory Neuroscience Symposium*. July 23-25, 2014, Omaha, NE (poster presentation)

Cox BC (2013) Spontaneous hair cell regeneration in the neonatal mouse cochlea and utricle in vivo. *Iowa Center for Molecular Auditory Neuroscience Symposium*, 2013 October 17, *University of Iowa, Iowa City* (Keynote speaker)

Cox, BC. Using mouse genetic models to investigate the mechanism of spontaneous hair cell regeneration in the neonatal mouse cochlea. *Department of Pharmacology & Physiology, Georgetown University*. November 20, 2014, Washington, DC. (seminar presentation)

Cox, BC. Using mouse genetic models to investigate the mechanism of spontaneous hair cell regeneration in the neonatal mouse cochlea. *Department of Physiology, Southern Illinois University Carbondale*. October 3, 2014, Carbondale, IL. (seminar presentation)